SUPPORTING DATA TO ACCOMPANY APPLICATION

FOR RETENTION LICENCE OVER THE

MOINA WRIGGLITE SKARN

1. Geology and Genesis of the F-Sn-W (-Be-Zn) Skarn (Wrigglite) at Moina, Tasmania. T.A.P. Kwak and P.W. Askins, 1981. Economic Geology, V 76, pp 439-467.

2. Drill Hole Summaries taken from Askins 1978, 1979 and later Shell reports.

3. Tonnage estimates after Askins, 1979.

4. Beneficiation Studies - Summaries from Askins, 1978 and 1979.

5. Financial Analysis - Summaries from Askins, 1979.

001

922002

Geology and Genesis of the F-Sn-W (-Be-Zn) Skarn (Wrigglite) at Moina, Tasmania

T.A.P. Kwak and P.W. Askins, 1981

Economic Geology, V 76, pp 439-467

Economic Geology
Vol 76, 1981, pp 439–467

Geology and Genesis of the F-Sn-W(-Be-Zn) Skarn (Wrigglite) at Moina, Tasmania

T. A. P. KWAK

Department of Geology, La Trobe University, Bundoora, Victoria 3083, Australia

AND P. W. ASKINS*

Comalco Limited, Exploration Department, P. O. Box 691, Devonport, Tasmania 7310, Australia

Abstract

The Moina skarn deposit, with its associated Sn-W-F veins and greisen, occurs at the margin of the Dolcoath leucogranite. The skarn occurs as a thick horizontal plate approximately one km in its longest dimension and up to 100 m thick and is separated from the granite's upper near-horizontal contact by approximately 200 m of the Moina sandstone. The necessary plumbing system for access of mineralizing fluids is probably a series of east-west-trending tension fractures, now Sn-W quartz veins, associated with a major northwest-southeast-trending fault known as the Bismuth Creek fault. Emplacement of the granite was at shallow depths (<3 km?).

The skarn unit section consists of: (a) a granular garnet-pyroxene-vesuvianite-fluorite skarn; (b) the main skarn ("wrigglite") consisting of fluorite-magnetite-vesuvianite (cassiterite-scheelite-adularia) and having a characteristic fine-grained, rhythmic, finely layered contorted structure; (c) a granular, pale green pyroxene skarn which occurs as thin units (<5 cm) within and near the base of unit (b) above; (d) a wollastonite-rich skarn (>80 vol % wollastonite); and (e) a granular garnet-pyroxene-vesuvianite-fluorite skarn overlying the other units. Unit (e) is relatively enriched in boron (≃600 ppm).

The skarn unit carries up to 25 weight percent F; 0.6 percent Sn, 0.5 percent W, 0.2 percent Be, 27.5 percent Zn, and 4.5 ppm Au. Sn, Be, and Fe values increase toward the upper part of the skarn sequence whereas Zn, Cu, and Mo values are erratic. Secondary Zn-Cu-In-Cd-Au sulfide-amphibole alteration of the primary F-Sn-Be oxide skarn is related to the Bismuth Creek fault. When the primary wrigglite skarn is altered, Sn is largely lost from that part of the skarn.

Introduction

THE Moina skarn deposit is located 40 km southwest of Devonport, Tasmania, near the margin of the Devonian Dolcoath granite. Quartz lodes (veins) which cut the skarn and underlying quartzite were mined for Sn and W until 1956 (Jennings, 1965), but only recently has an investigation of the Fe-F-Sn-W-Be-Zn-Au skarns been reported (Askins, 1978). Apart from studies by Sainsbury (1964, 1969) and Jahns (1944a, b), little has been published on this type of skarn in the western literature, although much has been published in the USSR (e.g., Govorov, 1958, Getmanskaya, 1972; Miroshnchenko and Gulyayev, 1978).

In addition to being of obvious potential economic interest, the relationship of these Sn-bearing oxide skarns to Sn-bearing sulfide replacement deposits such as the Renison Bell deposit (Patterson, 1976) needs more study. The purpose of the present study has been to determine the mineralogy, paragenesis, and bulk chemical relationships of the skarn and related rocks; the nature of the mineralizing fluids; and the distribution of economic elements in the skarn. With this information, a genetic model has been suggested and relations to Sn-sulfide replacement deposits inferred.

* Present address: The Shell Company of Australia Ltd., William Street, Melbourne, Victoria 3000, Australia.

Geology, Petrology, and Mineralogy

General

At Moina F-Sn-W-Be(-Zn) mineralization occurs as skarn, in veins, and in greisen (Fig. 1A). The skarns are a replacement of essentially flat-lying Ordovician limestone and calcareous siltstone (the Gordon Limestone) which conformably overlies quartz sandstone and siltstone (the Moina sandstone).

Mineralization is associated with a Devonian leucocratic granite (Dolcoath granite) which is never in contact with the limestone or skarn but is separated by about 200 m of Moina sandstone. The most intense mineralization occurs in a folded and fractured zone

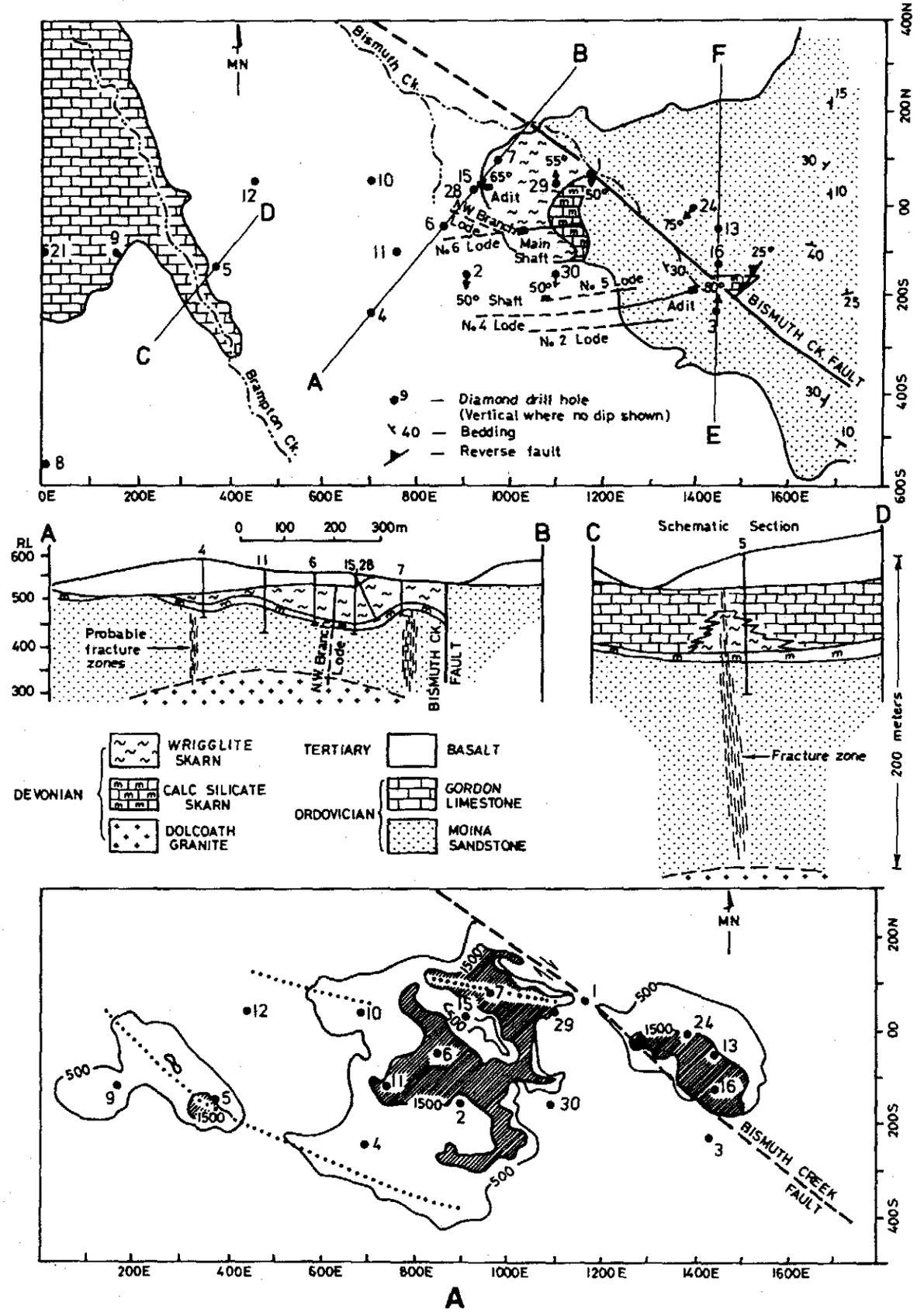

5 cm

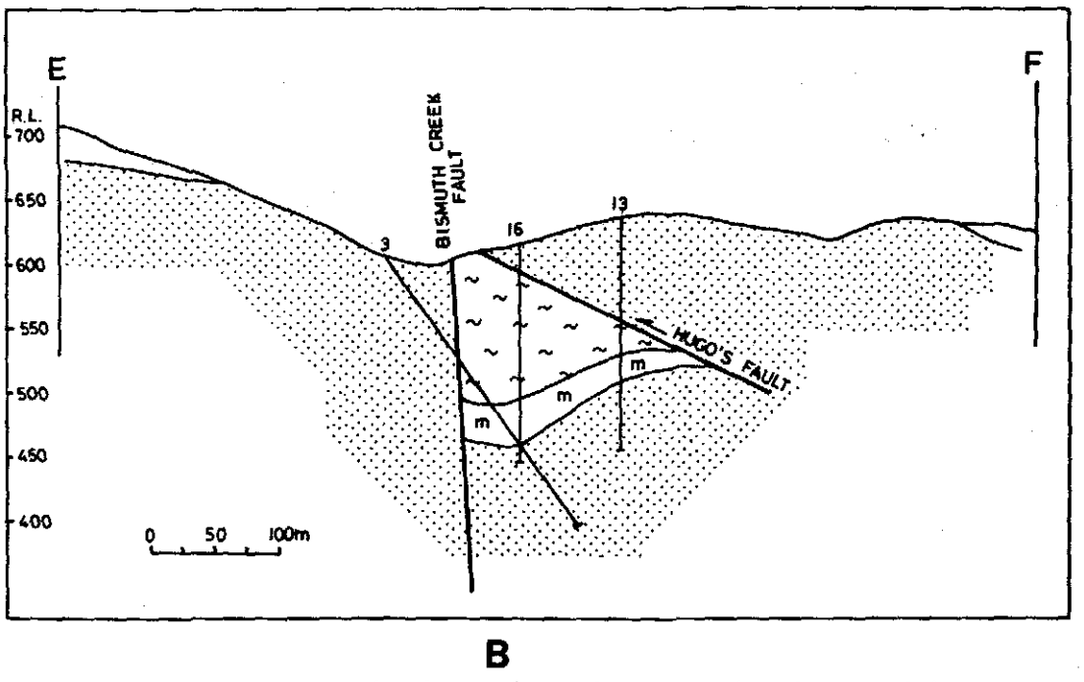

FIG. 1. B. Section E-F is an enlarged section showing skarn occurring beneath a reverse fault.

associated with a major fault. Tertiary basalt covers much of the area.

Granite

Granite has been intersected at a depth of approximately 200 m in diamond drill holes ML-1 and ML-2. Greisenization in the granite in ML-1 decreases downward from its contact at 279 to 317 m (distances down a hole of 50° dip) and consists of a grayish-white-colored zone nearest the contact (zone 1: 279 to 280.8 m), a gray zone (zone 2: 281.8 to 281.8 m), a green zone (zone 3: 281.8 to 292.7 m) and a pinkish-yellow zone (zone 4: 292.7 to 317 m) farthest from the contact. On the basis of color differences, the contacts between zones 1 and 2, and 2 and 3 are abrupt—over 5 cm—whereas that from zone 3 to 4 is less abrupt. Small areas of pinkish (zone 4) greisen appear in zone 3 and greenish (zone 3) greisen in zone 4. This indicates that irregularities of permeability may have existed and may account for minor chemical variations.

In zone 4, the least-altered samples consist of approximately 60 percent quartz, 20 percent white mica, <1 percent brown biotite, 20 percent orthoclase, 8 percent oligoclase, and accessory fluorite, pyrite, rutile, and hematite. By comparison, unaltered Dolcoath granite cropping out in the Forth River Valley 4 km east has an average composition of 35 percent quartz, 5 percent biotite, 40 percent K-feldspar, and 20 percent plagioclase (Gee, 1966), with accessory fluorite and zircon (Jennings, 1963). In zone 4, primary dark brown biotite occurs only as armored relicts in quartz. Fe calculated as Fe^{+2} is 4.451 atoms per molecule (24 oxygens per unit cell), F = 1.126, Ti = 0.431, and Cl = 0.106 with Fe^{+2}/Fe^{+2} + Mg = 91.5 (analysis 8, Table 1).

In zones 3 and 4, two types of white mica coexist having distinctly different compositions. Type 1 is coarse grained with high values of F (0.807 atoms/molecule), Fe(0.846), and Mg(0.123) and with relatively low Si and high Al for muscovite (analysis 4, Table 1). Type 2 in zone 4 occurs as fine-grained masses with low values of F(0.215), Fe(0.415), Mg(0.075), and high Si with lower Al than type 1 (analysis 6, Table 1). The Fe^{+2}/Fe^{+2} + Mg ratio of type 1 is higher than that of type 2 (87.3 vs 84.7). Texturally, type 2 commonly occurs between type 1 mica and unreplaced feldspar relicts. The modal ratio of type 1/type 2 decreases upward until no type 2 occurs in zones 1 and 2. This and the relatively great

FIG. 1. A. Geologic map, cross section, and magnetic anomaly map of the Moina Laminar skarn area. The geologic map shows the location of diamond drill holes. The position of shafts and cassiterite-wolframite-quartz lodes of the Murphy and Shepherd mine are shown. Section A-B is normal to fold trends and to the Bismuth Creek fault and is drawn to scale. Section C-D is schematic showing the probable nature of replacement of the limestone in fracture zones. The magnetic anomaly map is simplified fluxgate data (vertical component of the field) in nanoteslas and shows northwest-southeast and east-west trends.

TABLE 1. Electron Microprobe Analysis of Minerals Present in Greisenized Granite and Quartz Veins

	1	2	3	4	5	6	7	8	9	10	11
SiO_2	44.57	45.25	45.27	44.91	47.92	47.97	50.07	32.60	0.35	1.39	31.68
TiO_2	0.37	0.05	0.04	0.21	0.05	0.03	0.13	3.20	0.50	90.92	0.01
Al_2O_3	28.64	29.99	30.44	29.74	31.96	31.37	28.96	12.87	0.32	1.33	53.18
FeO	6.85	6.63	6.31	6.73	2.73	3.36	1.14	29.73	64.54	4.49	0.03
MnO	0.46	0.22	0.23	0.21	0.09	0.07	0.06	1.65	3.49	0.07	0.03
MgO	0.50	0.22	0.10	0.55	0.28	0.34	1.91	1.56	0.43	0.02	0.02
CaO	0.00	0.00	0.00	0.00	0.27	0.05	0.00	0.00	0.40	0.09	0.00
Na_2O	0.35	0.26	0.22	0.30	0.09	0.16	0.04	0.01	0.13	0.15	0.00
K_2O	10.22	10.19	10.01	10.21	9.24	9.22	10.58	9.11	0.01	0.29	0.02
F	1.90	1.55	1.02	1.70	0.30	0.46	1.38	1.99	0.05	0.09	4.07
Cl	0.02	0.05	0.05	0.02	0.11	0.04	0.01	0.35	0.04	0.07	0.01
Anhydrous total	93.88	94.41	93.69	93.58	93.04	93.07	94.40	93.15	69.76	98.94	96.05
Number of 0 ions	24	24	24	24	24	24	24	24	9	4	24
Si	6.680	6.742	6.793	6.745	7.072	7.087	7.214	5.836	0.040	0.038	3.949
Ti	0.043	0.006	0.005	0.024	0.006	0.004	0.014	0.431	0.000	1.866	0.001
Al^{IV}	1.120	1.258	1.207	1.255	0.928	0.913	0.786	2.164	0.044	0.064	0.051
Al^{VI}	3.941	4.010	4.178	3.833	4.623	4.551	4.133	0.552			7.764
Fe^{+2}	0.859	0.826	0.792	0.846	0.337	0.415	0.137	4.451	5.539[1]	0.102	0.003
Mn	0.059	0.028	0.029	0.027	0.012	0.009	0.007	0.251	0.343	0.002	0.003
Mg	0.112	0.030	0.023	0.123	0.061	0.075	0.410	0.416	0.008	0.001	0.004
Ca	0.000	0.000	0.000	0.000	0.043	0.008	0.000	0.000	0.005	0.003	0.000
Na	0.102	1.937	0.063	0.087	0.027	0.046	0.011	0.000	0.029	0.008	0.000
K	1.954	1.937	1.916	1.956	1.740	1.738	1.947	2.081	0.001	0.005	0.004
F	0.901	0.731	0.484	0.807	0.140	0.215	0.629	1.126	0.018	0.008	4.364
Cl	0.005	0.013	0.013	0.005	0.027	0.010	0.002	0.106	0.007	0.003	0.002

[1] Fe^{+3} not Fe^{+2}

1, type 1: white mica, average of 2, zone 1; 2, type 2: white mica, average of 2, zone 2; 3, type 1: white mica, average of 5, zone 3; 4, type 1: white mica, average of 8, zone 4; 5, type 2: white mica, average of 5, zone 3; 6, type 2: white mica, average of 8, zone 4; 7, white mica, alteration of 11; 8, Fe biotite, average of 3, zone 4; 9, Fe oxide (clot), zone 4 (rock 815, Table 2); 10, rutile, zone 4 (rock 862, Table 2); 11, topaz, in cassiterite-wolframite quartz veinlet. Chemical compositions were determined by means of a Joel JXA-5A electron microprobe with computer control, located at the Department of Geology, University of Melbourne, using a beam current of 0.1 mA and an accelerating potential of 15 kV. The following standards were used: SiO_2, wollastonite and quartz; Al_2O_3, corundum; TiO_2, rutile; Fe total and Ba, anandite; K_2O, potassium tantalite; Mn, Mn metal; Ni, Ni metal; F, fluorite; Cl, halite; and Na, jadeite. The computer program for the reduction of electron microprobe data was written by Mason et al. (1969) with modifications by A. K. Ferguson.

depth suggest that type 2 is not related to any surface alteration process. The occurrence of two coexisting micas may be due to the solid solution of another component such as Li. The Li content of type 1 (sample 799) is 770 ppm, but coexisting types 1 and 2 could not be separated. The Li content of the rocks is, however, relatively low (<700 ppm) (Table 2). The lower F content of type 2 may indicate that this mica formed late in the paragenesis at the expense of unreacted feldspar. Related Mn-rich hematite "clots" (analysis 10, Table 1) and fluorite may represent Fe-biotite relicts.

In zone 3, hematite clots are largely absent and only minor relicts of feldspar remain associated with type 2 mica clots. Also, Fe-biotite armored relicts are absent.

Zone 2 is probably a greisen vein which may originally have been a fault or shear zone prior to and/or during greisenization. It consists largely of coarse-grained type 1 mica (see analysis 2, Table 1), fluorite, quartz, pyrite, minor amounts of rutile (analysis 10, Table 1), and minute cassiterite grains. Throughout the zone there are quartz crystal-filled vugs suggesting high porosity (and permeability?) in the zone.

Zone 1 consists largely of quartz with type 1 mica (analysis 1, Table 1), fluorite, pyrite, and very minor amounts of sphalerite.

Above the granite, quartzite has been greisenized and some greisenized granitic dikes also occur.

The bulk chemistry and densities of 16 samples of the greisenized granite collected at regular intervals are shown in Table 2 with the average composition for each zone. For true comparisons to be made, these rocks should have the same densities. The densities of the samples in Table 2 do vary (e.g., 784 = 2.544 g/cm^3; 780 = 2.826 g/cm^3) and, accordingly, for comparison purposes, molar quantities per 100 cm^3 volume of rock were calculated (Fig. 2). As can be seen, Na_2O and Sr decrease systematically toward the contact representing, in part, the progressive break-

down of plagioclase. K_2O, CaO, Al_2O_3, Fe_2O_3, FeO, TiO_2, H_2O^+, Zn, Cl, Rb, Sn, Ga, Li, Yb, Cu, and to a lesser extent B are all enriched in zone 2. These enrichments reflect the large abundances of muscovite, fluorite, and cassiterite with some base metal sulfides. SiO_2, Zr, Th, U, Y, and Pb decrease in zone 2. MnO increases toward the contact. The inverse trends of Ti and Zr probably indicate that one (Ti?) or both of these elements are mobile in this environment.

Sedimentary rocks

The (meta-) sedimentary rocks of the area consist of the Ordovician Moina Sandstone (intertidal facies?), conformably overlain by Ordovician Gordon Limestone (intertidal to subtidal facies).

The Moina Sandstone is a well-bedded sequence of pale quartz sandstones and quartz siltstones with rare pebbly beds and rare shale. At the top of the sequence more finely grained silty beds predominate over sandy beds. Close to the granite, the sandstone has been recrystallized to a dense compact coarse-grained quartzite. For about 10 m below the skarn the unit consists dominantly of highly fractured dense gray fine-grained quartzite consisting of quartz ± biotite ± chlorite ± magnetite ± clinopyroxene ± amphibole ± fluorite ± calcite. The clinopyroxene is commonly partly altered to amphibole. Unaltered Gordon Limestone is dominantly a fine-grained, compact, pale to dark gray mudstone with well-defined bedding which was slightly disturbed, apparently by burrowing organisms. Particularly toward the base there are thin beds of silty or dolomitic limestone. When unaltered, the bottom transition to the Moina sandstone consists of about 10 m of limestone containing 0.5- to 10-cm-wide interbeds of siltstone, calcareous siltstone, and limestone. The bulk of the limestone is nondolomitic and contains less than 3 percent MgO.

Fracturing and veining

Fracturing and veining of skarn and quartzite is most intense near the contact between quartzite and skarn (Fig. 4A). Alteration of the massive quartzite has occurred out from fractures which are now filled with vein material. Early formed veins were intersected by later ones having different mineralogies and/or abundances of minerals. Thus, for a sample from drill hole SMD 12 at 62 m (see Fig. 1A for location), the general sequence of vein types is amphibole-biotite-muscovite, fluorite-adularia-scheelite, adularia-fluorite-biotite, and calcite-amphibole (Fig. 3B). Only the fluorite-rich fractures, which constitute the largest number, invariably have a magnetite-diopside selvedge separated from the vein by granular diopside (see Fig. 4A). Analyses 8 and 9 (Table 4) are of fractured and veined quartzite. On a 100 cm^3 basis it can be shown that relative to unveined quartzite (see 5 and 6, Table 5 and Fig. 7) the rocks are enriched in Be, Cl, Li, Cu, Zn, Sn, Sr, Rb, Th, W, Ca, Fe^{+2}, Fe^{+3}, K, F, Al, and Mn, with a loss of Si and Y. The fact that the most intense fracturing occurs nearest the lower contact and throughout the skarn but not nearer the granite suggests that the fracturing is produced by a skarn-forming process and is not directly related to the intrusion of the granite. The sequence of vein fillings reflects changing conditions (composition of the fluids, temperature, etc.) during skarn genesis as will be discussed later.

Quartz veins ("lodes" in Fig. 1A) from 0.5 mm to 1 m wide, generally striking east-west and dipping steeply north, are found throughout the quartzite and the lower part of the skarn unit. The widest and greatest abundance of these occur near the skarn-quartzite boundary (see Fig. 1A), although they are reported to have been mined to a maximum depth of 145 m into the underlying quartzite (Jennings, 1965). They were mined for Sn and lesser W until 1956 and consist of quartz containing wolframite, cassiterite, bismuthinite, native bismuth, sphalerite, molybdenite, chalcopyrite, pyrite, scheelite, arsenopyrite, galena, fluorite, topaz, beryl, phlogopite, muscovite, chlorite, and laumontite. Topaz from a cassiterite-wolframite-quartz vein (coordinates 1700E 100S, Fig. 1A) has a high F content (analysis 11, Table 1) and contains high-temperature (430°C, uncorrected for pressure), saline fluid inclusions as will be discussed. In the veins, the Sn:W ratio decreases from 20:12 near the surface (Williams, 1958) to 10:40 at depth (Reid, 1971).

Skarns

Skarn here refers to all calc-silicate-bearing rocks derived from Ca-rich sedimentary rocks. The generalized section consists of a lower calc-silicate skarn overlain by a wrigglite (magnetite-fluorite) skarn. The total skarn unit extends over more than 1 km in its longest dimension and is up to 100 m thick (Fig. 1A). The major magnetic anomalies shown in Figure 1A reflect the major skarn areas, but skarn thicknesses of up to at least 20 m exist below some areas of low magnetic relief (e.g., in drill hole SMD 12). Fortunately the overlying Tertiary basalt is relatively nonmagnetic, but there are pyrrhotite-rich and sphalerite-rich areas of as yet unknown extent which could complicate a simple interpretation of the magnetic picture.

The magnetic picture shows clearly a 300-m lateral displacement of the skarn along the Bismuth Creek fault, though some of this may actually be an apparent lateral movement caused by vertical displacement of shallowly dipping beds. Elsewhere in the

TABLE 2. Compositions of Greisenized Granite and Average of Zones in the Greisen

Sample no.	774	776	779	780	784	788	795	809	812
SiO_2	76.16	73.51	62.64	44.23	74.15	76.96	76.12	76.94	75.52
TiO_2	0.04	0.03	0.05	0.10	0.04	0.04	0.04	0.04	0.04
Al_2O_3	11.21	11.43	18.99	27.86	10.98	12.70	12.86	12.37	12.28
Fe_2O_3	0.00	0.19	1.36	2.15	1.10	0.42	0.70	0.91	0.49
FeO	4.63	4.37	3.78	5.08	4.35	1.12	1.09	0.77	1.54
MnO	0.10	0.17	0.19	0.18	0.26	0.04	0.03	0.03	0.06
MgO	0.10	0.15	0.10	0.35	0.16	0.12	0.14	0.14	0.13
CaO	0.01	1.29	1.68	2.22	0.51	0.41	0.62	0.30	0.46
Na_2O	0.23	0.22	0.30	0.45	0.20	1.38	0.48	0.56	2.03
K_2O	3.68	3.98	6.50	9.61	3.67	4.95	4.52	4.90	5.10
P_2O_5	0.00	0.00	0.00	0.02	0.00	0.05	0.01	0.00	0.00
S	1.17	0.56	0.00	0.54	0.02	0.05	0.21	0.09	0.06
H_2O^+	1.62	1.34	1.56	2.40	0.34	1.76	1.84	1.30	1.08
H_2O^-	0.26	0.15	0.11	0.25	0.35	0.38	0.46	0.93	0.35
CO_2	2.53	3.17	1.58	0.99	3.11	0.37	0.39	0.17	0.93
Total	101.74	100.54	98.84	96.70	99.24	100.76	99.51	99.45	100.07
−S = 0	0.59	0.28	0.00	0.27	0.01	0.03	0.10	0.04	0.03
Total	101.16	100.26	98.94	96.42	99.23	100.73	99.41	99.41	100.04
+F	0.34	1.36	2.27	3.43	0.51	0.46	0.60	0.29	0.41
Total	101.50	101.61	101.11	99.85	99.74	101.19	100.01	99.70	100.45
Sr	3.4	5.1	5.5	8.4	4.1	6.2	6.7	7.5	8.7
Y	78.4	97.3	0	0	95.9	785.7	212.0	156.7	84.0
Pb	200.0	25.2	12.2	14.9	214.4	114.5	45.6	57.9	38.8
Th	48.5	52.1	14.9	3.0	45.1	66.5	61.0	58.5	57.9
U	18.8	7.7	3.4	2.1	23.3	18.9	39.2	32.7	32.4
Rb	866.0	1,003.2	2,480.2	2,816.0	563.1	709.2	698.9	672.8	661.4
Zr	107.4	104.0	34.6	21.0	111.4	112.5	124.5	121.1	118.0
Nb	34.4	22.7	35.0	86.8	36.0	49.9	53.1	53.1	38.3
Ga	25	27	69	126	23	25	25	23	24
Be	25	30	40	60	50	30	40	30	50
Sc	0	0	0	30	3	0	0	3	3
Mo	0	0	3	3	15	0	0	0	10
Yb	10	25	25	40	10	80	25	30	20
Sn	85	360	330	560	36	50	55	46	50
Li	250	250	300	700	200	150	150	100	150
Gl	48	51	77	82	34	<20	39	38	<20
Ni	48	52	92	136	42	128	56	47	38
Cu	82	111	2	51	72	51	42	24	31
Zn	56	37	36	35	502	51	21	8	5
W	ND	20	ND	ND	ND	ND	ND	ND	ND
B	0	0	0	0	0	0	0	0	0
Density	2.6612	2.7268	2.7238	2.8265	2.5443	2.6180	2.6409	2.5989	2.6369

The major oxides SiO_2, TiO_2, Al_2O_3, Fe_{total}, MnO, MgO, CaO, P_2O_5, and SO_3 were analyzed by X-ray spectroscopy; K_2O and Na_2O by flame photometry; H_2O and CO_2 by weight differences on absorption of phosphorus pentoxide and "carbosorb," respectively; FeO by colorimetry at La Trobe University. F was determined by specific ion electrode analyses at Comalco Laboratories (Thomastown, Victoria, Australia). B and Li were determined by wet chemical means at the Australian Mineral Development Laboratories (Amdel). Be, Sc, B, and Mo were done spectographically; Sn and W were done by X-ray fluorescence at Amdel. Sr, Y, Pb, Th, U, Rb, Zr, Nb, Ga, Cl, Ni, Cu, and Zn were done by X-ray fluorescence at La Trobe University.

Assigning limits to the possible analytical errors for these analyses is problematical. For the trace elements the following detection

Moina area there is evidence of the opposite sense of displacement on the fault, and so it is possible that there has been more than one episode of movement. The magnetic picture also shows northwest trends and east-west trends. The northwest trends seem to correlate with known folding and/or faulting with northwest axes in an area close to the Bismuth Creek fault and the east-west trends seem to correlate with zones of tension fractures, which would have acted as the main part of the hydrothermal plumbing system. The major quartz lodes are part of this east-west system (Fig. 1A). The skarn east of Bismuth Creek is compositionally variable and lies beneath a reverse fault (Fig. 1B).

Three general types of calc-silicate skarn occur, namely, (a) a distinctive pale green pyroxene skarn,

from Diamond Drill Hole ML-1 (The sample positions are those shown in Figure 2.)

815	825	830	839	856	862	870	Avg. zone 1	Avg. zone 2	Avg. zone 3	Avg. zone 4
77.69	76.72	78.02	75.22	75.54	76.11	76.64	74.84	53.44	76.04	76.43
0.04	0.03	0.04	0.03	0.04	0.03	0.03	0.03	0.07	0.04	0.04
10.52	11.54	11.19	12.09	12.17	11.94	11.84	11.32	23.43	12.33	11.70
0.92	0.45	0.48	0.41	0.29	0.09	0.00	0.10	1.76	0.78	0.26
1.45	1.84	1.05	1.57	1.36	1.35	1.32	4.50	4.43	1.83	1.44
0.08	0.04	0.03	0.07	0.05	0.03	0.03	0.14	0.19	0.09	0.05
0.08	0.04	0.06	0.15	0.13	0.04	0.07	0.13	0.23	0.14	0.09
0.52	0.60	0.54	0.55	0.53	0.48	0.51	0.65	1.95	0.46	0.52
1.83	1.86	2.47	2.40	2.76	2.54	2.93	0.23	0.38	0.66	2.35
4.19	4.83	4.24	4.81	4.87	5.09	4.99	3.83	8.06	4.51	4.77
0.00	0.00	0.00	0.00	0.00	0.00	0.00	0.00	0.01	0.02	0.00
0.07	0.02	0.03	0.04	0.00	0.04	0.00	0.87	0.27	0.09	0.03
0.78	0.99	1.08	0.66	0.71	0.50	0.99	1.48	1.98	1.31	0.85
0.18	0.29	0.19	0.27	0.21	0.27	0.31	0.21	0.18	0.53	0.26
1.07	0.83	0.72	0.74	0.61	0.56	0.66	2.85	1.29	1.01	0.77
99.42	100.09	100.13	99.02	99.27	99.08	100.34	101.14	97.77	99.74	99.68
0.03	0.01	0.01	0.02	0.00	0.02	0.00	0.44	0.14	0.15	0.02
99.39	100.03	100.12	99.00	99.27	99.06	100.34	100.70	97.63	99.69	99.66
0.38	0.47	0.38	0.37	0.38	0.33	0.70	0.35	2.85	0.37	0.43
99.77	100.55	100.40	99.37	99.65	99.39	101.04	101.05	100.48	100.16	100.09
8.7	8.5	9.1	9.0	10.0	9.7	9.5	4.3	7.0	6.1	9.2
86.9	77.6	126.6	163.9	118.1	142.2	111.9	87.9	0	312.6	113.9
53.2	20.7	23.2	26.1	36.8	32.1	31.4	112.8	13.6	108.1	32.8
59.0	39.5	50.0	48.0	52.2	52.5	44.9	50.3	13.6	57.8	50.6
51.2	14.7	13.3	16.9	11.6	52.9	15.6	13.3	2.8	28.5	26.1
532.8	542.3	557.0	617.0	628.1	636.0	613.1	934.6	2,648.1	661.0	598.5
109.3	92.1	105.4	119.8	105.9	123.8	97.3	105.7	27.8	117.4	109.0
55.5	61.8	53.1	51.9	43.5	58.8	31.6	28.6	60.1	48.0	49.3
19	25	21	20	23	21	22	27	97.5	24.0	21.9
30	50	30	30	30	50	40	28	50	37.5	38.8
3	0	0	0	0	0	0	0	15	2	1
59	0	30	0	0	7	0	0	3	4	12
20	20	25	25	15	30	15	18	33	36	21.3
40	4	44	50	40	26	30	222.5	445.0	47	40.5
150	100	100	100	100	70	80	250	500	137.5	106.3
<20	20	20	20	20	39	21	50	79.5	27.8	7.5
30	27	38	43	40	40	33	50	114.0	68.3	36.1
181	3	8	9	16	15	15	96.5	27	47.3	34.8
7	11	5	4	6	4	3	46.5	36	146	6
				50		30	20	110		40[1]
0	0	0	0	0	0	0	0	0	0	0
2.6536	2.6155	2.6448	2.6183	2.6259	2.6074	2.6034	2.6940	2.7752	2.6005	2.6257

levels in ppm are suggested (R. Price, pers. commun.): Cu (0.5), Zn (0.5), Rb (0.4), Sr (0.3), Y (0.3), Zr (0.8), Nb (0.9), Pb (1.2), V (1.0), Cr (0.9), Ba (3.7), La (1.3), and Ce (4.0). The values for Mo, W, Th, and U are unknown but most likely are of the same order as the other elements (1.0 ppm or so). Analytical errors of major elements as suggested by Norrish and Hutton (1969) for X-ray spectroscopy-derived values are as follows (coefficient of variation of mean values percent) SiO_2 (0.30), TiO_2 (1.1), Al_2O_3 (0.63), Fe_2O_3 (0.71), MnO (2.4), MgO (0.92), CaO (0.81), and P_2O_5 (1.6). Values for Na_2O, K_2O, and SO_3 are (again) probably of the same order. Detection levels for the other trace elements in ppm are B (3), Yb (1), Mo (3), Sc (3), Y (10), Be (1), Sn (20), W (20), and Li (5). The samples were crushed in an Mo-W-free Mn-Cr Sieb mill, thus introducing the possibilities of Mn and Cr contamination.

(b) a garnet-vesuvianite-fluorite ± wollastonite ± amphibole ± epidote ± magnetite skarn, and (c) a wollastonite skarn (see Fig. 4B for types a (GS) and b (PS)). Type a consists of thin beds up to 3 cm wide having irregularities along strike but generally having a sharp contact with type b. Thin pyroxene skarn units are common nearest the lower contact of the overall skarn unit, becoming less common higher in the column. These represent replacement of calcareous siltstone interbeds which occur unaltered about 100 m west of SMD 21 (Fig. 1A) in the adjacent unreplaced Gordon Limestone and are bioturbated, with irregular bedding. This feature is retained in the skarn (Fig. 4C) which suggests that, apart from fracturing, the replacement of the units was a relatively passive event. In all of the skarn units, bimetasomatic zon-

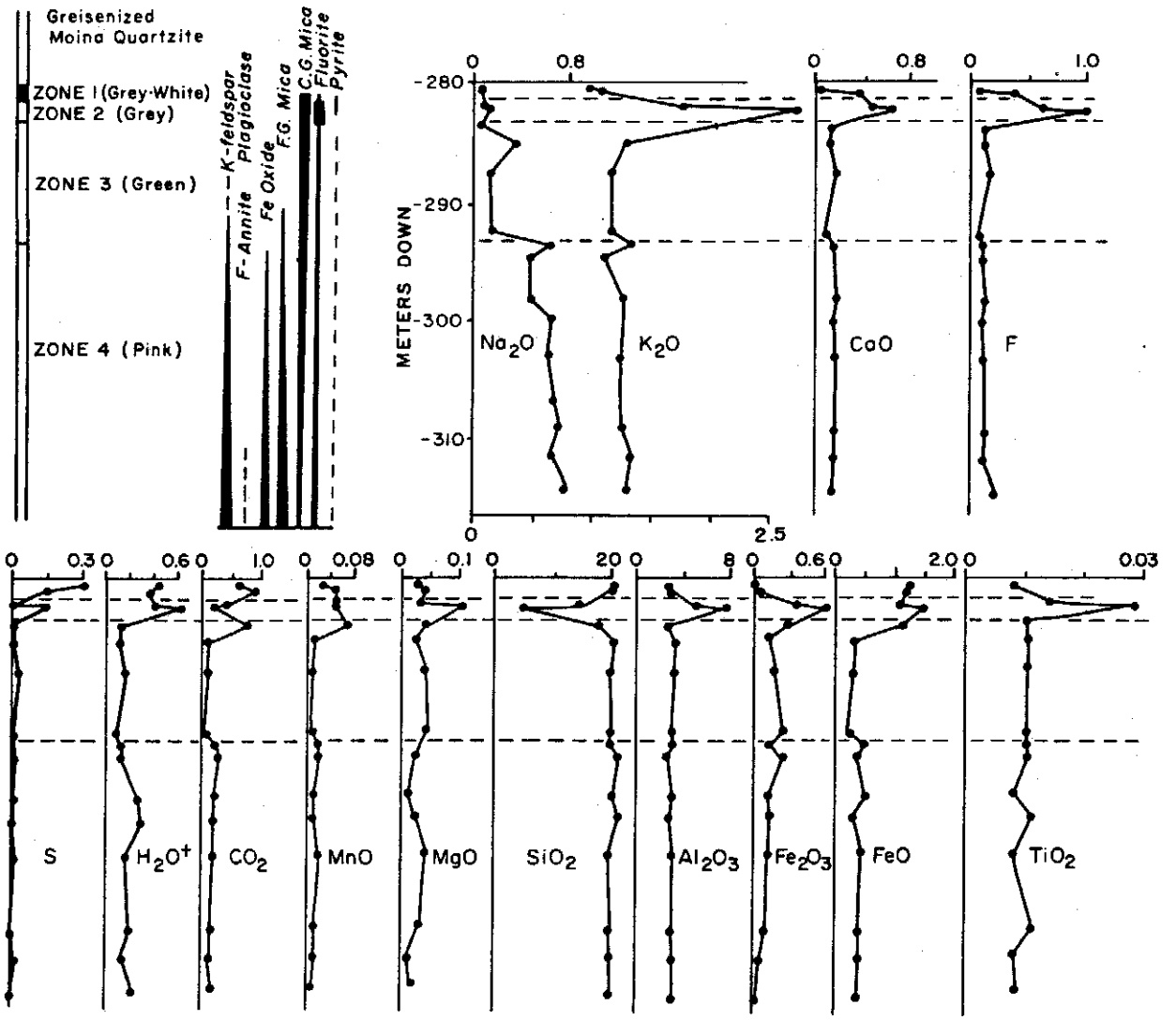

FIG. 2. Chemical variations of major and minor elements from the granite (greisen)-quartzite contact from 280 m down to 316 m in drill hole ML-1 (see Fig. 1 for location). The zones and mineralogy are explained in the text. The values are in moles per 100 cm^3 of rock (thus corrected for density differences). The values were calculated from those in Table 2.

ation is generally absent, reflecting the lack of major chemical or permeability gradients.

The pyroxene skarn consists mainly of fine-grained (<0.2 mm) diopside-hedenbergite pyroxene (ratio 40:60) with very minor amounts of fluorite and garnet. By comparing pyroxene skarn from SMD 5 at 56 m with similar interbeds beyond SMD 21 in unreplaced Gordon Limestone, (Table 4), it can be seen that Na, Sn, F, W, Zn, and Fe were added to the former (7, Table 5). This change could not have been produced solely by thermal metamorphism and indicates F metasomatism.

The second skarn, type b, occurs mainly near the base and in minor amounts interbedded with recrystallized limestone directly above the wrigglite skarn. All gradations exist but garnet is invariably present in large proportions. The garnet is andradite-grossularite (analyses 8 and 9, Table 3) and has concentric color zoning accentuated by anomalous anistropy in polarized light. Values of Sn of up to 0.70 weight percent were found in garnet. The pyroxene interstitial to and occurring as inclusions in garnet is diopside-hedenbergite (analysis 4, Table 3), whereas the accompanying vesuvianite is relatively Fe and F rich (analysis 1, Table 3). Fe-rich hornblendic amphibole (analysis 12, Table 3) and epidote occur replacing

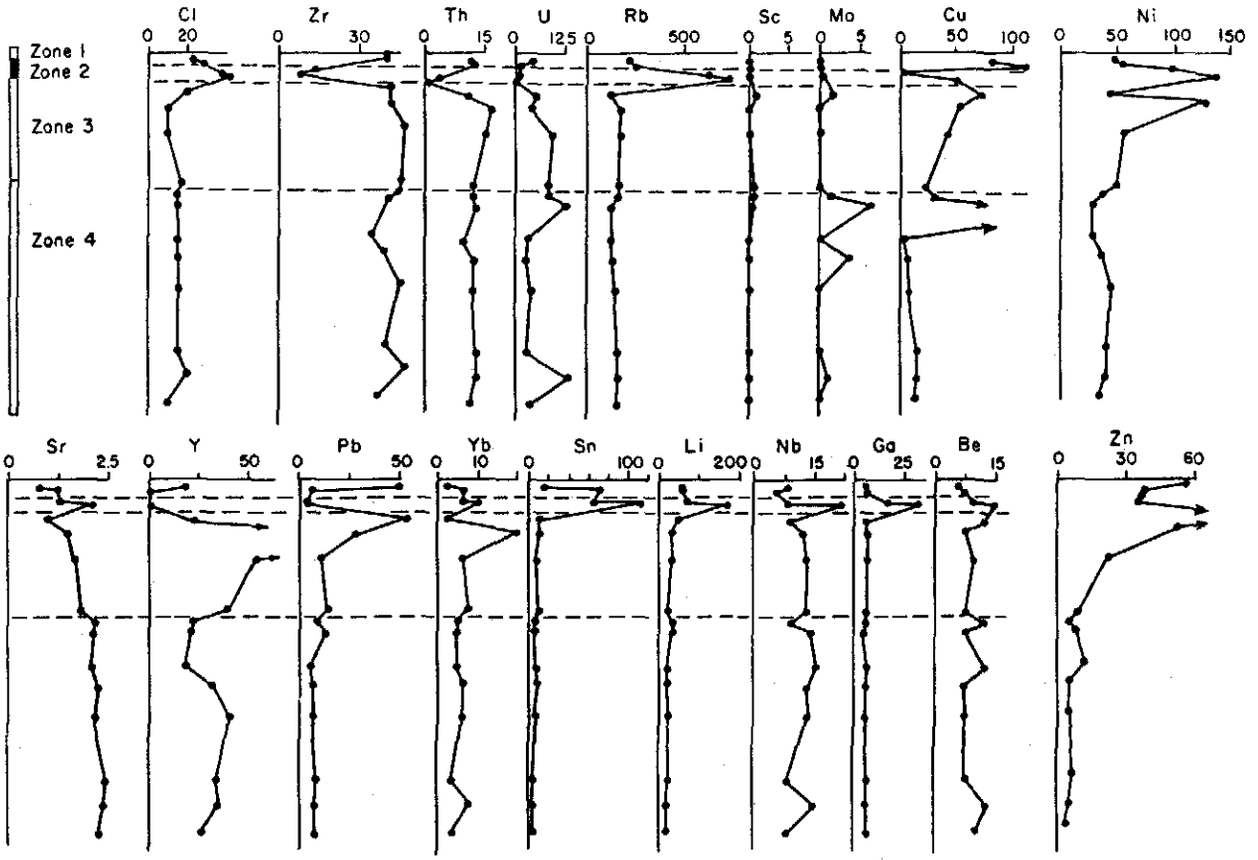

FIG. 2 (cont.)

pyroxene, vesuvianite, and garnet. Interstitial fluorite and adularia occur, occasionally with epidote and calcite in pods up to 2 cm long. Magnetite, scheelite, and pyrite occur as minute grains (to 0.1 mm across), but no cassiterite was observed.

Evidence that this skarn has formed from Gordon Limestone (marble) occurs in some cases (Fig. 4E). Bulk chemical analyses of garnet skarn (6, 11, and 18, Table 4) recalculated on a molar basis per 100 cm^3 volume (8, Table 5, and Fig. 7) show that relative to limestone (17 and 19, Table 4), Sn, H, U, Y, Zn, Li, Cl, Be, Si, Fe^{+2}, Fe^{+3}, F, Al, Mn, and B were added whereas Sr, C, and Ca were removed. The light elements Li, Be, B, and Cl are particularly enriched in garnet skarn overlying the wrigglite skarn (*see* Fig. 4E). Specific boron minerals were not found.

As in the quartzite, veinlet-filled fractures in calc-silicate skarn show a sequential deposition so that for SMD 5, 56 m down, the sequence is veins rich in: (1) muscovite, (2) potassium feldspar (adularia)-fluorite, and (3) calcite (in Fig. 4B and C). The sequence may be only partly shown in any one sample so that in Figure 3A only (2) above is present. The margins of fluorite-bearing veins commonly show marginal alteration to magnetite ± amphibole of garnet and pyroxene skarn (i.e., Fig. 4B).

Calc-silicate skarn type c consists mainly of wollastonite (>80 vol %) with lesser amounts of garnet, pyroxene, vesuvianite, and fluorite. It is probably a variation of type b in representing the metamorphism of extremely quartz-rich impure limestone interbeds, which occur up to 3 m thick. Like the other calc-silicate skarns, it is enriched in F, Sn, Fe, W, and Cl (10 and 14, Table 4).

The main skarn type is a dark, heavy, fine-grained rock showing chaotic laminar patterns of alternating light and dark lamellae which are up to 0.5 mm wide. The rock type has been called "ribbon rock" skarn (Jahns, 1944a), "rhythmically banded rock" (Shabynin, 1977), "wrigglite" skarn (Askins, 1975), and "apocarbonate greisen" (Govorov, 1958).

The skarn here called wrigglite skarn occurs first as thin interbeds within the upper part of the lower calc-silicate skarn unit (see Fig. 5A). Higher in the column wrigglite skarn occurs interbedded with pyroxene skarn (Figs. 5B and 4C) but generally not with

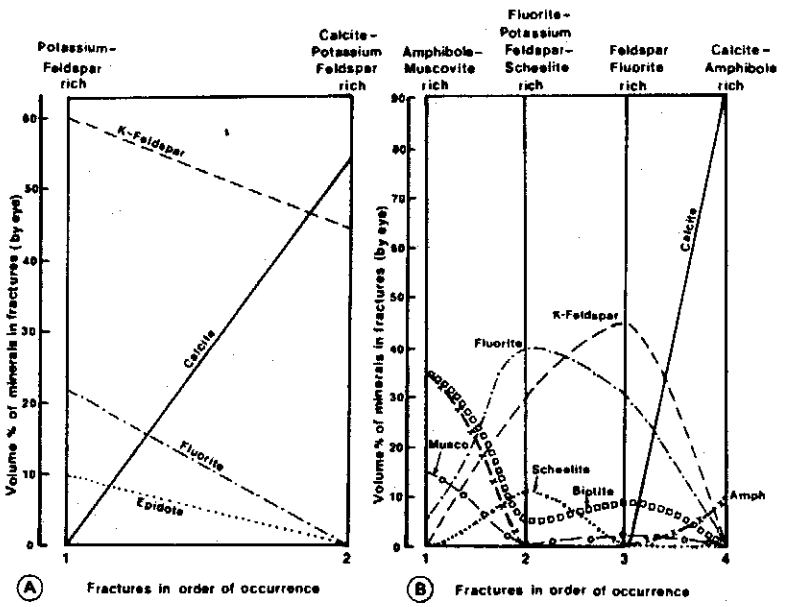

FIG. 3. Graphs showing the mineral contents of sequentially deposited veins in quartzite (B, SMD 5, -65 m), calc-silicate skarn (C, SMD 12, -65 m) and laminar skarn (A and D, SMD 5, -46.2 m). The vein contents were estimated by eye. In most cases between three to ten veins of the same period were averaged to produce the graphs.

garnet skarn. The wrigglite skarn terminates upward against unreplaced marble (where it is not removed by erosion) and septa of skarn occur along fractures extending into the marble (Figs. 5C and D).

The lamination is closely related, and parallel, to fractures (Figs. 5C and D), not bedding (Fig. 5B). In some cases the skarn-marble contact is irregular enough to produce embayments (Fig. 5D) or even pockets of unaltered material. These latter are interpreted eventually to form augen-type structures ("1" in Fig. 5C and "3" in Fig. 5B) or foldlike areas as in Figure 6A. The augen often occur where two or more fractures intersect (Figs. 5C, 4C, and 4D).

The normal primary mineralogy of the wrigglite skarn is magnetite in the dark lamellae and vesuvianite + fluorite in the light-colored lamellae. More rarely, adularia + fluorite and pyroxene ± garnet + fluorite and pyroxene ± garnet + fluorite from the light-colored lamellae. Minor cassiterite occurs, particularly in the magnetite layers, and minor Sn-rich sphene, scheelite, and bismuthinite crystals occur scattered throughout. Molybdenite, sphalerite, pyrite, scheelite, cassiterite, amphibole, bismuthinite, adularia, topaz, unusual K-Ca silicates (on which study is still in progress), and laumontite occur in veinlets. As seen in Figure 6A, the dark layers need not be continuous but pinch and swell making the exact classification of which minerals belong to which lamellae difficult.

Vesuvianite has Fe > Mg (analysis 3, Table 3) and high F (2.369 atoms per formula of 78 oxygens). Pyroxene is rarely found in the light layers, but when it is present it is hedenbergitic (i.e., Fe/Fe + Mg = 0.619, analysis 5, Table 3). This is in sharp contrast to diopsidic pyroxene in accompanying garnet skarn (analysis 4, Table 3). Adularia + fluorite wrigglite probably occur only where high Sn values are found (>0.4 % Sn?). The adularia has few impurities (analysis 16, Table 3). Tin values of 6.31 weight percent are found in rare Sn-rich sphene. Magnetite contains little Sn or W (analysis 15, Table 3) whereas cassiterite, which forms irregular patches up to 15 μm in diameter, contains less than 2.00 weight percent FeO.

As in the quartzite and lower calc-silicate unit, the wrigglite skarn has numerous intersecting fractures and veinlets. For example, in a sample from SMD 5 at 46.5 m (Fig. 3D) the general sequence is veins rich in (1) garnet + fluorite, (2) adularia + fluorite (+ to 2% topaz and 8% scheelite), and (3) fluorite + adularia.

The alteration of the primary wrigglite skarn to form amphibole and/or sulfide-rich equivalents occurs at Moina, as in many skarns throughout the world. The distribution of alteration in the skarn is difficult to define because of the limited number of drill holes and poor surface exposure. Variable amounts of amphibole (±sulfide) alteration occur throughout. In some cases the wrigglite skarn may

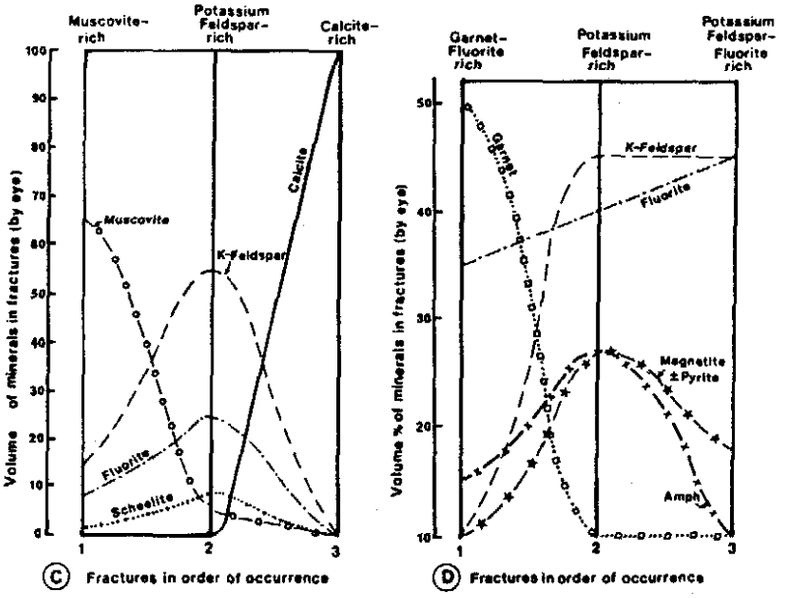

FIG. 3. (cont.).

be altered producing an amphibole-rich area having sharp contact with unaltered skarn (e.g., at "2", Fig. 5D); in others magnetite ± cassiterite relict layers are retained in an amphibole-Fe sulfide matrix. Apart from intermittent alteration throughout the skarn, major areas are known to occur in SMD 9 at the skarn extremity where there is a pyrrhotite-rich skarn and in SMD 13 near the Bismuth Creek fault, beneath a reverse fault, where there is a coarse-grained, sphalerite-rich rock. In both examples, but particularly in the former, relict wrigglite structure occurs with a superposition of a later structure consisting of plates of hematite (SiO_2 = 0.021 moles, CaO = 0.009 moles per 3 oxygens) with marginal Fe-F biotite (analysis 13, Table 3 and Fig. 6D). Amphibole is Fe rich with considerable K + Na (analysis 10, Table 3). Pyrrhotite has the composition $Fe_{0.955}S$ in sample SMD 9 at 97.2 m (Figs. 5F and 6D) whereas hematite (0.027 moles SiO_2 per 3 oxygens) occurs with chalcopyrite.

Near the Bismuth Creek fault the replacement of wrigglite skarn by base metal sulfides, Fe sulfides, and hematite is common (Fig. 5E). Sphalerite in sample SMD 16 at 65 m, has the composition $Zn_{0.863}Fe_{0.164}Mn_{0.020}S_{1.067}$ whereas coexisting pyrrhotite has the composition $Fe_{0.936}S$ and hematite has 0.008 moles SiO_2 (3 oxygens per formula) as impurities. Garnet (and vesuvianite?) alter to hematite + quartz (Fig. 6B); pyroxene, to amphibole (Fig. 6C) and magnetite to sulfides. The amphibole in the alteration is similar to that found in less-altered wrigglite skarn (analyses 11 and 12, Table 3).

Mass Balance Relationships

Mass balance calculations were done to gain some insight into the amount of materials added by the mineralizing solution on traversing the rock units and to see if the constituents were produced by either redistribution in the skarn column, derivation from the quartzite column, or derivation from the greisenized granite. Most of the trace element contents of the skarn are so anomalously high that these could not have been produced by redistribution within the columns and rock types analyzed. To account for density differences, the mass balance calculations for major constituents are shown in Table 5 on the basis of molar changes per 100 cm^3 of rock. Columns 1 to 3 and 5 to 11 are for changes of rock compositions caused by replacement from a previous rock type whereas columns 4 and 12 represent the gains and losses to the fluid from the greisenized granite (column 4) and the skarn (column 12). As can be seen in Figures 2 and 7, when the fluid traversed and reacted with the column of granite, the solution gained Si, Na, and K whereas all other major constituents were lost. For the skarn column, including some quartzite, the solution gained only Ca, a minute amount of P, and large amounts of CO_2. The major constituents added to the greisenized granite column are Al, Fe^{+2}, Fe^{+3}, S, and F; Si, Al Fe^{+2}, Fe^{+3}, Mg, Na, K, S, H_2O, and F were added to the skarn column. Much Si could have been added when the solutions traversed the quartzite (column 5), but clearly most

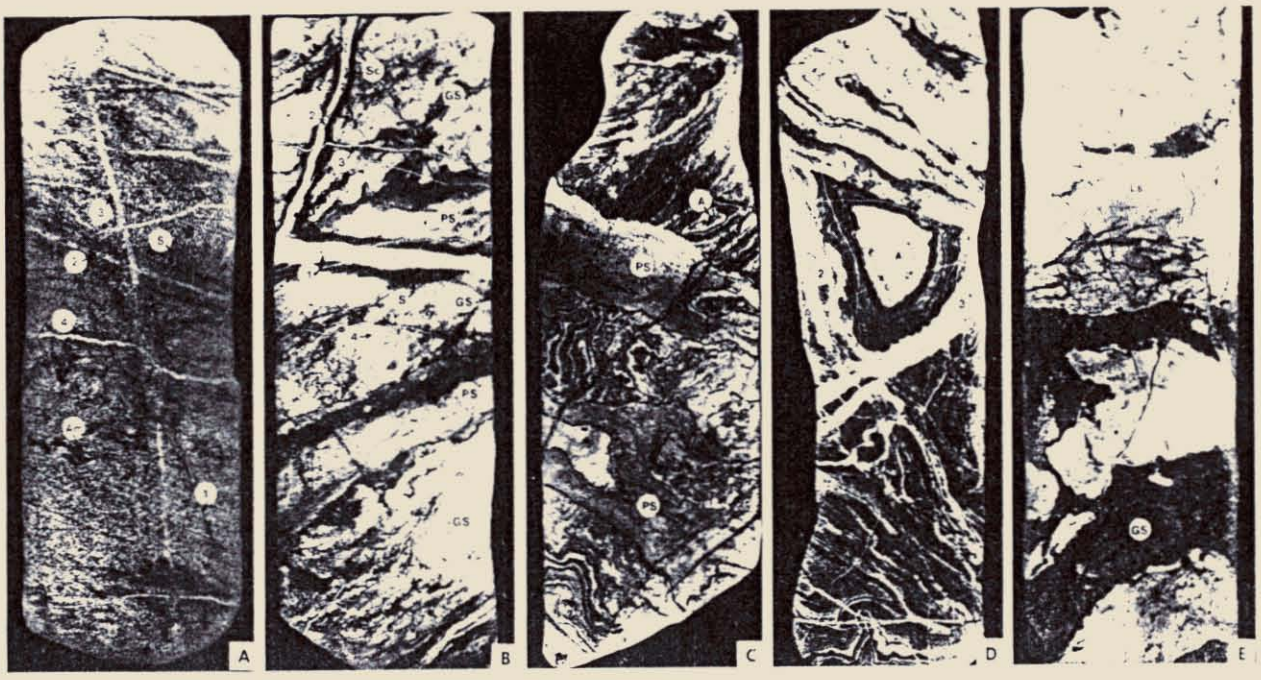

FIG. 4. Examples of drill core from an idealized section through the skarn layer at Moina. The core is approximately 4 cm wide.

A. Photograph of intensely fractured and veined quartzite immediately beneath the skarn units (SMD 5, -62 m). Numbers 1 to 4 = the sequence of vein fills described in the text; S = the magnetite-diopside selvage found at fluorite-rich vein margins described in the text; Am = to amphibole (-epidote)-rich pods.

B. Transmitted light photo of basal skarn showing alternating garnet (GS) and pyroxene skarn (PS) units (SMD 5, -56 m). Numbers 1 to 4 = the sequential nature of intersecting veins; Sc = scheelite grains observable in vein 2; S = the magnetite (-diopside) selvage peripheral to the fluorite-bearing veins (1 and 2).

C. Transmitted light photo of alternating layers of wrigglite skarn and pyroxene skarn (PS) common near the base of the main wrigglite skarn unit. A = a concentrically zoned area of wrigglite skarn. An enlargement of this wrigglite skarn-pyroxene skarn contact is shown in Figure 5B (SMD 12, -101.25 m).

D. Transmitted light photo of wrigglite skarn showing sequential vein fillings (1 to 3) and granular skarn area A (SMD 5, -46.5 m). The latter consists of garnet + fluorite + pyrite.

E. Transmitted light photo of garnet (+ vesuvianite + fluorite) skarn-marble. The skarn is enriched in B, Li, etc., but is not wrigglite. It is a replacement of undisturbed limestone with dolomitic siltstone interbeds.

of the constituents that must have been added to produce the relatively thin skarn column of SMD 12 could not have been derived solely by alteration of quartzite or greisenization of an amount of granite equivalent to the column studied in drill hole ML-1. Also, the skarn overlying adjacent areas of ML-1 is much thicker than that found in SMD 12.

Distribution of Economic Constituents

In the course of exploration by Comalco Limited, approximately 5,000 analyses of Pb, W, Bi, Sn, Mo, Cu, Zn, Be, Sc, Y, Cd, In, Ge, Au, and Ag were done of drill cores SMD 4, 11, 6, 15, and 7 (traverse 1, section line A-B in Fig. 1A) and ML-3, -16, and -13 (traverse 2, section line E-F in Fig. 1A) by the Australian Mineral and Development Laboratories (AMDEL). These are traverses both out from and across the Bismuth Creek fault. The data were analyzed by computer to see (a) the degree of correlation between all possible element pairs, (b) whether there is a relation between the concentration of an element and depth, and (c) whether there is a lateral relation of concentration and proximity to the Bismuth Creek fault. Correlation coefficients were calculated relative to a linear model. Scatter can result from the data not filling a linear model, analytical variation, and the fact that the analyses were done on different skarn rocks and quartzite where density differences were not accounted for. The correlation coefficient data of (a) above shows (Table 6) that elements fall approximately into two groups, namely, (1) Be, F, Sn, and Ag and (2) Zn, Cd, In, Ge, Au, and possibly Bi. The

TABLE 3. *Composition of Representative Skarn Minerals*

	1	2	3	4	5	6	7	8	9	10	11	12	13	14	15	16
SiO_2	36.87	35.19	34.21	53.07	48.94	37.62	37.21	36.89	37.01	36.80	36.55	39.14	34.90	45.61	0.81	66.42
TiO_2	0.07	0.08	0.20	0.00	0.07	0.17	0.20	0.22	0.56	0.20	0.25	0.34	0.00	0.00	0.06	0.02
Al_2O_3	13.70	15.64	13.65	0.19	0.37	5.97	6.09	6.97	8.29	11.54	13.23	14.44	10.90	30.59	0.20	18.73
FeO	5.43	3.98	6.62	4.97	18.33	22.02[1]	21.12[1]	22.29[1]	20.64[1]	27.14	26.16	23.83	36.19	6.76	51.14[1] 46.02	0.32
MnO	0.75	0.83	1.20	0.27	2.83	1.79	1.00	1.86	2.41	0.83	1.42	1.26	1.77	0.00	0.34	0.00
MgO	3.00	2.28	2.15	15.01	4.74	0.09	0.08	0.00	0.01	3.39	2.62	2.00	3.40	0.53	0.00	0.07
CaO	35.19	35.11	35.84	24.86	22.68	31.78	32.51	31.35	31.25	11.22	9.64	11.05	0.15	0.00	0.25	0.00
Na_2O	0.01	0.04	0.02	0.04	0.15	0.05	0.09	0.00	0.01	1.53	1.49	0.28	0.00	0.28	0.01	0.01
K_2O	0.00	0.01	0.04	0.01	0.00	0.02	0.02	0.00	0.02	2.22	2.93	2.25	8.10	10.77	0.00	13.01
F	1.70	1.35	1.40	0.11	0.22	0.23	0.31	0.31	0.32	0.60	0.45	0.29	2.22	2.89	0.00	0.00
Cl	0.24	0.23	0.17	0.02	0.00	0.02	0.06	0.00	0.05	0.52	0.61	0.62	0.24	0.00	0.00	0.00
Anhydrous total	97.05	94.84	95.62	98.56	98.34	99.76	98.69	99.89	100.57	95.99	93.35	95.50	97.78	97.43	98.83	98.58
Number of 0 ions	78	78	78	6	6	12	12	12	12	24	24	24	24	24	4	
Si	19.014	18.558	18.304	1.986	1.976	5.978	6.104	5.992	5.943	6.288	6.268	6.608	6.044	6.439	0.033	12.168
Ti	0.056	0.063	0.081	0.000	0.002	0.020	0.025	0.027	0.068	0.026	0.032	0.026	0.000	0.000	0.002	0.003
Al^{IV}	8.330	9.724	8.611	0.002	0.018	0.022	0.00	0.008	0.057	1.712	1.732	1.392	1.956	1.561	0.010	4.045
Al^{VI}				0.000	0.000	1.096	1.178	1.327	1.512	0.614	0.943	1.583	0.269	3.530		0.000
Fe^{+2}	2.342	1.755	2.962	0.156	0.619	0.000	0.000	0.000	0.000	3.878	3.752	3.878	5.228	0.000	1.557	0.050
Fe^{+3}	0.000	0.000	0.000	0.000	0.000	3.015	2.607	2.725	2.491	0.000	0.000	0.000	0.000	0.718	1.557	0.000
Mn	0.328	0.371	0.544	0.009	0.097	0.241	0.139	0.256	0.312	0.120	0.206	0.120	0.260	0.000	0.012	0.000
Mg	2.306	1.792	1.714	0.837	0.285	0.021	0.020	0.000	0.002	0.863	0.670	0.863	0.877	0.111	0.000	0.019
Ca	19.446	19.840	20.548	9.997	0.981	5.411	5.714	5.457	5.377	2.054	1.771	2.054	0.028	0.000	0.011	0.000
Na	0.010	0.041	0.021	0.003	0.006	0.015	0.014	0.000	0.003	0.507	0.495	0.507	0.000	0.076	0.000	0.002
K	0.000	0.006	0.013	0.000	0.000	0.004	0.002	0.000	0.002	0.484	0.641	0.484	1.788	1.939	0.000	3.041
F	2.772	2.251	2.369	0.011	0.028	0.031	0.161	0.159	0.163	0.324	0.244	0.324	1.215	1.290	0.000	0.000
Cl	0.210	0.205	0.154	0.002	0.000	0.005	0.017	0.000	0.014	0.150	0.177	0.150	0.070	0.000	0.000	0.000

[1] = Fe_2O_3 instead of FeO

Analyses were done as explained in caption of Table 1. 1, vesuvianite: SMD 5, −56 m, in calc-silicate skarn; 2, vesuvianite: SMD 12, −104.18 to −104.29 m, lower calc-silicate skarn; 3, vesuvianite: SMD 12, −93.00 to −93.09 m, wrigglite skarn; 4, pyroxene: SMD 5, −56 m, in calc-silicate skarn; 5, pyroxene: SMD 12, −93.00 to −93.09 m, wrigglite skarn; 6, garnet edge: SMD 12, −93.00 to −93.09 m, wrigglite skarn; 7, garnet core: as 6 above; 8, garnet: SMD 5, −56 m, in calc-silicate skarn; 9, garnet: SMD 12, −92.00 to 92.12 m, upper calc-silicate skarn; 10, amphibole: SMD 12, −93.00 to 93.09 m, wrigglite skarn; 11, amphibole: SMD 12, −104.18 to −104.29 m, lower calc-silicate skarn; 12, amphibole: SMD 12, − 92.00 to −92.12 m, upper calc-silicate skarn; 13, annite: SMD 9, −97.2 m, sulfide-wrigglite skarn; 14, muscovite: SMD 16, −126.557 m, altered wrigglite skarn; 15, magnetite: SMD 12, −93.00 to −93.09 m, wrigglite skarn; 16, adularia: SMD 12, −39.00 to 93.09 m, wrigglite skarn.

TABLE 4. Composition of

The analyses were determined as described in Table 2 except that instead of being calculated as oxides they were calculated in terms

	1	2	3	4	5	6	7	8	9	10
Si	4.39	21.53	31.69	10.06	23.80	12.27	18.41	37.97	22.36	17.87
Ti	0.06	0.34	0.13	0.13	0.49	0.13	0.30	0.21	0.28	0.20
Al	1.08	5.48	2.38	4.68	7.56	4.73	6.46	1.58	4.25	4.08
Fe^{+3}	0.00	0.00	0.95	4.33	1.89	9.83	4.75	0.00	1.47	9.38
Fe^{+2}	0.63	1.95	2.88	14.55	3.68	6.34	2.64	1.76	6.23	0.96
Mn	0.05	0.02	0.12	0.12	0.62	0.59	0.85	0.10	0.30	0.95
Mg	0.95	1.39	2.61	1.14	1.75	1.15	1.39	2.05	5.09	1.88
Ca	36.83	13.41	7.00	18.20	11.70	22.95	20.80	4.34	13.51	21.68
Na	0.14	0.42	0.35	0.59	2.66	0.46	0.42	0.27	0.33	0.08
K	0.62	3.60	1.75	2.48	0.51	0.35	0.27	0.97	1.42	0.01
P	0.02	0.04	0.12	0.02	0.05	0.06	0.05	0.23	0.13	0.10
S	0.21	0.81	0.02	2.63	0.01	0.18	0.02	0.03	0.22	0.01
H^+	0.69	0.17	0.17	0.13	0.17	0.12	0.06	0.04	0.10	0.05
H^-	0.01	0.04	0.02	0.03	0.02	0.01	0.02	0.01	0.02	0.02
C	9.14	3.75	0.08	1.26	0.23	0.28	0.24	0.17	0.36	0.30
F	0	0.84 (?)	10.03	24.86	3.01	23.93	8.09	0.09	4.26	3.54
Total	54.82	53.79	60.30	85.21	58.05	83.38	64.77	49.82	68.33	61.11
wt. oxygen inferred (approx.)	45.18	46.21	39.70	14.79	41.95	16.62	35.23	50.18	32.67	48.89
Sr	344	272	38	97	188	36	34	50	100	11
Y	13 (40)	8 (60)	32 (100)	0 (60)	11 (60)	4 (70)	22 (50)	61 (100)	28 (70)	31 (60)
Pb	1	13	18	4	4	51	2	1	24	14
Th	4	15	8	123	15	148	15	10	67	16
U	0	1	1	5	1	5	1	1	1	2
Rb	20	102	591	791	217	42	60	158	233	6
Ga	3	14	10	44	19	24	20	4	17	13
Be	5	20	400	300	100	400	80	40	70	60
Sc	5	15	5	7	20	7	6	3	7	5
Mo	0	0	20	300	15	70	0	0	0	0
Yb	4	3	15	10	5	8	8	10	5	5
Sn	<20	<20	280	1,000	180	940	220	20	130	900
Li	5	25	100	65	25	30	15	20	50	5
Ci	0	0	99	35	0	1,799	230	32	116	750
Ni	28	45	77	112	111	62	65	42	100	79
Cu	20	27	7	869	36	289	25	16	66	26
Zn	0	28	89	67	131	173	82	45	334	129
W	<50	<50	2,400	2,100	130	500	190	<50	160	<50
B	0	50	3	0	3	300	0	3	5	150
Density	2.7382	2.6773	2.8479	3.6349	3.0090	3.5914	3.4473	2.8035	2.9698	3.5498

1, Gordon Limestone, field specimen from Iris River, CO_2 too high to do by the methods available; 2, siltstone interbed in Gordon Limestone (analysis 1); 3, SMD 5, −62 m, whole rock, fractured quartzite; 4, SMD 5, −46.5 m, whole rock, wrigglite skarn; 5, SMD5, −56 m, No. 1, green pyroxene-rich layer *in calc-silicate rock, silty interbed in original limestone*; 6, SMD 5, −56 m, No. 2, whole rock, calc-silicate, highly fractured + veins + green pyroxene-rich layer; 7, SMD 5, calc-silicate next to analyses 5 (free of veins and green pyroxene layer); 8, SMD 12, −111.36 to −111.46 m, pure quartzite whole rock; 9, SMD 12, −110.08 to −110.18 m, quartzite with vein-filled fractures, whole rock; 10, SMD 12, −106.02 to 106.13 m, calc-silicate rock, whole rock; 11, SMD 12, −104.18 to −104.29 m, calc-

correlation coefficients between the individual members from the two groups are usually negative (i.e., Zn:F = -0.13; Sn:Zn = -0.16) The two groups are believed to relate to the composition of the primary wrigglite skarn (group 1) and the later sulfide-rich alteration (group 2). These data imply that group 1 is removed by solution when sulfide (group 2) alteration occurs, as will be discussed. The distribution of W is erratic except for its correlation with Ge which may be accidental as only 13 pairs were analyzed. The W distribution is probably related to its irregular occurrence in veinlets (e.g., Fig. 4B). The Sc and Y correlations are erratic which may in part reflect the possible inaccuracy in the analysis (semiquantitative). Bi may have been redistributed during sulfide-amphibole alteration but not lost to solution as were the group 1 elements.

Table 7 shows the correlation coefficients of elemental concentrations as a function of depth in each drill hole. Those from group 1, namely Sn, F, and to

Quartzite, Skarn, and Limestone

of elemental abundances. The numbers in brackets are semiquantitative analyses by AMDEL.

11	12	13	14	15	16	17	18	19	20	21
12.63	8.68	10.40	16.67	5.13	12.19	3.06	16.78	7.67	10.79	5.06
0.16	0.06	0.08	0.28	0.07	0.13	0.05	0.37	0.14	0.11	0.08
4.55	5.49	5.21	5.18	1.34	5.10	0.64	5.45	2.56	5.01	1.41
9.50	2.48	2.85	5.33	0.17	1.65	0.18	3.57	0.00	4.16	0.09
5.87	18.26	16.80	1.53	2.08	11.75	1.36	2.14	1.30	13.45	1.34
0.88	0.35	0.54	1.48	0.23	0.60	0.21	0.98	0.02	0.50	0.14
1.13	0.86	0.92	1.74	1.42	1.80	1.40	2.92	1.47	1.17	1.31
22.79	18.26	18.66	23.46	36.58	21.88	36.90	21.66	33.11	19.96	35.86
0.30	0.30	0.18	0.01	0.10	0.38	0.01	0.04	0.15	0.35	0.10
0.46	1.31	1.57	0.02	0.22	0.76	0.12	0.03	1.26	1.32	0.56
0.06	0.02	0.03	0.04	0.02	0.03	0.03	0.06	0.03	0.03	0.03
0.01	1.96	2.48	0.01	0.15	1.95	0.10	0.04	0.37	1.81	0.21
0.12	0.35	0.22	0.06	0.00	0.22	0.02	0.13	0.02	0.21	0.18
0.02	0.03	0.03	0.01	0.04	0.03	0.06	0.04	0.04	0.03	0.03
0.15	0.64	0.66	0.38	9.53	1.23	10.18	1.06	8.44	0.79	9.32
24.05	23.25	22.32	13.78	0	21.84	0	3.31	0	23.26	0
82.68	81.20	81.94	69.98	47.08	81.54	54.32	58.58	56.56	82.95	55.72
17.32	17.70	17.05	30.02	42.92	18.46	45.68	41.42	43.44	17.05	44.28
21	61	57	21	279	109	225	16	361	69	302.3
13 (60)	0 (50)	0 (40)	20 (60)	9 (40)	0 (40)	13 (40)	16 (60)	12 (50)	3	12
20	0	0	6	2	0	0	6	0	5	1
64	238	298	37	4	190	7	27	7	183	5
3	8	2	2	1	4	1	2	1	4	1
32	605	699	4	37	84	28	7	58	442	31
20	33	32	14	4	26	4	16	7	31	4
300	400	300	200	70	400	30	100	5	340	28 (?)
7	4	3	30	3	4	3	15	7	5	4
0	70	5	0	0	60	0	0	0	87	0
5	5	3	4	2	2	3	4	3	5	3
950	660	780	200	100 (?)	620	30 (?)	310	<20	802	33 (?)
10	130	75	10	10	50	5	30	15	66	1
2,001	924	904	649	0	1,732	0	1,403	0	1,119	0
88	54	69	58	20	35	31	56	30	72	27
59	738	1,140	11	45	523	100	25	17	666	46
183	165	189	170	82	258	140	264	8	172	58
100	530	480	100	<50	240	<50	<50	<50	690	<50
200	40	50	150	3	200	0	600	3	98	1
3.5117	3.2988	3.4620	3.5368	2.8973	3.4285	2.8491	2.9431	2.7586	3.4672	2.8108

silicate rocks + wrigglite skarn, whole rock; 12, SMD 12, −99.13 to −99.20 m, wrigglite skarn, whole rock; 13, SMD 12, −97.5 to −97.59 m, wrigglite skarn, whole rock; 14, SMD 12, −96.19 to −96.28 m, calc-silicate rock, whole rock; 15, SMD 12, −93.00 to −93.09 m, unreplaced marble, whole rock; 16, SMD 12, −93.00 to −93.09 m, wrigglite skarn replacement of (15), whole rock; 17, SMD 12, −92.00 to −92.12 m, unreplaced marble, whole rock; 18, SMD 12, − 92.00 to −92.12 m, calc-silicate replacement of (17), whole rock; 19, SMD 12, −83.32 to −83.48 m marble, whole rock; 20, average wrigglite skarn (this table); 21, average marble (this table).

a lesser extent Be, show a decreasing concentration trend with depth in traverse 1 but not traverse 2. The values from group 2, namely Mo, Cu, and Zn, are erratic throughout. This is interpreted to show that the sulfide-rich replacement, particularly common near the Bismuth Creek fault, is somewhat erratic and selective, relating to permeability present after the primary skarn crystallization.

In traverse 1, the average value of the concentration for each drill hole of the group 1 elements (F, Sn, and Be) as well as W, Mo, and Bi is approximately constant relative to their proximity to the Bismuth Creek fault. Cu shows a decrease while Zn shows an almost three-fold increase toward the fault. In traverse 2, where there are only three values per element, Zn increases to the west while Sn, F, Be, and Mo decrease. The data suggests that Zn is derived from the Bismuth Creek fault whereas the group 1 elements were derived from a more extensive plumbing system (east-west fracture systems incorporating

TABLE 5. Differences of Composition between Rocks and Their Unreplaced Equivalents

The values are in terms of molar differences per 100 cm^3 of rock analyzed. The molar values were calculated from Tables 2 and 4 using the density data.

	1	2	3	4	5	6	7	8	9	10	11	12
Si	0.0073	−0.4074	−0.0229	0.6639	−1.4261	−0.5768	2.7273	0.4974	0.8256	0.9587	1.4479	−7.5205
Ti	−0.0002	0.0007	0	−0.0039	0.0049	−0.0065	0.0170	0.0117	0.0032	0.0050	0.0199	−0.1105
Al	−0.0006	0.0891	0.0028	−0.1230	0.3034	0.0869	0.6806	0.2993	0.4969	0.5040	0.5270	−6.8172
Fe^{+3}	−0.0007	0.0089	0.0033	−0.0440	0.0077	0.0048	0.2924	0.1017	0.2577	0.0924	0.1790	−2.7357
Fe^{+2}	0.0903	0.0921	0.0106	−0.3699	−0.0102	0.0586	0.0967	0.1049	0.7674	0.6136	0.0435	−6.0764
Fe^{total}	0.0910	0.1010	0.0139	−0.4139	−0.0025	0.0634	0.3891	0.2066	1.0251	0.7060	0.2225	−8.8121
Mn	0.0027	0.0044	0.0012	−0.0223	0.0113	0.0013	0.0465	0.0329	0.0246	0.0251	0.0416	−0.4025
Mg	0.0016	0.0060	0.0019	−0.0298	0.3856	−0.2223	0.0480	0.0636	0.0153	0.0845	0.1894	−1.7957
Ca	0.0049	0.0516	−0.0022	−0.0867	0.6975	0.1939	−0.6870	−0.0175	−0.7881	−0.7728	−1.0327	5.4418
Na	−0.0650	−0.0599	−0.0522	1.7911	0.0100	0.0105	0.0512	0.2992	0.0406	0.0421	0.0039	−1.1623
K	−0.0097	0.0434	−0.0034	0.0083	1.0091	0.0581	−0.0158	0.2075	0.0770	0.0503	−0.0064	−4.4106
P	0	0	0.0001	−0.0011	−0.0082	−0.0096	0.0027	0.0013	0.0007	0.0017	0.0028	0.0125
S	0.0706	0.0209	0.0048	−0.1977	0.0018	−0.0008	−0.0159	−0.0668	0.1777	0.1948	−0.0053	−1.0659
H^+	0.0054	0.0101	0.0036	−0.0191	0.1849	0.3720	−0.2914	0.0564	0.2222	0.7543	0.3257	−1.5751
C	0.0351	0.0097	0.0038	−0.0592	0.0493	−0.0207	−2.0787	−0.7784	−1.9531	0.3415	−2.1550	20.9970
F	−0.0098	0.3569	0.0049	−0.4256	0.6526	1.4905	1.4679	0.3583	4.2445	3.9411	0.5127	−36.841

1, average of zone 4, average of zone 1, Table 2

2, average of zone 4, average of zone 2, Table 2

3, average of zone 4, average of zone 3, Table 2

4, molar gains and losses by the solution for the greisenized section; values are in moles/100 cm^3-meters; intersections of zones used are: zone 1, 1.75 m; zone 2, 1.05 m; zone 3, 10.87 m; and zone 4, 21.49 m

5, replacement of quartzite: veined quartzite (9, Table 4), pure quartzite (8, Table 4)

6, replacement of veined quartzite (3, Table 4), pure quartzite (8, Table 4); veined quartzite is shown in Figure 4A

7, replacement of silty sediment pyroxene skarn (5, Table 4), siltstone (2, table 4); pyroxene skarn is shown in Figure 4B

8, replacement of marble; calc-silicate skarn (7, Table 4), average marble (21, Table 4); calc-silicate skarn is shown in Figure 4B

9, replacement of marble; wrigglite skarn (20, Table 4), unreplaced average marble (21, Table 4)

10, replacement of marble; wrigglite skarn (16, Table 4), unreplaced adjacent marble (15, Table 4); see figure 5C for relation

11, replacement of marble; calc-silicate skarn (18, Table 4), unreplaced adjacent marble (17, Table 4); see Figure 4E for relation

12, molar proportions of elements lost to and gained from solutions while traversing and reacting in section (SMD 12); values are in moles/100 cm^3 m; thicknesses are: veined quartzite, 3.31 m; lower calc-silicate unit, 3.81 m; laminar skarn, 7.40 m; and upper calc-silicate unit, 0.97 m

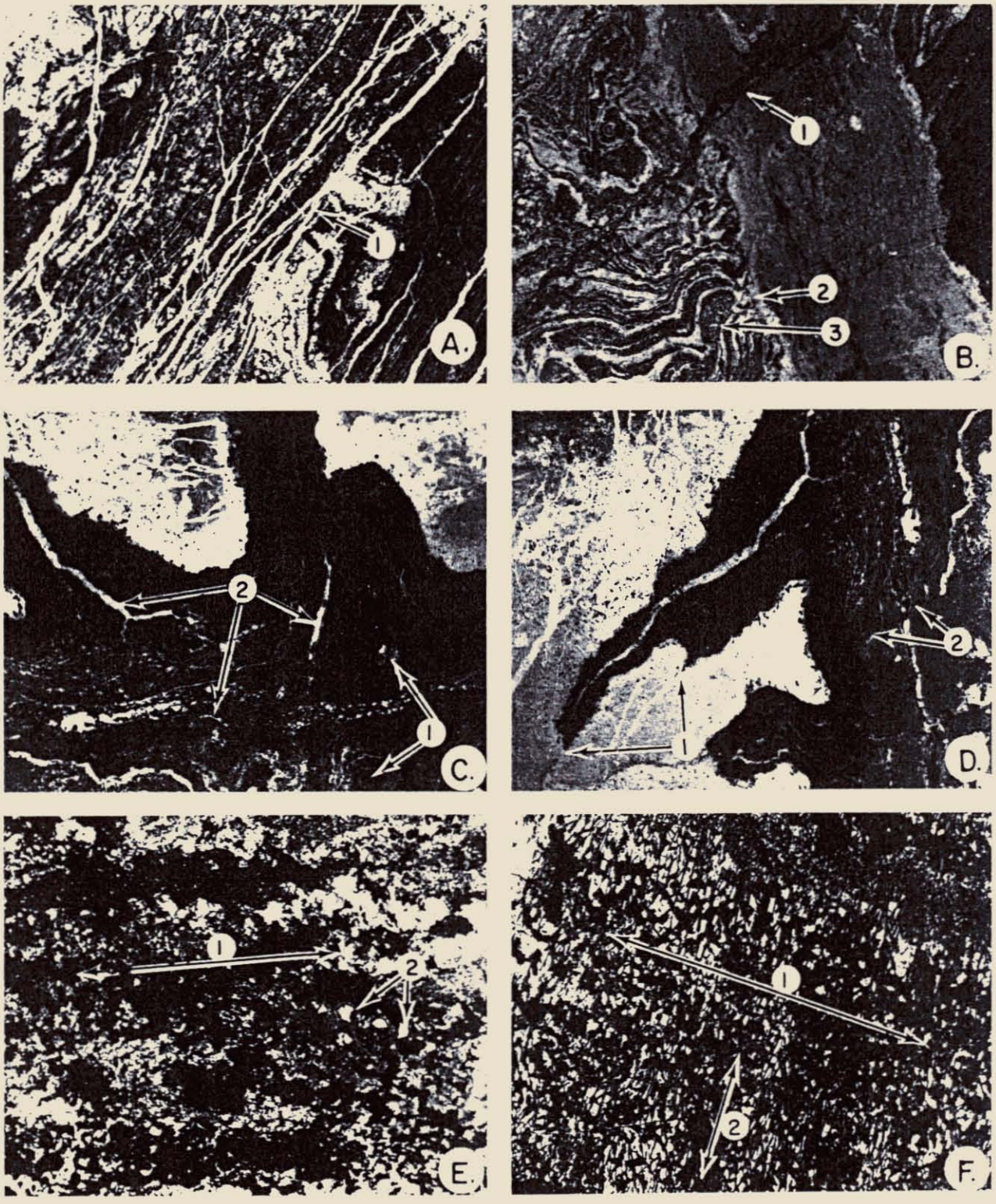

FIG. 5 Features of primary wrigglite skarn and secondary sulfide replacement.

A. SMD 5, -56 m, shows the extremely fractured "sheeted" appearance of wrigglite skarn and garnet skarn common near the skarn-quartzite contact. (1) shows a mineral-filled fracture. The field of view is 4 cm wide.

the quartz lodes?). This is consistent with the Bismuth Creek fault being active after as well as during wrigglite skarn deposition.

The Occurrence of Elements of Economic Importance in the Skarns

At Moina, Sn occurs in a number of ways, namely, in solid solution in garnet (to 0.70 wt %), in Sn sphene, and as cassiterite. AMDEL (1978) regarded the tin content partly as a solid solution in garnet (45%) and also as cassiterite of very fine grain size (55%). Green (1979) has shown that at Moina, cassiterite occurs as laminar inclusions of 1.5 to 5 μm long in garnet. These were not found by the present authors although cassiterite grains to 15 μm in size were observed in the magnetite-rich layers in the wrigglite skarn. No distinct Be mineral such as helvite was found and Be is presumed to occur in vesuvianite. Beus (1966, p. 144) found Be values in vesuvianite up to 9.20 weight percent and in garnet, 0.39. W is in scheelite in the skarn fabric and in wolframite plus scheelite in veins; no significant values of W in any of the other minerals was found. F is mainly in fluorite (>90%) with topaz + F-micas in veins; similarly, Bi is in bismuthinite, Mo in molybdenite, Cu in chalcopyrite, and Cd and In in sphalerite. Au may occur as a solid solution in bismuthinite, as the correlation data suggest, or simply as free gold.

Fluid Inclusions

Primary fluid inclusions in the skarn minerals were not found, reflecting their fine-grained nature, whereas measureable inclusions occur only sparingly in vein minerals. Fluid inclusions should represent those present during skarn genesis because the mineralogy of the veins is similar to that of the skarn; the intersecting nature of successive periods of vein deposition suggests cogenesis (Fig. 3). In quartz (SMD 12 at 155 m), liquid CO_2 is a common but not constant constituent (Fig. 8B, E, and F). The daughter products are NaCl (D_1) and fluorite (D_2) as confirmed by SEM analyses, with a rare reddish opaque which is possibly hematite (Fig. 8D) and a number of minute grains of unidentified nonopaque daughter products. Homogenization temperatures were 331° ± 12°C (average of 12; gas dissolved into the liquid phase in seven cases and liquid into gas in five). This variation, together with the fact that gas-rich and saline liquid-rich inclusions occur together (Fig. 8H), suggests the inclusions were trapped from a boiling solution. NaCl dissolved before the homogenization temperature was reached while CaF_2 did not, perhaps due to slow kinetics. The first melting of previously frozen inclusions gave temperatures of −23.1° ± 0.4°C (average of six) and the last melting of ice, −15.3° ± 2.2°C (average of six).

Fluid inclusions in fluorite in a fluorite-rich vein (SMD 16 at 43.9 m depth) contain no liquid CO_2. Homogenization temperatures of the commonly five-phase inclusions are 482.8° ± 9.2°C (average of eight; three homogenized into gas, five into liquid), with a first melting temperature of −19.5° ± 3.0°C (average of eight) and a last melting of −7.0° ± 1.5°C (average of eight). Fluid inclusions in topaz in a cassiterite-wolframite-bismuthinite quartz vein (stratigraphically below the skarn, reference points 1700E, 100S, Fig. 1A) contained no liquid CO_2 and generally two daughter products (Fig. 8G). Homogenization was at 416° ± 5.2°C (average of 10; eight dissolved into liquid, two into gas), with a first melting temperature of −15.0° ± 1.5°C (average of seven) and a last melting of −6.4° ± 0.8°C (average of seven). The pressure correction for the homogenization temperatures is unknown but is probably small as the deposit was likely formed at near-surface conditions.

On the basis of the limited data available, the following conclusions are drawn: the homogenization of fluid inclusions constituents into both the liquid and the gas phase, with the large variation of ratios ob-

B. SMD 12, -101.28 m, showing the interface (2) between wrigglite and pyroxene skarn. (3) shows a concentrically zoned wrigglite skarn area. (1) shows a fluorite-rich fracture which obviously has altered pyroxene skarn to a greater extent than wrigglite skarn. Field of view is 2 cm wide.

C. SMD 12, -80 m; wrigglite skarn replacement of marble. The central fractures (2) have been filled in by a variety of vein materials. (1) refers to augen-type features near the intersection of major fractures. Field of view is 3 cm wide.

D. SMD 12, -80 m, wrigglite skarn replacement of marble showing the parallel relationship between the original fracture and the lamination of the skarn. (2) shows the interface between amphibole-sulfide replacement area and unreplaced wrigglite skarn. Field of view 3 cm wide.

E. SMD 16, -65 m, transmitted light photomicrograph of layered sphalerite base metal sulfide skarn after garnet or wrigglite skarn. The lamination is parallel to (1). (2) shows garnet partly altered to hematite quartz. Field of view is 1 cm wide.

F. SMD 9, -97.2 m, transmitted light photomicrograph of pyrrhotite replacement of primary laminar skarn. Relict wrigglite skarn lamination is parallel to (1) whereas a later superimposed fabric is shown by (2). Field of view is 1 cm wide.

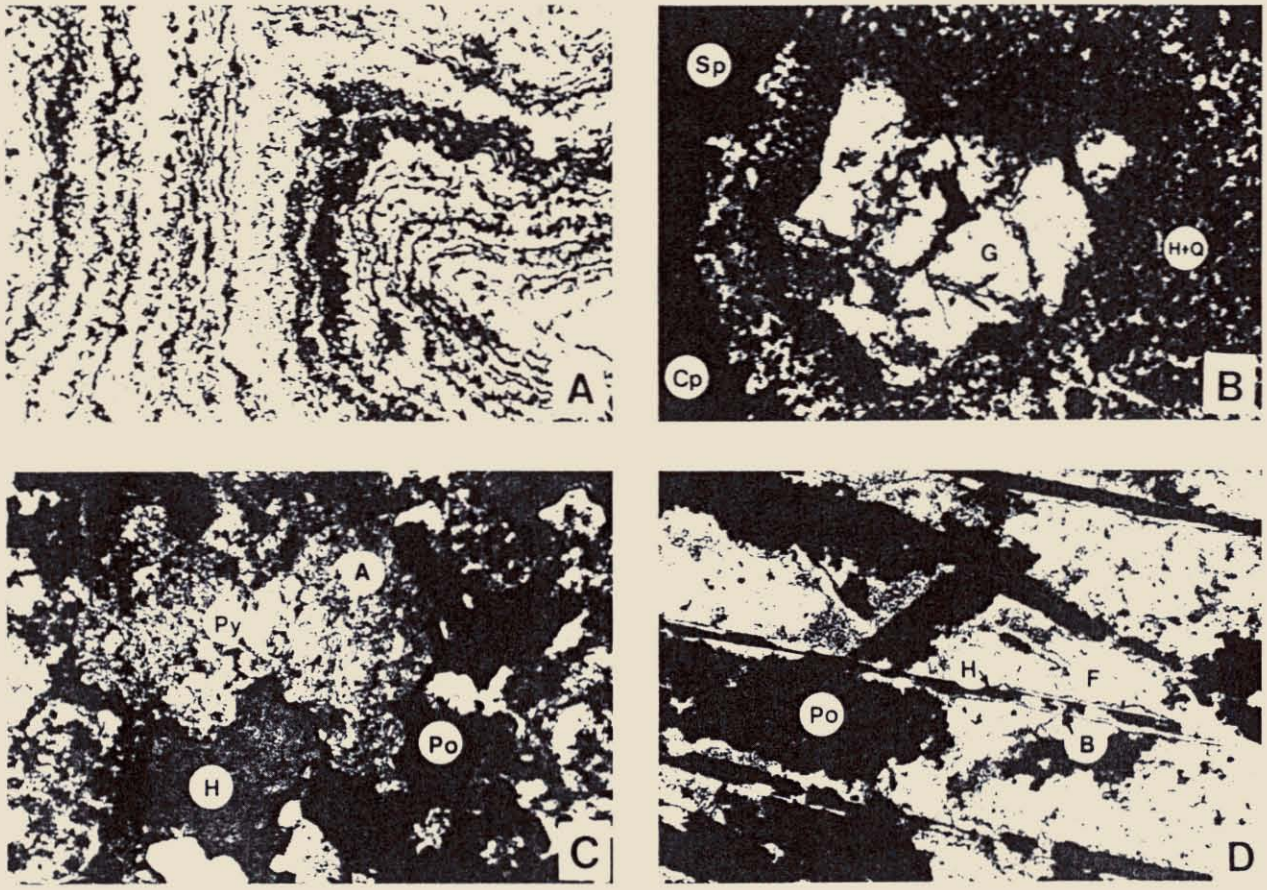

FIG. 6. Textures in primary wrigglite skarn and replacement of this skarn.

A. Typical wrigglite skarn showing that the dark (magnetite ± cassiterite) lamellae are not continuous. The apparent foldlike form is due to irregularities in permeability (see text for explanation); SMD 5, -46.5 m. Field of view is 0.9 cm wide.

B. Replacement of garnet (G) by hematite + quartz (H + Q) with sphalerite (Sp) and chalcopyrite (Cp). Enlargement of replacement feature in Figure 5E; SMD 16, -65 m. Field of view is approximately 1 mm wide.

C. Replacement of pyroxene (Py) by amphibole (A) with associated hematite (H) and pyrrhotite (Po). Field of view is approximately 1.1 mm wide; SMD 16, -65 m. Some of the light areas are fluorite.

D. Replacement of wrigglite skarn by pyrrhotite (Po) with fluorite (F) retained. Enlargement of a part of Figure 5F, SMD 9, -97.2 m. A later fabric consisting of hematite plates (H) with marginal F annite (B) has been superimposed upon the already replaced laminar skarn. This suggests hematite is a postsulfide replacement. Field of view is approximately 1 cm wide.

served, implies that boiling the hydrothermal solutions occurred at some time during genesis, and salinities were high (≥30–40 equiv. wt % NaCl). The major constituents in the fluid phase are NaCl, (KCl?), H_2O, and CO_2. Some CaF_2 occurs either as a daughter product or as accidental crystals. The first melting temperatures near −20°C confirm that NaCl (+KCl?) is the major salt present and that $CaCl_2$ is not present. Systems involving the latter salt show first melting temperatures near −52°C (the ternary eutectic in the system $CaCl_2$-NaCl-H_2O).

Sulfur Isotopes

Table 8 shows sulfur isotope values from the Moina area done by Dr. Shen-Su Sun of the Division of Mineralogy, CSIRO. These values are relative to the Cañyon Diablo standard and the analytical uncertainity is believed to be better than 0.2 per mil. As can be seen sulfides from wrigglite, pyrrhotite-rich (amphibole), pyrite-rich (amphibole), and sphalerite-rich skarns have similar sulfur isotopic values (8.4 to 9.3‰) to those of pyrite in the greisenized granite

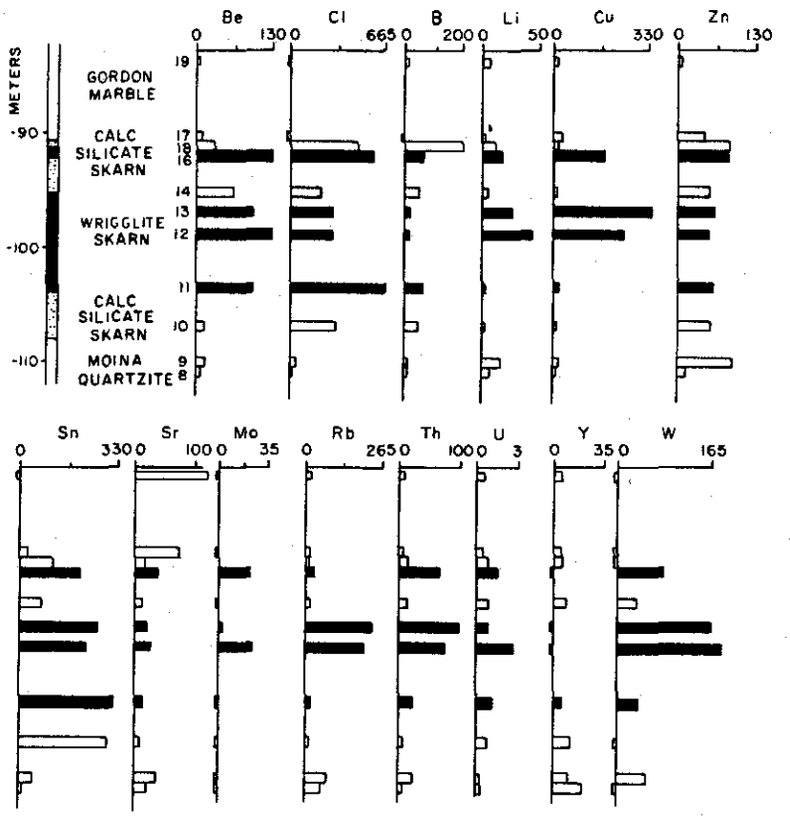

FIG. 7. Histograms of chemical variations through the quartzite-skarn-limestone section of SMD 12 (see Fig. 1A for location). The numbers 8 to 19 refer to the analyses in Table 4. The values are in moles per 100 cm^3 of rock (to account for density differences). The dark bars to the right of the vertical line refer to wrigglite skarn composition values. Values shown to the left of the vertical line indicate that the analysis yielded no values of the element.

(8.9‰). Pyrrhotite from SMD 14 (at 38 m depth below the collar) limestone and framboidal pyrite from the Moina sandstone have negative values (−4.2 and −6.9‰, respectively). Pyrite from metasomatized sandstone (SMD 18 at 102.5 m depth) and pyrite and pyrhotite from the margin of the skarn (Moina) have intermediate values (≃4.5‰).

Sulfur isotope $\delta^{34}S$ values of hydrothermal fluid can be as much as 4 per mil larger that the $\delta^{34}S$ melt if the volume ratio fluid to melt is small (Ohmoto and Rye, 1979, p. 527). Average $\delta^{34}S$ values of silicic igneous rocks of as high as 10 ± 5 per mil have been suggested (Holser and Kaplan, 1966), and individual values as high as 30 per mil have been recorded (Shima et al., 1963). Presently accepted values, however, are approximately 0 ± 3 per mil (Ohmoto and Rye, 1979, p. 524).

The greisenized granite and skarn values (≃9‰) have a sulfur source which is quite constant but is unlikely to be purely magmatic in origin. Coexisting pyrrhotite-pyrite pairs in SMD 9 (−102.50 m) and Moina 13 have similar values. On the basis of sulfur fractionation thermometers (Ohmoto and Rye, 1979, p. 518), this would suggest they crystallized at very high temperatures (>700°C), which is geologically unlikely, or they did not coexist stably (not formed at the same time). The latter explanation is most likely on textural evidence. Sulfur isotope values are known for the Renison Bell Sn replacement body (Patterson and Ohmoto, 1976). Here, $\delta^{34}S$ values of pyrrhotite in the ores are near 6.5 per mil and the primary (?) sulfide in the associated granite have $\delta^{34}S$ values near 3.5 per mil. Patterson and Ohmoto (1976) interpreted this to mean the sulfur has a magmatic source.

Discussion

Origin of wrigglite skarn at Moina and elsewhere

Fluorite-rich wrigglite skarns are known from many other localities including: Dragoon Mountains,

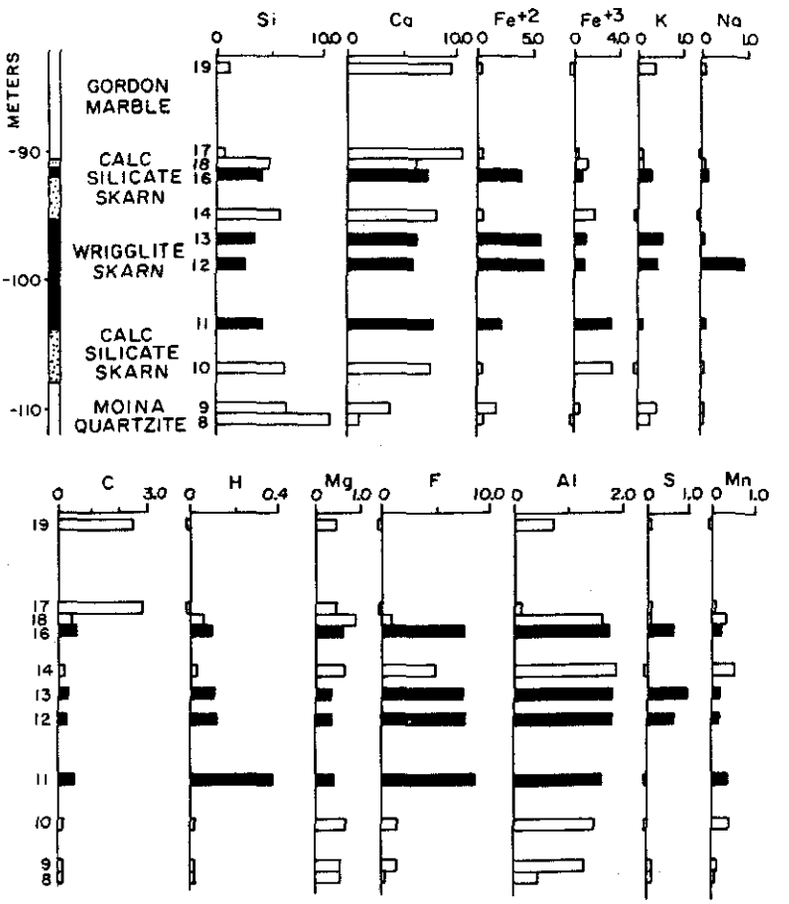

FIG. 7 (cont.).

Arizona, (Perry, 1964); Iron Mountain, New Mexico (Jahns, 1944b); Lost River, Alaska (Knopf, 1908; Sainsbury, 1964, 1969); south China (Meng, 1937; Hsieh, 1963; Beus, 1966); Chugako, Japan (Miyake, 1965); Kazakhstan, USSR (Beus, 1966; Zasedatelev, 1973; Ermilova and Senderova, 1959); Iten' Yrginsk, Chukotka, USSR (Shcherba, 1970; Getmanskaya, 1972); various other deposits in the Far Eastern Province, USSR (Govorov, 1958); Dal'negorsk, Primor'ye, USSR (Aleksandrov, 1975); Kristiana, Norway (Twelvetrees, 1913); Mt. Garnet, Queenland (Askins, 1976); and Mt. Bischoff, Tasmania (observed by one of us—P.W.A.). They are related to leucogranite plutons or dikes exhibiting greisenization and are usually found in Paleozoic limestone terrains (Govorov, 1968). There is invariably intense fracturing and faulting and, at least in some cases, boiling of the hydrothermal solutions can be demonstrated (evidence from the study of W. Brown at Mt. Garnet, pers. commun., 1979; at Moina and Mt. Bischoff, P. Collins, pers. commun., 1979). The primary skarn is enriched in F, Fe, Sn, W, Be, Li, B, and Bi whereas secondary alteration commonly produces skarn rich in Zn, S, Pb, and Cu (e.g., at Mt. Garnet, Askins, 1976; Dal'negorsk, Aleksandrov, 1975; and at Moina). Anomalously high values of such elements as B, In, Cd, and Li may occur (Sainsbury, 1969).

Bulk chemical analyses of wrigglite skarn by Zasedatelev (1973), Miroshnchenko and Gulyayev (1978), Waite (1978); Sainsbury (1969), and the present authors indicate that when the fluorine content is less than about 9 weight percent the wrigglite structure does not form and granular skarn forms instead. In a cuspidine wrigglite skarn from Mt. Garnet (Askins, 1976), the lamination is indistinct and F $\simeq$ 9.0 weight percent.

Wrigglite skarn is fine grained, has a contorted structure, and is commonly associated with coarser grained, F-poor, granular skarn. Individual lamellae, which contain restricted mineral assemblages, pinch and swell and may contain crosscutting septalike veinlets of magnetite (at Moina) or tourmaline (at

TABLE 6. Correlation Coefficients of Elemental Abundances of Elements Relative to Others

	Pb	W	Bi	Sn	Mo	Cu	Zn	Be	F	Sc	Y	Cd	In	Ge	Au	Ag
Pb		−0.22	0.27	−0.11	0.09	0.30	0.41	−0.20	−0.21	−0.02	−0.24	0.21	0.34	0.26	0.56	−0.12
W	262		0.13	0.00	0.06	0.14	−0.01	0.18	0.15	0.03	−0.00	−0.35	−0.13	0.58	−0.01	−0.32
Bi	263	344		0.08	−0.11	0.30	0.28	0.13	0.15	−0.09	−0.27	0.33	0.47	0.49	0.80	0.25
Sn	285	401	364		0.59	−0.05	−0.16	0.32	0.20	−0.49	−0.56	−0.06	0.06	0.16	−0.18	−0.03
Mo	229	313	305	321		−0.05	−0.05	0.06	−0.03	0.07	0.08	−0.63	−0.30	0.39	−0.12	−0.24
Cu	278	265	260	282	228		0.62	−0.09	−0.06	−0.11	−0.16	0.77	0.54	−0.05	0.45	0.22
Zn	290	324	324	347	284	287		−0.22	−0.13	−0.05	−0.09	0.99	0.74	0.04	0.71	0.01
Be	284	359	358	382	316	281	346		0.26	−0.11	−0.11	0.06	−0.04	0.40	−0.26	0.39
F	287	364	364	387	321	284	349	384		−0.46	−0.47	−0.41	−0.16	0.33	−0.24	0.44
Sc	56	130	132	145	109	57	109	50	148		0.71	−0.14	−0.00	0.41	−0.13	0.00
Y	56	125	127	140	104	57	105	145	143	144		−0.00	−0.03	0.10	−0.34	0.00
Cd	20	8	18	20	6	20	20	20	20	20	20		0.74	−0.05	0.46	0.00
In	41	25	33	40	16	42	42	42	41	42	42	18		0.25	0.39	0.00
Ge	19	13	17	19	8	19	19	19	19	19	19	8	15		0.17	−0.15
Au	93	80	85	96	73	90	96	90	96	46	46	18	35	18		
Ag	25	20	24	25	23	17	25	19	24	0	0	0	0	0	20	

The upper right hand part of the table gives the correlation coefficients between elements and the lower left hand part gives the number of pairs used. When the concentration of an element was zero, the value was not used for correlation. The program used was written by Ms. Judy Hannah of the Department of Geology, University of California, Davis, California. The program fits the data to a linear function and calculates correlation coefficients.

TABLE 7. Correlation Coefficients of Elemental Abundance of Economically Important Elements in Weight Percent vs. Depth in the Skarn Profile

Also given are the range of values and the average value for each drill hole. All rock types that contain mineralization are included, of which wrigglite skarn predominates.

Traverse 1	W	Bi	Sn	Mo	Cu	Zn	Be	F
DDH 4 (32 analyses each)								
Cor. coef.	−0.214	−0.678	−0.755	−.026	−0.249	−0.362	−0.650	−0.751
Range	70–2,220	0–780	30–2,100	0–150	5.350	18–1,240	70–700	0.63–12.89
Average	744	305	1,178	43	117	130	266	5.86
DDH 11 (42 analyses each)								
Cor. coef.	0.162	−0.678	−0.357	0.301	0.165	−0.027	−0.411	−0.535
Range	50–6,500	8–820	620–2,950	0–370	10–350	30–450	70–500	2.91–12.41
Average	1,040	402	1,490	50	120	116	252	7.98
DDH 6 (70 analyses each)								
Cor. coef.	−0.073	−0.266	−0.372	0.380	−0.234	0.133	−0.036	−0.587
Range	55–4,600	0–2,100	46–5,000	0–360	5–190	45–4,550	70–600	1.51–14.60
Average	879	430	1,302	62	45	216	2.44	7.74
DDH 15 (41 analyses each)								
Cor. coef.	0.171	−0.680	−0.672	0.355	ND	ND	−0.391	−0.699
Range	45–3,650	0–700	60–3,600	0–150	ND	ND	80–500	0.73–12.41
Average	1,092	403	1,321	43	ND	ND	256	7.88
DDH 7 (60 analyses each)								
Cor. coef.	−0.193	−0.305	−0.780	0.104	−0.232	−0.200	−0.264	−0.268
Range	95–3,400	0–2,050	180–2,750	0–290	2–440	55–9,800	80–300	1.31–14.07
Average	878	391	1,169	47	46	366	200	8.17
Traverse 2								
DDG ML-3 (38 analyses each)								
Cor. coef.	0.307	0.364	−0.481	−0.209	−0.078	0.000	−0.532	−0.432
Range	0–1,400	0–1,060	1–8,200	0–2,075	0–910	10–435	1–370	0–15.00
Average	317	259	2,223	245	64	147	180	6.69
DDH 16 (53 analyses each)								
Cor. coef.	−0.018	0.049	−0.059	0.052	ND	−0.096	0.292	0.120
Range	15–6,500	20–2,000	190–2,650	0–200	ND	55–154,000	50–5,000	0.34–12.05
Average	728	416	933	42	ND	11,852	160	5.14
DDH 13 (57 analyses each)								
Cor. coef.	0.213	−0.180	−0.361	0.434	−0.228	−0.082	0.312	0.244
Range	0–1,850	0–2,100	8–720	0–34	2–910	42–275,000	2–1,000	0.01–5.60
Average	69	266	299	9	151	24,182	81	0.60

The samples represent analyses of split core of 1 m length, in most cases. The positions of the drill holes are shown in Figure 1A. W, Bi, Sn, Mo, Cu, Zn, and Be are in terms of ppm while F is in terms of weight percent. Values of Pb, Sc, Y, Cd, In, Ge, Au, and Ag are not included because they are only minor constituents of the skarn. Their ranges in ppm are Pb (0–110), Sc (0–20), Y (0–70), Cd (0–1340), In (0–90), Ge (0–5), Au (0–4.5), and Ag (0–2).

Lost River). The following mineral assemblages, occurring in the alternating dark and light lamellae, respectively, were observed by the authors in skarn(s) from different areas: (a) magnetite ± cassiterite: vesuvianite + fluorite (most common); (b) magnetite + cassiterite: adularia + vesuvianite + fluorite (rare, Moina); (c) magnetite ± cassiterite: hedenbergite + fluorite ± andradite (rare, Moina); (d) f annite + magnetite: fluorite (rare Mt. Garnet); (e) magnetite rimmed by gahnite: f cuspidine + vesuvianite + fluorite (rare, Mt. Garnet); (f) pyrrhotite + cassiterite ± stannite: F biotite + F-Na tourmaline + fluorite + sellaite (rare, Mt. Bischoff); and (g) chrysoberyl + F margarite + F-Na tourmaline: fluorite + F margarite (Lost River).

Other common minerals are: helvite, danalite, hematite, spinel, lithian mica, and Ca-rich plagioclase (Govorov, 1968; Shabynin, 1977). Wrigglite-like skarn consisting of alternating magnetite and garnet has been recorded from the Kearney mine, Hanover, New Mexico (D. M. Burt, pers. comm., 1979).

Different authors believe that wrigglite skarns rep-

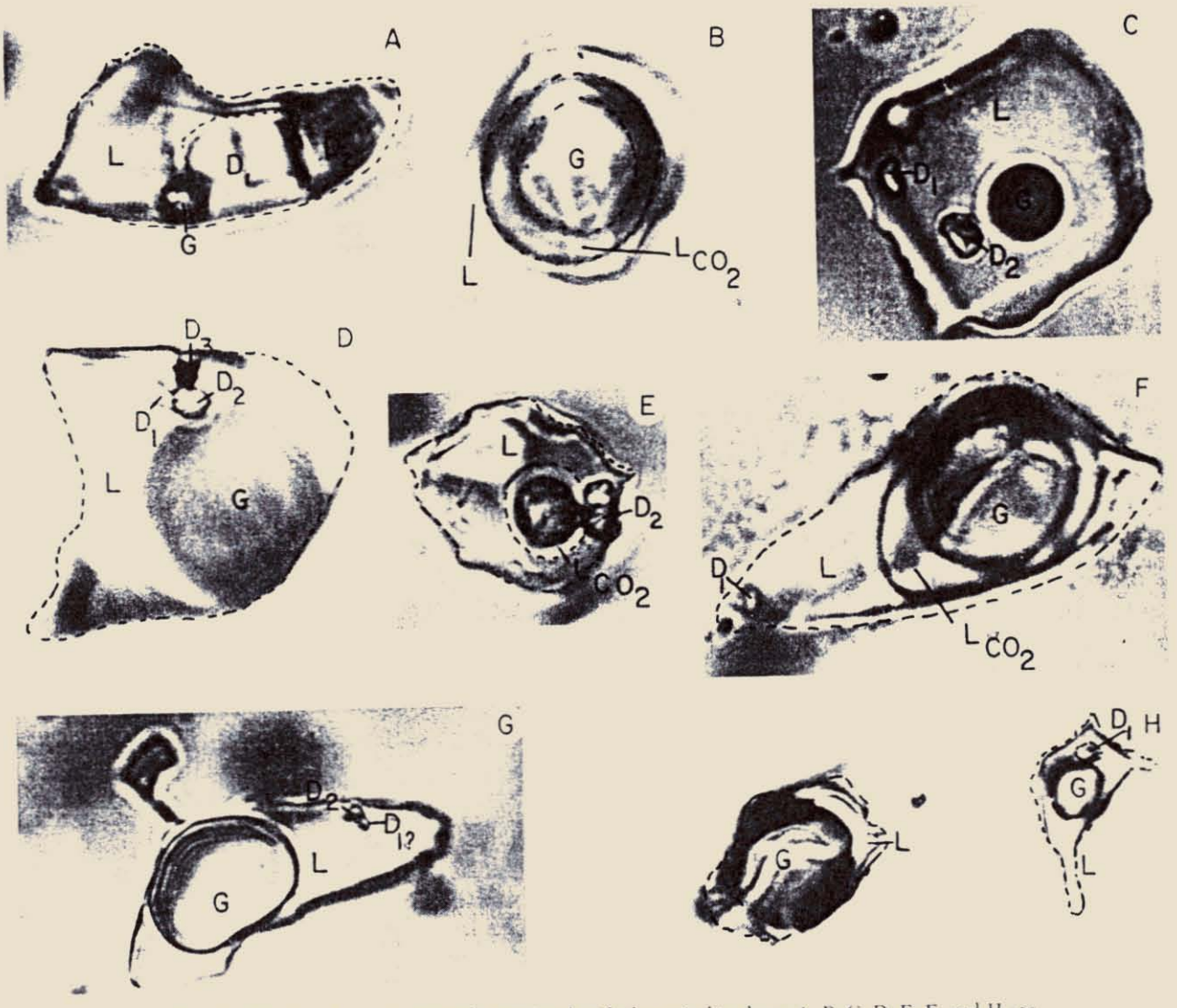

FIG. 8. Fluid inclusions in minerals associated with the wrigglite skarn. A, B, C, D, E, F, and H are from a quartz (-cassiterite-fluorite) vein in SMD 12 at 155 m. Note the liquid CO_2 (L_{CO_2}) daughter products (D), gas (G), and liquid (L). D_1 = NaCl, D_2 = fluorite, and D_3 = probably hematite. The coexisting gas-rich and liquid-rich fluid inclusions (H) have been interpreted to indicate that boiling occurred during trapping. G shows a highly saline fluid inclusion in topaz (described in text). All the fluid inclusions are generally 15 to 30 microns wide.

resent: (1) bedding in an unusual sediment (Zasedatelev, 1973), (2) replacement of fine bedding and/or stromatolites (P. W. Stainton, pers. commun.), (3) colloform, solidified gel precipitates (as in Stevenson and Jeffery, 1964), (4) rhythmical deposition in cavities (Trustedt, 1907), and (5) deposition by replacement at diffusion fronts moving outward from fractures (Knopf, 1908; Jahns, 1944a; Eskola, 1951; Beus, 1966; Sainsbury, 1969; Georgievskaya, 1955; Shabynin, 1977).

In Zasedatelev's model, wrigglite skarn is formed as chemical sediment in small, strongly evaporated basins, the unusual components (F, Be, Sn, W, etc.) being attributed to thermal springs of volcanic association. The rhythmic layering is a possible seasonal effect and chemical deposition is a colloidal precipitate producing colloformlike textures. Diagenesis, regional metamorphism, and finally contact metamorphism by a granite caused recrystallization of the sediment to its present mineralogical composition. The evidence against such an origin is strong. The laminations consist of folded, commonly pipelike

TABLE 8. Sulfur Isotope (δ^{34}) Values Relative to Meteoric Sulfur

The sample numbers refer to drill holes and depth shown in Figure 1A. The depths are in meters down from the collar of the drill hole. Numbers such as Pait, Moina 11, 12 refer to specific surface samples collected. The analyses were performed by Dr. Shen-Su-Sun, CSIRO Laboratories, North Ryde, N.S.W.

Drill hole and distance of sample down hole	Rock	Mineral	Value $\delta^{34}S$	Remarks
ML-1, 237 m	greisenized granite	pyrite	8.9	top of cupola is at 279 m
SMD 18, 102.50 m	metasomatized impure sandstone	pyrite	4.5	between wrigglite skarn and granite
Pait, Moina 11, 12	wrigglite	pyrite	8.8, 9.1	surface sample from near mill site, Shepherd and Murphy Mine
SMD 9, 102.50 m	pyrrhotite-rich skarn	pyrrhotite	8.6	pyrrhotite after magnetite wrigglite
		pyrite	8.4	
SMD 14, 38 m	fine-grained dark dolomitic interbed in limestone	pyrrhotite	−4.1	above wrigglite, unaltered or metamorphosed
SMD 13, 93.50 m	sphalerite-rich skarn	sphalerite	9.3	sulfide-replaced wrigglite?
		pyrite	8.4	on NE side of Bismuth fault
Surface sample	fine-grained dolomitic layer in limestone	pyrrotite	4.4	1.5 km from skarn
		pyrite	4.6	
Pait, Moina 10	pyrite-rich skarn	pyrite	9.1	1.5 km from Moina skarn
Pait, Moina 7	framboidal pyrite, Moina sandstone	pyrite	−6.9	5 km from skarn

shapes which are not geometrically equivalent to folds in sedimentary bedding. The early stages of wrigglite skarn formation can clearly be demonstrated to be a replacement of preexisting limestone along fractures (Fig. 5C and D).

Superficially many wrigglite skarns appear to be a very selective specialized replacement of stromatolite layering (model 2). However, no stromatolites exist in the unreplaced carbonate host rocks known to the authors and in any case replacement demonstrably takes place outward from fractures, not specifically along a preexisting layering.

In model 3, limestone is progressively dissolved by acidic fluoride solutions and at the same time iron hydroxide and fluorite form as a gel precipitate, separating out by mutual attraction into separate layers as replacement proceeds. The gel crumples as replacement of the limestone proceeds irregularly, and the gel slowly ages to the present texture and mineralogy. Various similar processes have been proposed by Stevenson and Jeffery (1964), Boydell (1925) (quoted in Lovering, 1962), and Garrels and Dreyer (1952), for replacement of limestone by magnetite or sulfides. The model does explain the colloformlike texture of wrigglite skarn. However, Roedder (1968) demonstrated that colloformlike textures do not necessarily indicate that colloids have been present. Continuous layers in a gel when deformed would produce concentric folded shapes, not the reentrant angles commonly observed, and the volumetrically significant shrinkage cracks that occur in real gels are not observed in the lamination. If a gel intermediate stage existed on a large scale, the rock would have little strength and would be structurally unstable.

The model proposing that wrigglite skarns are crustiform precipitates in cavities (model 4) was first favored by Trustedt (1907). Presumably acid fluids infiltrate through limestone channels and produce fissurelike and pipelike openings. In the forward zone of the advancing front of fluids, the fluid passing by a given point is neutral to alkaline, and fluorite and magnetite (etc.) begin to precipitate. Slight fluctuations in the pH of the fluid cause the rhythmic layering until the cavity is filled or nearly filled. Crustiform layers necessarily build up from the walls of a cavity and are parallel to the walls. However, at Lost River and Moina, delicate argillaceous beds are preserved in wrigglite skarn whose layering is continuous on either side of the bed (Fig. 4C; and Sainsbury, 1969) suggesting that cavities could not have been present.

In model 5, fluids infiltrate along areas of high permeability while the components in the fluid replace and diffuse into the marble due to activity (and concentration) gradients. Wrigglite skarn forms by replacement at diffusion fronts advancing from the highly permeable area until the effective limiting distance of diffusion from the fracture is reached or until the fluid infiltrating along the fracture is spent. There are irregularities in the advancing diffusion fronts caused by slightly differing rates of diffusion from one place to another resulting in local thickening

and thinning. This produces the irregular fold forms in the wrigglite skarn. The last phase in the process is the filling of the fracture itself, to produce a coarser grained central vein of fluorite and other minerals, or further infiltration occurs producing alteration of wrigglite skarn by fluid(s) of different composition.

The mechanism to explain the rhythmic nature of the skarn is probably that discovered by Leisegang (quoted in Knopf, 1908). If a drop of $AgNO_3$ is placed upon a gelatin plate impregnated with $K_2Cr_2O_7$, a series of concentric rings of $Ag_2Cr_2O_7$ forms. These become progressively more widely spaced with increasing distance from the center, although the widening of the rings outward does not take place if the concentration at the center is kept constant by a continuous influx of material (Watanabe, 1924b). Five theories to explain the phenomenon and about 600 papers have been produced, as summarized by Stern (1954). Stern concluded that Ostwald's 1897 explanation is the most satisfactory. He believed that dichromate ions diffuse inward as Ag ions move outward. The continued diffusion caused super saturation of $Ag_2Cr_2O_7$ and precipitation at a front normal to the diffusion direction. Just beyond the front there is a zone of low concentration of dichromate and here Ag diffuses outward through this zone until it reaches inward-diffusing dichromate and supersaturation occurs once more, forming a new ring. The process can take place in solids and even in water (e.g., Leisegang, 1931; Stern, 1954). Watanabe (1924a) conducted experiments on the diffusion of mixed zinc and iron sulfate solutions through a sodium sulfide-impregnated gel. He produced alternating ZnS and FeS rhythmic layers. One boundary condition is that if the solution contains much Zn^{+2} and less Fe^{+2}, no rhythmic layering occurs, presumably because FeS can only precipitate when Zn^{+2} is exhausted at the leading edge. This rhythmic layering was found to be metastable, with the system eventually reverting to a granular structure. This may also be true of wrigglite skarns.

Beus (1966) and Eskola (1951) have attempted to explain the mechanism in exact terms. Beus believes that the leading front of the acidic solution is partly neutralized by reaction with carbonate and Fe oxide precipitates. The solution, now containing F-Al-Si-Be-Sn, etc., diffuses through this Fe oxide layer and a layer of fluorite plus other calc-silicate minerals precipitates. A new front of solution diffuses through this couplet, a new couplet forms, and so on. Beus's model is questionable because it does not explain the origin of wrigglite skarn in which no Fe oxide phase is present, such as some that occur at Lost River, Alaska. It also offers no adequate explanation for the fact that wrigglite skarn does not generally form in skarns poor in F, where granular skarn forms.

The mechanism proposed here is that extreme supersaturation of one component is necessary so that minerals containing that component (usually F) nucleate rapidly. Because of the extreme supersaturation of F in the carbonate environment, many small crystals of F minerals from the first layer. When this supersaturated component is depleted in the solution, other elements diffuse or perculate through the first formed layer to form the next wrigglite consisting of other minerals.

In the examples studied, when the thickness of successive couplets reaches a critical thickness of between 1 mm and 5 cm, fracturing and replacement of unreplaced marble occurs. At both Moina and at Mt. Garnet this critical thickness is greatest nearest the contact with the granite and least nearest the marble. Repeated periods of fracturing and vein filling explain the sequential nature of the vein contents shown in Figure 3. By sequential fracturing and replacement the entire marble unit is replaced (Fig. 4C) or if repeated fracturing does not occur, unreplaced marble is retained (Fig. 5C and D). The fracturing is interpreted to be in response to clogging of the system when the constituents of the solution can no longer diffuse across the distance to unreplaced marble and instead precipitate in the fracture system. The pressure needed to cause the fracturing may be caused by development of a CO_2 overpressure due to reactions occurring elsewhere in the skarn and, possibly, due to a tectonic component. This hypothesis best explains why fracturing is most intense within and peripheral to the skarn unit but not nearer the granite at Moina. The augen-type features containing granular skarn (Fig. 5C) are believed to represent the replacement of embayed marble where the conditions necessary for wrigglite skarn growth were not met (slow, systematic loss of CO_2?).

The rhythmic nature of the lamination could be caused by a constant supply of new solution passing through the fracture system as described by Watanabe (1924a). Alternatively, it could be caused by periodic opening and closing of the system at the end of each period of couplet formation. Spent CO_2-rich fluid would be flushed out of the system and wrigglite skarn formation would proceed from new introduced fluid. The periodic loss of volatiles (CO_2) may be essential for wrigglite skarn genesis because some skarns do contain much fluorine with Ca-Si silicates but do not have a wrigglite structure. This needs more study.

A model for the genesis of the skarn, quartz veins, and greisen at Moina

The assertion that the skarn, Sn-quartz veins, and greisen are cogenetic is supported by their close spatial relations and unique chemistry. As is shown by

the relict granite fabric and relict mineralogy in the greisen, fine-grained granite crystallized first. Its mineralogy was K-feldspar, plagioclase, quartz, F annite, and fluorite. The anomalous mica composition suggests the granite crystallized from a high f_{F_2} melt having high Fe/Fe + Mg and/or f_{O_2}, and relatively high SiO_2. The aqueous phase which evolved could not have been greatly out of equilibrium with the granite and some other process was needed to produce the greisenization.

When the pluton developed a solid granite carapace and dense surrounding hornfels, evolving aqueous solutions from lower levels were partly trapped. Rupturing of the carapace either by tectonic or fluid overpressure decreased P_{fluid} from values of $P_{lithologic}$ or more to values near $P_{hydrostatic}$. Boiling occurred producing an acidic, volatile-rich (HF, HCl, H_2S, etc.) vapor phase and a basic saline aqueous phase. As such, the system resembles a (small) porphyry copper system. The vapor phase caused greisenization of the granite and hornfels and facilitated the transport of much F and associated elements.

At Moina and many other wrigglite skarn deposits, massive granular skarns commonly occur between granite and wrigglite skarn (Govorov, 1958). The granular skarns consist mainly of garnet, vesuvianite, magnetite, pyroxene, and some fluorite. The garnet may be Sn rich (0.70 wt % at Moina to 0.3 at Iron Mountain, Jahns, 1944b) whereas vesuvianite commonly is Be bearing (to 1.30 wt % at Iron Mountain, Jahns, 1944b). Sn values in granular skarn are commonly high (e.g., in SMD 12, this study; at Iron Mountain, Jahns, 1944b), indicating that associated granular skarn is genetically related to the F-Sn-Be-bearing mineralization. However, this granular skarn has invariably been cut and partly altered by fluorine-adularia (-scheelite) veins (i.e., see Fig. 4B of this study for Moina; p. 80 of Sainsbury, 1969 for Lost River; p. 59 of Jahns, 1944b, for Iron Mountain). The veins are interpreted to have been the conduits for solutions which replaced marble to form wrigglite skarn higher in the sequence. The interpretation suggested here is that the granular skarn and hornfels were produced cogenetically with the granite and that the processes of greisenization, alteration of granular skarn, and formation of wrigglite skarn are associated with later boiling of the solutions.

The alteration of primary wrigglite and calc-silicate skarn by Zn-Cu-S-Cd-In-Au (group 2) precipitating solutions has been reported elsewhere (e.g., Aleksandrov, 1975) and occurs at Moina. At Moina, a zonal arrangement occurs on a regional scale with wolframite-cassiterite and accessory molybdenite nearest the Dolcoath granite; cassiterite with accessory wolframite and bismuthinite farther out; and Bi-Au and Ag-Pb-Au(-Zn) mineralization at the outer edge (Jennings, 1965, p. 513). A similar zonation associated with Sn-F skarn has been reported by Miroshnechenko and Gulyayev (1978, p. 54). The replacement of group 1 elements by group 2 metals occur outward from the Bismuth Creek fault. The alteration is interpreted to have occurred during the time when the system telescoped inward near the end of the mineralizing episode, superimposing base metal mineralization on group 1 mineralization. That primary (group 1) mineralization occurred by way of multiple fractures and faults (see Fig. 1A, magnetics), best explains the relatively even concentration of Sn, F, and Be in different drill holes. These fractures were eventually sealed by the precipitation of Sn-W-quartz veins.

The local alteration of the skarn to a hematite-quartz assemblage may have postdated the sulfide replacement as suggested by textural evidence (Fig. 5F). Whether the crystallization of type 2 mica, found associated with hematite in the greisen, is associated with hematite crystallization in skarn is not known. Presumably these minerals could have been produced when cooler, mainly meteoric water circulated through the system near the end of the mineralizing episode. Laumontite, which occurs in fractures in the skarn, may also relate to this episode, or may have formed later. The unreplaced limestone and siltstone above and peripheral to the skarn are of low metamorphic grade because they contain epidote + tremolite and calcite + quartz assemblages (Fig. 4E). The skarns, however, represent higher grade metamorphism as is indicated by the assemblage wollastonite + garnet + pyroxene. This, with the unique composition of all the skarns, suggests the skarn forms a pocket of high-grade metamorphism superimposed on a lower grade environment. The hydrothermal solutions may thus be the main source of the heat for the high-grade metamorphism and the heat was not produced from outward-moving isograds in response to conductive heat gained by the rocks from the cooling pluton.

Relation to other Sn-F replacement deposits

The relation between Sn-bearing wrigglite skarn deposits and massive Sn sulfide replacement deposits such as the Renison-Bell (Patterson, et al., 1981), Mt. Bischoff (Orr, 1976; Groves et al., 1972), and Cleveland (Palmer, 1976) deposits of Tasmania is unclear. These examples are replacements of both dolomite and limestone, and the mineralogy includes cassiterite, fluorite, and pyrrhotite. In each case extensive faulting occurred. However, magnetite-bearing wrigglite skarns occur near granite contacts (<250 m) and the other sulfide Sn-F deposits occur farther away (>500 ms?). Parts of the Mt. Bischoff and part of the

Moina deposits (Fig. 5E) appear to be transitional in having the assemblage pyrrhotite + fluorite + F-biotite ± cassiterite and also in being wrigglite.

Limited fluid inclusion data indicates that wrigglite skarns are at least partly produced from a boiling, high-temperature, saline solution whereas the non-wrigglite Sn replacement deposits are produced from nonboiling, lower temperature, and less saline solutions. The data of Collins (1979) suggest that for fluid inclusions studied from the Renison Bell and Cleveland deposits, homogenization temperatures range from 250° to 430°C, salinities are 10 to 15 weight percent (NaCl equivalent), and no evidence of boiling occurs. At Mt. Bischoff boiling appears to have occurred (Collins, 1979) with homogenization temperatures near 530° to 510°C and with fluid inclusions containing cubes of sylvite and halite (therefore, >26 equiv. wt % NaCl). Similar data has been produced in this study and in a study of the Mt. Garnet wrigglite skarns (study in progress by W. Brown and T. A. P. Kwak).

The relative importance of dolomites versus limestones as hosts is unclear because wrigglite skarn forms in dolomites (e.g., at Pitkaranta, USSR, Trustedt, 1907; at Chukotka, USSR, Getmanskaya, 1972; at Mt. Bischoff) as well as limestones.

Although more study is clearly needed, the above data can be used to imply that when suitable carbonate horizons exist near a "Sn"-leucogranite (<250 m) with the required plumbing system (i.e., faults), the result is the precipitation of a magnetite-cassiterite-fluorite wrigglite skarn from a boiling, high-temperature saline solution. However, if the carbonate horizon occurs at great distances from the pluton (>700 m) and the required permeability exists (such as the mineralized Bassett Federal fault at the Renison Bell deposit) and there is a source of sulfur, a massive cassiterite-pyrrhotite-fluorite-stannite replacement body forms from a lower temperature, nonboiling, more dilute solution. This has important economic consequences because only the latter type contains cassiterite in a form and quantity that is economically recoverable under present conditions.

Acknowledgments

Permission to publish this paper has been given by Comalco Limited. Discussions with D. M. Burt, A. Waite, and D. Veblen were very helpful. The Australian Research Grants Committee is thanked for giving access to electron microprobe facilities at the University of Melbourne and D. Sewell and P. Kelley of that institution are thanked for their help with the analyses. K. Palmer is thanked for help with the bulk chemical analyses. J. Hannah of the University of California, Davis, is thanked for help with computational problems and last, but certainly not least, B. Taylor of the same institution is thanked both for much helpful discussion and for supplying some mineral analyses.

May 15, 1979; September 8, 1980

REFERENCES

Aleksandrov, S. M., 1975, The geochemistry of formation of skarns and ores in the crushed zones of carbonate rocks: Geochemistry Internat., v. 12, no. 5, p. 2–18.

AMDEL, 1978, Report on the distribution of tin in ores from Moina, Tasmania: Adelaide, AMDEL, Rept. R 745. 6 p.

Askins, P. W., 1975, "Wrigglite"—an unusual fluorite bearing skarn, Mt. Garnet region, North Queensland, Australia: Unpub. M.Sc. thesis, Cairns, Australia, James Cook Univ., 185 p.

—— 1978, "Wrigglite"—a fluorite rich skarn at Moina, Tasmania, and The Shepherd and Murphy Mine, *in* Geology and mineralization of N. W. Tasmania: Hobart, Geol. Soc. Australia Spec. Pub. p. 9–10.

Beus, A. A., 1966, Geochemistry of beryllium and genetic types of beryllium deposits: San Francisco, W. H. Freeman and Co., 401 p.

Boydell, H. C., 1925, The role of colloidal solutions in the formation of mineral deposits: Inst. Mining Metallurgy Trans., v. 34, sec. B, p. 145–337.

Collins, P. L. F., 1979, Fluid inclusions in cassiterite-sulphide metasomatic replacement deposits, *in* Kwak, T. A. P., ed., Fluid inclusion workshop notes, Study Group for Economic Geology, La Trobe University, Feb. 26–29: Melbourne, Geol. Soc. Australia, 85 p.

Ermilova, L. P., and Senderova, U. M., 1959, Strontianite from the West Kara-Ob deposit in central Kazakhstan: Materialy po geologii rudnykh mesotorozhdenii, petrografii mineralogii i geokhimii, Izdatel-stvo AN SST, p. 294–300.

Eskola, P., 1951, Around Pitkaranta: Soumalaisen Tiedeakatemian Toimituksia (Annales), ser. A., v. 3, no. 27, 90 p.

Garrels, R. M., and Dreyer, R. M., 1952, Mechanism of limestone replacement at low temperatures and pressures: Geol. Soc. America Bull., v. 63, p. 325–380.

Gee, C. E., 1966, The geology and mineral deposits of the Moina-Lorinna area: Unpub. B.Sc. Honours thesis, Univ. Tasmania, 132 p.

Georgievskaya, O. G., 1955, Genesis of the rhythmic-folded laminated texture of ore bodies of some contact-metasomatic deposits (K. vopruso o genezise vitmichno-vitievato-potoschatoi tekstury vudnykh tel nekotorhykh kontakto-metasomatischeskikh mestoroschdeneii) Akad. Nauk SSSR Doklady, v. 101, no. 5, p. 87–96.

Getmanskaya, T. I., 1972, Beryllium mineralization in a polymetallic ore district in Siberia: Internat. Geol. Rev., v. 14, p. 829–836.

Green, D. C., 1979, Moina "wrigglite": Tasmania Dept. Mines, unpub. rept. R.758, R.745, R.731, 5 p.

Govorov, M. M., 1968, Specific features of mineralogy and genesis of tin-beryllium-fluorite deposits of the Far East: Akad. Nauk SSSR Izv., Ser. Geol., no. 1, p. 62–73.

Groves, D. I., Martin, E. L., Mruchies, H., and Wellington, H. K., 1972, A century of tin mining at Mount Bischoff, 1871–1971: Tasmania Dept. Mines Geol. Survey Bull. 54, p. 3–10.

Holser, W. T., and Kaplan, I. R., 1966, Isotope geochemistry of sedimentary sulfates: Chem. Geology, v. 1, p. 93–135.

Hsieh, C. Y., 1963, A study of tin deposits in China: Scientia Sinica, v. 12, p. 373–390.

Jahns, R. H., 1944a, "Ribbon Rock," an unusual beryllium-bearing tactite: Econ. Geol., v. 39, p. 173–205.

—— 1944b, Beryllium and tungsten deposits of the Iron Mountains

district, Sierra and Socorro Counties, New Mexico: U. S. Geol. Survey, Bull. 945-L, 79 p.

Jennings, I. B., 1963, Middlesex, one mile geological series, explanatory report: Tasmania Geol. Survey, Expl. Rept., p. 512–514.

Jennings, I. B., 1965, Middlesex mineral district, *in* McAndrew, J., ed., Geology of Australian ore deposits: Melbourne, Australasian Inst. Mining Metallurgy, v. 1, p. 512–514.

Knopf, A., 1908, Geology of the Seward Penninsula tin deposits, Alaska: U. S. Geol. Survey Bull. 358, 71 p.

Leisegang, R. E., 1931, Colloid chemistry and geology, *in* Alexander, J., ed., Colloid chemistry, vol. 3: Cambridge, Chem. Category Co., 187 p.

Lovering, T. G., 1962, The origin of jasperoid in limestone: ECON. GEOL., v. 62, p. 861–889.

Mason, P. K., Frost, M. T., and Read, S. J. B., 1969, Computor programs for calculating corrections in quantitative X-ray mind-analysis: United Kingdom, Nat. Physics Lab., Div. Inorganic Metallic Structure, rept. 2, 45 p.

Meng, H. H., 1937, Tin deposits of China: Geol. Soc. China, Bull. 17, p. 439–449.

Miroshnchenko, L. A., and Gulyayev, A. P., 1978, Skarn-greisen metasomatism: Alma-Ata Nauka, Kazakstan SSR, 167 p.

Miyake, H., 1965, Study on genesis on skarns and the related minerals: Hiroshima Univ. Jour. Sci., ser. C., v. 4, p. 37–49.

Norrish, K., and Hutton, J. T., 1969, An accurate X-ray spectrographic method for the analysis of a wide range of geological samples: Geochim. et Cosmochim. Acta, v. 33, p. 431–453.

Ohmoto, H., and Rye, R. O., 1979, Isotopes of sulfur and carbon, *in* Barnes, H. L., ed., Geochemistry of hydrothermal ore deposits, 2nd ed.: New York, Wiley-Interscience, p. 509–567.

Orr, D., 1976, The Mt. Bischoff tin deposit: Internat. Geol. Cong., 25th, Sydney 1976, Excursion Guide 31AC, p. 19–23.

Palmer, K. C., 1976, The Cleveland tin deposit: Internat. Geol. Cong. 25th, Sydney 1976, Excursion Guide 31AC, p. 27–31.

Patterson, D. J., 1976, The Renison tin deposit: Internat. Geol. Cong., 25th, Sydney 1976, Excursion Guide 31AC, p. 37–39.

Perry, D. 1964, Genesis of the contact rocks at the Abril mine, Cochise Country, Arizona: Unpub. M.Sc. thesis, Univ. Arizona, 156 p.

Reid, K. O., 1971, Moina area: Queenstown, Mt. Lyell Mining Railway Co. Internal. memorandum E. L. 8/65, 52 p.

Roedder, E., 1968, The non-collodial origin of "colloform" textures in sphalerite ores: ECON. GEOL., v. 63, p. 451–471.

Sainsbury, C. L., 1964, Geology of the Lost River mine area, Alaska: U. S. Geol. Survey Bull. 1129, 80 p.

—— 1969, Geology and ore deposits of the central York Mountains, western Seward Peninsula, Alaska: U. S. Geol. Survey Bull. 1287, 69 p.

Shabynin, L. I., 1977, The origin of rhythmically banded skarn-greisen structures: Geokhimiya, no. 9, p. 1424–1435.

Shcherba, G. N., 1970, Greisens; Internat. Geol. Rev., v. 12, p. 114–150, 239–255.

Shima, M., Gross, W. H., and Thode, H. G., 1963, Sulfur isotope abundances in basic sills, differentiated granites and meteorites: Jour. Geophys. Research, v. 68, p. 2835–2846.

Stern, K. H., 1954, The Liesegang phenomenon: Chem. Rev., v. 54 (1), p. 79–99.

Stevenson, J. S., and Jeffery, W. G., 1964, Colloform magnetite in a contact metasomatic iron deposit, Vancouver Island, British Columbia: ECON. GEOL., v. 59, p. 1298–1305.

Trustedt, O., 1907, Die Erzlagerstatten von Piktaranta am Ladoga: Comm. Geol. Finlande Bull., no. 19, 57 p.

Twelvetrees, W. H., 1913, The Middlesex and Mt. Claude mining field: Tasmania Geol. Survey Bull. 14, 28 p.

Waite, A., 1978, The petrology, mineralogy and genesis of the tin-fluorine-tungsten skarn of Moina, Tasmania: Unpub. B.Sc. Honours thesis, Bundoora, Australia, La Trobe Univ., 57 p.

Watanabe, M., 1924a, Zonal precipitation of ores from a mixed solution: ECON. GEOL., v. 19, p. 497–503.

—— 1924b, Some problems of diffusion, with special reference to study of ore deposits: Tohoku Imp. Univ. Sci. rept., ser. 3., v. 3, p. 105–189.

Williams, K. L., 1958, Tin-tungsten mineralization at Moina, Tasmania: Australasian Inst. Mining Metallurgy, Proc., no. 185, p. 29–50.

Zasedatelev, A. M., 1973, The problem of genesis of berylliferous skarns: Internat. Geol. Rev., v. 15, p. 213–224.

DRILL HOLE SUMMARIES

16. DIAMOND DRILLING

A. PRELIMINARY

Initial drilling on the sheet areas was carried out by the Mt. Lyell Mining and Railway Co. Ltd. in 1970, 71. The Mines Department drilled 3 holes in 1972-73. Comalco commenced drilling of the Shepherd and Murphy Mine area early in 1976.

B. MT. LYELL DRILLING

Mt. Lyell's drilling consisted of 3 holes ML1A, ML2, ML3A, angled to test extensions of the known lodes at the Shepherd and Murphy Mine, (McKibben, 1971). The sites of the holes are plotted on the geology plan, TAS-76-46.

No significant intersections of mineralized quartz veins were found. Wrigglite was intersected in ML2 and ML3A but it was not recognized as a fluorite rich skarn and it was not split and analysed. Greisenized granite was intersected in ML1 and ML2 at about 200 m below the surface.

The Mt. Lyell core was kindly made available to Comalco and has been logged, split and analysed.

C. MINES DEPARTMENT DRILLING

Three holes, with a total depth of 521 m, were drilled on sheet 2 area to test mineralized skarns. Full details of core logs, analyses etc. are in Collins, (1975).

Pulps of the skarn intersections were given to Comalco so that analyses for fluorine and other elements could be carried out by the Comalco laboratory. Permission was also granted to sample other sections of the core.

D. COMALCO DRILLING

(a) Methods:

All drilling was carried out with Comalco personnel and equipment. The drill was a Joy 22HD mounted on a 6 x 6 GMC truck.

The first Comalco drill hole was labelled SMD 4, the number being consecutive to the 3 prior holes of Mt. Lyell.

All core was logged, marked for splitting, photographed, split, analysed and stored at the Devonport base.

Many holes were scanned with a McPhar TV1 scintillometer to check for radioactive minerals but none have been found.

All holes except SMD 14 were logged by P. Askins. P.W. Stainton logged SMD 14 (and logged several other holes in addition, with sedimentological emphasis).

(b) Aims:

Initial drilling was aimed at delineating the extent and grade of the wrigglite. Most holes were therefore sited as close as physically practicable to magnetic highs.

Later drilling was designed to test M.I.P. anomalies which were thought to possibly be due to massive pyrrhotite-cassiterite mineralization.

(c) Results:

Full geological logs and analyses are given in Appendices 24 and 25. Recovery logs are in Appendix 26. Comments on all Moina holes, including Mt. Lyell and Mines Department drilling, are listed below:-

DOM 1: 360W/100N, vertical, depth 325 m. Is probably sited where the sequence of Gordon Limestone is thickest. Calc-silicate rock with only very minor wrigglite is at the base of the limestone.

DOM 2: 1340W/860S, vertical, depth 101 m. Sited in outcropping skarn. Magnetite-fluorite skarn, some pyrite and pyrrhotite rich, plus calc-silicate rocks to only 15 m.

DOM 3: 1200W/940S, vertical, depth 95 m. Sited on basalt, to 10 m. Magnetite skarn virtually absent, only calc-silicate rock to 23 m. Magnetite skarns probably stripped off here by erosion.

ML 1A: 1170E/070N, 50° towards 180°M, depth 265 m. Commenced probably in the Bismuth Creek fault zone in altered sandstone. No skarns intersected. Greisenized granite intersected at 225 m. Extra analyses and petrological studies of greisenized granite are being carried out at present:- will be included in a later report.

ML 2: 910E/150S, 50° towards 180°M, depth 335 m. Intersects wrigglite limestone partly replaced by wrigglite at about 168 m; this is one of the few intersections showing partial replacement relationships. Greisenized granite intersected at 331 m. No significant mineralized quartz veins.

ML3, ML3A: 1450E/125S, 50° towards 000°M, depth 260 m. Hole collared in sandstone, drilled through Bismuth Creek fault into wrigglite. Wrigglite in places is chloritic and relatively poor in fluorite and magnetite; here fluorine analyses are low. A petrological description of this rock is in Appendix 4.

The highest Sn analyses in core are in this hole; some sections richest in Sn might be due to chloritic alteration of pre-existing wrigglite; higher Sn values tend to correlate with low F values, Fig.10. Sn values are up to 8200 ppm; analyses of separate intervals are not continuous, but complete bulked samples were analysed. Bulk analyses over the full intersection of wrigglite are:

342 - 377.5 ft. i.e. 35.5 ft. (10.8m), 2750 ppm Sn, 10.0% F
377.5 - 403.5 ft. i.e. 26.0 ft. (7.9m), 4200 ppm Sn, 2.3% F
403.5 - 478 ft. i.e. 74.5 ft. (22.7m), 2500 ppm Sn, 11.4% F

SMD 4: 700E/240S, vertical, depth 109 m. To test one of the outer limits of the main magnetic anomaly. Sited on basalt. Basalt and Tertiary sediments to 68 m. Patchy wrigglite interbedded with calc-silicate rock to 92 m.

SMD 5: 370E/130S. vertical, depth 81 m. To test the area well to the west of the Shepherd and Murphy Mine, at a point where magnetic anomaly is relatively weak. 22 m of basalt and Tertiary sediments, then limestone to 46 m showing partial replacement to wrigglite near base, then interbedded wrigglite and calc-silicate rock to 61 m.

SMD 6: 860E/50S, vertical, depth 102 m. To test area covered by basalt close to Shepherd and Murphy Mine where magnetic anomaly is pronounced. 21 m of basalt, then wrigglite with some interbedded metasiltstone to 83 m.

SMD 7: 975E/90N, vertical, depth 71 m. Area of outcropping wrigglite in Shepherd and Murphy Mine area, pronounced magnetite anomaly. 45 m of wrigglite, with some interbedded wrigglite and calc-silicate rock to 65 m.

SMD 8: 00/550S, vertical, depth 61 m. To test I.P. chargeability high trending east. Basalt and much Tertiary sediments to 32 m, then wollastonite hornfels, calc-silicate rocks and only a few cm of wrigglite to 46 m. I.P. anomaly as explained in Section 12 possibly due to Tertiary deep lead sediments.

SMD 9: 150E/100S, vertical, depth 130m. Designed to further test the relatively weak magnetic anomaly on which SMD 5 is sited. Intersected limestone to 91 m, then pyrrhotite-magnetite-fluorite-actinolite skarn to 118 m; then fault zone with coarse fluorite to 125 m, sub parallel to core. Pyrrhotite skarns are crudely layered, wispy and contorted. Sn values disappointingly low:- Maximum 1700 ppm, generally about 100 - 900 ppm.

SMD 10: 700E/50N, vertical, depth 117 m. To test northern part of main magnetic anomaly. Basalt and Tertiary sediments to 39 m, then wrigglite variously interbedded with metasiltstone and calc-silicate rock to 83 m. Some mineralized quartz veins intersected.

SMD 11: 750E/100S, vertical, depth 120 m. To test central part of main magnetic anomaly. Basalt with mudstone interbeds to 31 m, then wrigglite interbedded with various metasiltstone and calc-silicate rock to 69 m.

SMD 12: 450E/50N, vertical, depth 123 m. To test an area with no magnetic high, to determine rock types, at NW perimeter of the main magnetic anomaly. Basalt with underlying deep lead sediments to 40 m, then cavernous limestone to 91 m, then relatively minor wrigglite interbedded with calc-silicate rock and metasiltstone to 109 m.

SMD 13: 1450E/50S, vertical, depth 182 m. To test the magnetic anomaly to the east of Bismuth Creek. Anomaly was puzzling since sandstone occurs at the surface.

Sandstone to 84 m, then through a fault into skarn to 113 m. Skarn is very rich in sphalerite in places; up to 27.5% Zn (89.10 to 90.00) and averaging 8.6% Zn over 16.65 m from 87.35 to 104.00 (see Table below). This skarn seems to be replacement of pre-existing calc-silicate rock and wrigglite. Below skarn there is calc-silicate rock to 124, then sandstone.

SMD 16 was drilled into the same anomaly and established that the fault is a flat lying reverse fault, where older sandstone has been brought over the top of limestone or skarn. It is not known whether this reverse fault predates or post dates mineralization.

From	To	Int.	% Zn	Int x Zn
87.35	88.50	1.15	6.30	7.25
88.50	89.10	0.60	13.80	8.28
89.10	90.00	0.90	27.50	24.75
90.00	91.00	1.00	14.50	14.50
91.00	92.00	1.00	5.25	5.25
92.00	93.00	1.00	12.50	12.50
93.00	94.00	1.00	11.50	11.50
94.00	95.00	1.00	8.50	8.50
95.00	96.00	1.00	13.00	13.00
96.00	97.00	1.00	5.40	5.40
97.00	98.25	1.25	0.43	0.54
98.25	99.25	1.00	1.31	1.31
99.25	100.25	1.00	7.75	7.75
100.25	101.25	1.00	10.40	10.40
101.25	102.25	1.00	7.00	7.00
102.25	103.25	1.00	4.65	4.65
103.25	104.00	0.75	1.63	1.22
Total 16.65 m			wt.av. 8.63%	143.76

SMD 14: 100W/175N, vertical, depth 194 m. Not logged by PWA, see graphical sedimentological log of P.W. Stainton. To test E.I.P. chargeability anomaly (Post Office anomaly).

Limestone from surface to 192 m, then wollastonite hornfels. Hole if continued would probably have penetrated calc-silicate rocks from this point. E.I.P. anomaly explained by fine pyrite, pyrrhotite associated with stylolitic limestone and thin dark dolomitic beds concentrated in top 60 m of hole (see Section 12 for details and some petrological descriptions).

SMD 15: 900E/018N, vertical, depth 116 m. Designed to test a relative magnetic low trending NW within the main magnetic anomaly. Thought to be due to faulting and late stage alteration of pre-existing wrigglite, with possibly high Sn values as for example in ML 3A.

Hole was probably sited too far south and missed fault zone (if it exists). It is recommended that this feature be drilled again with an angled hole.

Basalt to 20 m, then deep lead sediments to 33 m, then calc-silicate rock to 109 m, with metasiltstone below.

SMD 16: 1450E/125S, vertical, depth 171 m. To further test the area around SMD 13. Sandstone to 24 m, then through a fault into calc-silicate rocks, wrigglite and some patchy sphalerite bearing skarns to 129 m. Tin contents higher than SMD 13, but not as high as ML3A. Tungsten, occurring mainly as scheelite disseminated in the wrigglite or in the relatively common pink felspar veins, is relatively abundant in this hole.

The four holes which have penetrated the skarn zone to the east of Bismuth Creek i.e. ML3A, SMD 13, SMD 16, SMD 24, have shown that the body is complex, in part Sn rich, in part W rich, in part Zn rich. See Fig.6, which is a geological cross section.

SMD 17: 810W/060S, vertical, depth 74 m. To test magnetic anomaly well away from Shepherd and Murphy mine. No surface outcrop. Intersected interbedded sandstone and limestone to 26 m, then interbedded calc-silicate rock, normal wrigglite, metasiltstone to 42 m thence through into sandstone-siltstone. Sn and W contents quite low.

Holes 18 and 19: drilled at Mt. Jacob (see separate report).

SMD 20: 300W/275S, vertical, depth 95 m. To determine source of an M.I.P. 'D type' anomaly which could feasibly have been due to massive pyrrhotite-cassiterite mineralization similar to that at Renison. For details see Section 13. Intersected cavernous broken limestone to 53 m, thence calc-silicate rocks to 70 m, with siltstone sandstone below. No pyrrhotite rich skarns.

SMD 21: 000/075S, vertical, depth 155 m. To determine source of another M.I.P. 'D type' anomaly. Limestone to 106 m, thence calc-silicate rock with minor normal wrigglite

to 124 m, thence metasiltstone. No pyrrhotite rich skarns. Hole geophysically logged; shows proximity to caverns, for details see Section 13.

SMD 22: 100W/275S, vertical, depth 110 m. Final hole to test M.I.P. 'D type' anomalies. On same anomaly as SMD 20 but 200 m to the east. Cavernous limestone to 69 m, thence limestone and calc-silicate rock, with a few cm of wrigglite at the base, to 91 m; metasiltstone-sandstone below. No pyrrhotite rich skarns.

Holes SMD 20, 21, 22 demonstrated that the cause of the M.I.P. anomalies is not massive pyrrhotite mineralization but is due to non chargeable conductive wet clay etc. in sink holes and underground caverns within relatively resistive and chargeable limestone. Full details in Section 13.

SMD 23: 200W/675S, vertical, depth 37 m. To test long narrow relatively weak magnetic anomaly south of areas previously tested. Basalt to 6 m, thence interbedded wrigglite calc-silicate rock and metasiltstone to 27 m, thence metasiltstone. Anomaly therefore due to normal wrigglite, not pyrrhotite rich skarns.

SMD 24 SMD 25: 1380W/010S. These are holes sited east of Bismuth Creek angled towards the fault, designed to further test the complex skarn zone, then explore for vein stockworks associated with the fault and mineralized greisenized granite. Very difficult drilling conditions were encountered and the holes were abandoned before target depths.

The holes have not yet been logged in detail nor analysed; they will therefore be reported on in a later report.

Drilling continued on various targets using Comalco personnel and equipment. The drill was either a Joy 22HD mounted on a 6 x 6 GMC truck or a skid/trailer mounted Longyear 38.

Aims and summary of results of each hole are:

SMD 24 1380E/010S, 75° towards 215°M, depth 169.80m.
This hole was sited east of Bismuth Creek angled towards the fault, designed to further test the complex skarn zone, then explore for vein stockworks associated with the fault and mineralized greisenized granite. Very difficult drilling conditions were encountered and the holes were abandoned before target depths. Ultimately we lost over 80m of rods, 2 barrels, recovery gear and casing due to difficulties in Hugo's fault at about 86m.

A summary log of the hole is:

0	-	86m	Moina sandstone
86	-	89m	Fault zone (Hugo's fault)
89	-	98m	Wrigglite, altered weathered
98	-	125m	Wrigglite, calc-silicate rock, interbedded
125	-	126m	Sandstone
126	-	143m	Wrigglite
143	-	170m	Calc-silicate rock
170m			(Hole abandoned with 3m core in barrel down the hole)

Analyses for the wrigglite are typical of results elsewhere. However up to 7000 ppm Sn over 2.05 metres occurs in leached altered skarn. No concentration of sphalerite as in SMD 13 and 16 was intersected; the highest Zn value is 1.7% over 3.1 metres at 143.65m in calc-silicate rock.

SMD 25 1380E/010S, 65° towards 215°M, depth 44.80m.
This hole was commenced in an attempt to redrill the targets attempted in SMD 24, but difficult drilling caused the hole to be abandoned at 44.80m after penetrating only sandstone.

SMD 26 2150E/675S, vertical, depth 202m.
Designed to test for possible tin-tungsten mineralization in broken argillized greisenized Cambrian acid pyroclastics and clastics within the Bismuth Creek Fault zone on Sheet A. The hole was sited in lease 8M/72 which we hold under option. No mineralization nor greisenization was intersected; granite was not intersected.

A summary log is:

0	-	12m	Completely weathered tuff, very clayey
12	-	20m	Slightly to moderately weathered tuff
20	-	60m	Porphyritic quartz chlorite? welded tuff, very broken, locally pyritic.
60	-	162m	Tuffaceous siltstone-sandstone, well bedded.
162	-	202m	Porphyritic quartz hornblende? welded tuff some barren quartz veining at 162, and after 180.

Much of the core was analysed as a check against fine cassiterite not readily visible to the eye. The highest values occur in the topmost weathered rock - 240 ppm Sn and 100 ppm W; elsewhere values are negligible.

SMD 27 1900E/575S, vertical, depth 73m.

This hole is on Sheet A, outside the leased areas, within the Bismuth Creek Fault zone, and as for SMD 26, was designed to test broken argillized greisenized Cambrian acid pyroclastics and clastics. Unfortunately, as in SMD 26, no mineralization nor greisenization was intersected.

A summary log is:

0	-	14m	Completely weathered tuff, (clay).
14	-	73m	Porphyritic quartz hornblende(?) welded tuff, locally very broken and pyritic.

SMD 28 900E/025N, 65° towards 040°M, depth 101m.

The aim of the hole was to test a relative magnetic low trending NW through the centre of the main wrigglite body; this low was previously drilled with SMD 15, vertical, but had apparently missed the target. It was thought that the low could be due to altered and weathered wrigglite in a fault zone paralleling the Bismuth Creek Fault - altered wrigglite could carry cassiterite in in discreet recoverable grains rather than locked in garnet and magnetite.

A summary log is:

0	-	18m	Basalt with some included weathered brecciated wrigglite (? flow foot breccia)
18	-	32m	Wrigglite, HW - CW
32	-	38m	Wrigglite, MW - Frst.
38	-	42m	Wrigglite and calc-silicate rock, interbedded
42	-	44m	Calc-silicate rock, pale, in part wollastonite rich
44	-	48m	Wrigglite
48	-	50m	Calc-silicate rock, some hornfels (metasiltstone).

040

50	-	58m	Wrigglite, some calc-silicate rock
58	-	60m	Calc-silicate rock
60	-	91m	Wrigglite, some interbedded calc-silicate rock towards 91m
91	-	95m	Calc-silicate rock
95	-	101m	Wrigglite, calc-silicate rock, interbedded
101m			Hole abandoned due to mechanical breakdown.

The hole failed to intersect altered or weathered wrigglite or thick deep lead or any other feature which might explain the magnetic low. In fact the wrigglite at this point is the thickest and deepest in the whole area drilled to date.

Analyses of wrigglite from SMD 28 are typical of those found elsewhere.

SMD 29 1100E/050N, 55° towards 000°M, depth 122m.

The hole was designed to test wrigglite in an area with many scheelite bearing feldspar veinlets and also penetrate the Bismuth Creek Fault zone from the western side, to evaluate the nature of the skarn in the fault zone. It was thought that there may be altered skarns with free cassiterite or a stockwork of mineralized veinlets in the fault zone.

A summary log is:

0	-	23m	Wrigglite, many scheelite bearing veinlets
23	-	95m	Calc-silicate rock with many scheelite bearing feldspar veinlets, and some quartz-wolframite-cassiterite veinlets to 78m
95	-	96m	Wrigglite
96	-	100m	Limestone breccia in Bismuth Creek Fault
100	-	122m	Moina sandstone with no Sn, W mineralization

Tungsten occuring as scheelite/wolframite in veinlets in wrigglite and calc-silicate rock averages 1760 ppm from surface to 83.5m including 0.6m of 1.07% and 0.9m of 1.7%; tin averages 2180 ppm in wrigglite from surface to 23m and only 330 ppm in the calc-silicate rock below. It is possible that an E-W trending vertical "stockwork" of veinlets occurs here. With photometric sorting as a possible beneficiation method this area may warrant further exploration.

SMD 30 1100E/150S, 50° towards 180°M, depth 126m.

The hole was designed to test for possible quartz-cassiterite-wolframite stockworks in sandstone between No's 2 and 5 lodes. The target area lies within the general pay shoot area which plunges west within the east-west lodes.

A summary log is:

0	-	71m	Moina sandstone, only minor quartz veinlets with minor wolframite. Some calc-silicate layers to 45m.
		71m	Old working - in No.5 lode not shown on mine plans.
71	-	126m	Moina sandstone, only minor veinlets as above
		126m	Old working - No.4 lode. Barrel lost, hole abandoned. Working is at or close to No.3 level.

The hole did not penetrate through to No.2 lode, but because of the difficulty of drilling in old mine workings, plus the lack of significant veining in the core drilled, no further drilling was attempted.

There is one intersected interval of 0.55 metres at 62.45m of quartz veins carrying 1.46% Sn but elsewhere quartz veins are volumetrically insignificant and/or are relatively unmineralized. Much of the surrounding sandstone was analysed to check for non visible cassiterite but generally values do not exceed a few hundred ppm for Sn and for W.

SMD 31 1400W/700S, vertical, depth 41m.

Three drill sites on magnetic anomalies in the Tea Tree Creek area were cleared with a small dozer. Hole SMD 31 was the first site. The target was pyrrhotite bearing skarns with possible significant Sn content. Since pyrrhotite skarn was not intersected the other two drill sites at 1300W/775S and 1275W/625S were not used.

A summary log is:

0	-	11m	Basalt
11	-	17m	Calc-silicate rock and magnetite skarn, interbedded
17	-	41m	Calc-silicate rock and hornfels (metasiltstone) interbedded.

The magnetite skarn is not wrigglite and contains only about 1% CaF_2; also Sn does not exceed 900 ppm and W does not exceed 75 ppm. The content of other elements including Be, Bi, Au is also negligible.

SMD 32 1300E/035S vertical, depth 152.4 metres.

This is east of the Bismuth Creek Fault to intersect possible high grade wrigglite beneath Hugo's Fault, adjacent to the Bismuth Creek Fault.

0 - 11 metres Soil-Basalt, 11 - 16 metres garnet-diopside-chlorite skarn, 16 - 31 metres strong shearing (Hugo's Fault) 31 - 100 metres wrigglite skarns, brecciated, altered and veined, 100 - 115 metres calc-silicate rocks, 115 - 152 metres Moina sandstone.

042

Mineralisation shows -

61.44 - 65.08 - 3.61 metres @ 11.0 g/t Ag.
28.31 - 95.67 - 67.36 " @ 0.21 % Sn
70.11 - 100.14 - 29.97 " @ 0.11 % W
129.00 - 141.56 - 12.56 " @ 0.03 % Mo

MD 33 650E/222N vertical for 164 metres. Drilled to test for possible fringing sulphide zones between SMD 10 and the Bismuth Creek Fault. 0 - 51 metres basalt and deep lead. 51 - 87 metres Limestone, 87 - 133 metres skarns - wrigglite and garnet-diopside-magnetite chlorite. 133 - 140 metres Moina quartzite, 140 - 141 quartz-talc chlorite skarn, 141 - 164 metres Moina quartzite.

Assays: 88.0 - 104.21 - 16.21 1185 ppm Sn 350 ppm W
139.8 - 141.15 - 1.35 55 ppm Sn 6900 ppm W

Highest values (Cu 180 ppm, Zn 1%, Pb 6300 ppm, Mo 820 ppm Au 0.19 ppm).

The hole indicates a slight thinning of the skarn sequence to the north of the main wrigglite zone, a decrease in grade and a thickening of the overall limestone unit. No significant sulphide skarn located.

MD 34 400E/175N vertical for 196 metres. Drilled to test for fringing sulphides between SMD 9 and Bismuth Creek Fault. 0 - 24 metres Basalt, 24 - 28 metres Weathered Limestone, 28 - 92 metres Limestone minor cave fill occasionally pyritic. 92 - 93 metres Calcareous quartzite, 93 - 141 metres Limestone 141 - 144 metres Garnet skarn, 144 - 150 metres Limestone, 150 - 154 metres Garnet-Talc skarn, 154 -160m Interbedded wrigglite and garnet-diopside skarn, 160 -161 metres Wrigglite, 161 - 196 metres Diopside-quartz-chlorite skarns.

Assays: 150.47 - 161.25 - 10.78 metres 1065 ppm Sn 480 ppm W
170.00 - 172.00 - 2.00 metres 22 ppm Sn 1650 " "

Highest values (Cu 510, Pb 130, Zn 810, Mo 1100, Au 0.06 Ag 2, As 580, Ba 1000).
No significant sulphides intersected and the skarn sequence thins from SMD 9.

043

922044

MD 35 240E/008N vertical for 161 metres. Drilled to test the extent of the pyrrhotite skarn to the east of SMD 9. 0 - 4 metres No recovery, 4 - 96 metres Massive and banded limestone, 96 -101m Limestone with calc-silicate bands, 101 - 158 metres Variety of skarns some intervals contain up to 10 percent pyrrhotite. 158 - 161 metres Moina quartzite.

Assays:	100.65	- 124.05	- 23.4 metres	1180 ppm Sn	1035 ppm W
	141.00	- 143.00	- 2 "	110 ppm Sn	3000 ppm W
	153.75	- 154.70	- 0.95 "	95 ppm Sn	1300 ppm W

Highest values (Cu 530, Pb 25, Zn 280, Mo 270, Au 0.42 Ag 1, Bi 860, Ba 400)

Only minor sulphides intersected although Tin slightly better than in SMD 9. The massive pyrrhotite in SMD 9, does not appear to extend very far to the north east.

MD 36 699E/648N vertical, depth 170.5 metres. Drilled on the east side of the Bismuth Creek Fault to obtain stratigraphic information.
0 - 60m Tertiary, 60 - 101m Limestone, 101 - 108m Limestone and skarn bands, 108 - 125m Calcareous and carbonaceous mudstone on cave fill. 125 - 159m Various skarns, 159 - 160m Limestone, 160 - 171m Impure Moina quartzite.

Assays: 122.20 - 153.20 - 31.0 metres @ 20 ppm Sn 50 ppm W. Highest values (Cu 55, Pb 60, Zn 260, Mo 4, Au 0.02, Ag 0.11, Bi 10, As 270).

The hole confirmed the presence of limestones but they were unmineralised. The area maybe too far from the source of mineralising fluids.

MD 37 450E/338N vertical, depth 176.6 metres. Drilled to test an I.P. anomaly and to investigate a replaced section of limestone between MD 34 and the Bismuth Creek Fault.

044

922045

0 - 18 metres Basalt, 18 - 144 metres Limestone, massive to banded, extensive cavities. 144 - 145 metres Calcareous quartzite, 145 - 176.6 metres Various skarns,some containing pyrite/pyrrhotite/sphalerite.

Assays:

160.9 - 163.42 - 2.25 metres @ 1140 ppm Sn 315 ppm W

Highest values (Cu 200, Pb 25, Zn 1800, Mo 40, Au 0.04, Ag 0.2, Bi 470, As 260).

This hole indicated a much reduced skarn section and lower Tin and Tungsten values. The I.P. anomaly maybe due to extensive cave fill sediments.

MD 38 575E/475N angled at 70° towards 215° magnetic on the east side of the Bismuth Creek fault and planned to drill South West to intersect the Bismuth Creek Fault. Depth 263.1 metres. 0 - 8 metres Basalt, 8 - 178 metres Limestone, 178 - 250 Various skarns, limestones and occasional Meta-siltstone bands, Bismuth Creek Fault at 195 metres.
250 - 260 metres Metasiltstone/quartzite.

Assays: 195.2 - 197.3 - 21.1 metres @ 240 ppm Sn 10 ppm W

Highest values (Cu 1500, Pb 150, Zn 2800, Mo 8, Au 0.01, Ag 1, Bi 30, As 340).

This shows a further thinning of skarn and Tin/Tungsten mineralisation form MD 37.

The Bismuth Creek Fault also proved to be non-mineralised.

MD 39 1301E/106N vertical, depth 260.4 metres. To test magnetite - sphalerite skarn below Hugo's Fault to the north of the previous intersections MD 32, SMD 13, SMD 16.

0 - 96 metres Moina sandstone, 96 - 146 metres Roland Conglomerate, 146 - 153 metres Hugo's Fault, 153 - 260.4 metres Variety of skarns.

045

Assays: 176.0 - 193.0 - 17.0 metres @ 1150 ppm Sn 220 ppm W
193.0 - 202.0 - 9 metres @ 770 ppm Sn 130 ppm W

Highest values (Cu 2200, Pb 135, Zn 2700, Mo 170, Au 1.85 Ag 25, Bi 2400, As 90, Ba 1200).

This hole suggests a large syncline of skarned limestone may occur to the north of previously recognised mineralisation below Hugo's Fault. This drillhole also suggested the possibilities of major tonnages of skarn to the east of the Bismuth Creek Fault.

MD 40 975E/100N angled at 45° towards 210° magnetic to investigate the economic potential of a suspected sheeted East-West system developed in the wrigglite zone. Depth 157 metres.

0 -14m Wrigglite, 14 - 85 metres Various skarns, 85 - 91 metres Breccia-shear zone, 91 - 157 metres Variety of different skarns.

Feldspar/feldspar quartz veining is best developed in the wrigglite section and zones with the highest density of veining occur between 37 - 47 metres, 63 - 67 metres, and 77 - 82 metres.

Assays: 10.0 - 88.8 - 78.8 metres @ 1525 ppm Sn 1120 ppm W
18.7 - 49.4 - 30.7 metres @ 1585 ppm Sn 1330 ppm W

Highest values (Cu 370, Pb 230, Zn 2.15%, Mo 2000, Au 1.15, Ag 4, Bi 760).

No well developed sheeted or stockwork vein system was intersected. The scheelite present occurs in irregular feldspar veins along minor joints and fractures, and as very finely disseminated powellite.

046

MD 41 975E/153N and angled at 45° towards 210° magnetic to investigate the presence of scheelite bearing veins beneath MD 40. Depth 150.7 metres.
0 - 10 metres Rubble and wrigglite, 10 - 92 metres Various skarns-magnetite-chlorite -garnet- dipside, 92-93 metres Wrigglite, 93-124 metres skarn-magnetite-garnet.
124-150 metres quartzite with minor diopside skarn.

Veining was best developed between 21-27 metres. Quartz mica veins were best developed in the magnetite - chlorite - garnet skarn.

Assays:

0 - 28.5 metres @ 1560 ppm Sn and 820 ppm W
97.6 - 98.6 - 1m @ 490 ppm Sn and 3800 ppm W and 1500 ppm Mo
101.0 - 103.3 - 2.3 metres @ 195 ppm Sn and 9570 ppm W.

Highest Values (Cu 470, Pb 65, Zn 2.15% Mo 1600, Au N/D, Ag 1, Bi 4500, As 270).

Drillholes DM 40,41 have changed the inferred structures of the main outcropping wrigglite. It now appears that the folds are more open than previously thought. There is no discrete, recognisable, intense zone of feldspar veining and the veins die out at dpeth below the main wrigglite/garnet-magnetite mineralisation.

MD 42 1170E/97N vertical, depth 208 metres just east of the Bismuth Creek Fault to intersect the wrigglite skarn below Hugo's Fault. It was hoped this zone would have higher grade mineralisation than holes further from the fault.

0 - 137 metres Moina sandstone, 137 - 158 metres Hugo's Fault, 158 - 165 metres Wrigglite skarn, 165 - 166 metres Fractured quartzite, 166 -193m Various skarns, 193 - 195 metres Chlorite-garnet-pyrite (10%),195 - 208 metres Chloritic sandstone - Moina sandstone.

Assays:

158.0 - 177.0 - 19.0 metres @ 1350 ppm Sn and 475 ppm W.
Highest values (Cu 540, Pb 1050, Zn 2.95%, Mo 55, Au 0.05, Ag 1, Bi 830, As 365).

This hole has indicated either a rapid steepening of the dip of Hugo's Fault or the presence of an extra North-South fault (indicated by magnetics) between MD 39 and MD 42. The skarn intersected did not show any notable increase in Tungsten and Tin grades.

MD 43 1400E/100N vertical, depth 325 metres. Drilled to investigate extensions of the sphalerite skarn to the north of SMD 13 and indicate the depth to granite.

0 - 81 metres Moina sandstone, 81 - 134 metres Roland Conglomerate, 134 - 137 metres Mixed zone - conglomerate and magnetite rich quartzite, 136 metres Mineralised breccia, 137 - 139 Sericitised sedimentary quartz breccia, 139 - 225 metres Cambrian volcanics, 225 - 325 metres Moina sandstone occassionally mineralised by magnetite, pyrite, chlorite, sphalerite, chalcopyrite and garnet.
Small granitic dyke 1 centimetre wide at 292 metres.

Assay:

136.6 - 136.9 - 0.3 metres @ 670 ppm Sn 770 ppm W and 12% Cu
Highest values (Cu 12% then 570, Pb 50, Zn 2700, Mo 9500, Au N/D, Ag 34, Bi 24, As 65).

The presence of the apparently fault bounded block of Cambrian volcanics in this hole complicates the structure of this area to the east of the Bismuth Creek Fault. Hugo's Fault is possibly represented by the quartz breccias with minor mineralisation from 134.3 - 138.9 metres. Two high angle faults probably post dating Hugo's Fault bound the Cambrian volcanics. Metasomation has affected much of the core but it has not introduced significant amounts of metals.

In March 1982 a reinterpretation of MD 43 occurred because the hole had complicated the structure on the eastern side of the Bismuth Creek Fault. The volcanics intersected may be either a faulted sliver or as a normal O - ϵ succession.

048

If Cambrian volcanics represent the normal succession the skarn below Hugo's Fault maybe the metasomatic product of Cambrian volcanics. Therefore the whole Cambrian volcanic succession could be prospective for skarns. This is true to a small extent at the All Nations Mine where drillholes have intersected minor zones (2 metres) within skarned Cambrian volcanics. No large volumes of metasomatised Cambrian volcanics have been recognised elsewhere in the region.

The sandstone intersected at the bottom of the hole was originally logged as Moina Sandstone on appearance. Trace element geochemistry was tried using Nb, Y and Zr to determine if it may have been a sandstone intercalation within the Cambrian volcanics. The results tentatively support a Moina (i.e.) Ordovician origin more than a Cambrian origin and so it is now thought MD 43 has intersected a sliver of infaulted Cambrian volcanics which complicate the structural picture east of the Bismuth Creek Fault.

MD 44 1450E/100N vertical, depth 325 metres. Drilled to test for extensions to the Sphalerite skarn to the north and east of SMD 13 and to attempt to intersect granite.

0 - 80 metres Moina sandstone, 80 - 134 metres Roland Conglomerate, 134 - 137 metres Mixed zone Hugo's Fault?, 137 - 138 metres Quartz-pyrite-magnetite-arsenopyrite vein, 138 - 225 metres Volcanics - slightly greisenised and metasomatised, 225 - 325 metres Moina sandstone with some thin calc-silicate zones.

TONNAGE ESTIMATES

(Askins, 1979)

050

14. WRIGGLITE TONNAGES AND GRADES

A. GENERAL

A preliminary calculation of the tonnage and grade of wrigglite at Moina was made in September 1976 and included in the 1978 report.

Revised calculations have been made on the basis of extra drilling and a more refined interpretation of the geology.

All sections previously presented have been revised; these plus additional north-south sections form plans TAS-79-356 to 373 These north-south sections have not been used for the revised calculations; instead oblique sections approximately normal to the fold directions and faulting have been used.

B. SUMMARY

The total wrigglite resource is

"indicated" tonnage	26,500,000t
grade	approx. 18% CaF_2, 0.1% Sn, 0.1% W
Overburden over "indicated" wrigglite	8,500,000t
Ratio "indicated" wrigglite to overburden	3 : 1

The deposit is probably the largest single fluorite resource in Australia.

C. METHODS, ASSUMPTIONS

(a) Plans, sections

Based on all available drilling data, outcrop geology and underground mapping by the Mines Department. Structure contours on the base of the wrigglite and on the base of Tertiary alluvium and/or basalt were constructed. These are plans TAS-79-376 and 375. The structure contours are necessarily very interpretive in places due to the paucity of data, but show clearly that there are a series of anticlines and synclines, with axes trending NW sub parallel to the Bismuth Creek Fault, with probably vertical axial planes, and with plunges varying from about 65° NW close to the lodes in the south east to perhaps subhorizontal in the north west of the area. Close to the mine there seem to be more folds and steeper plunges than away from the mine but this might be partly an apparent feature due to the lack of data points.

Structure contours on the base of the wrigglite and on the fault in the area east of Bismuth Creek were also constructed; see plan TAS-79-376

Geological sections along lines A to G normal to the folds were constructed, plan# TAS-79-374. These use the best fit of information from outcrop geology drill hole exposures, underground mapping of the Mines Department, the structure contour data, and on assumption that wrigglite is approximately outlined by the 62 500nT contour of the proton precession total field.

(b) Tonnage calculations:

Tonnage calculations are shown in Appendix 12. Tonnages are quoted as "indicated" in accordance with Aus. I.M.M. usage. The degree of faulting and folding in the prebasalt rocks and the rugged pre basalt relief make accurate "measured" tonnage calculations impossible. Closer spaced drill holes will be necessary to obtain "measured" tonnages. The "indicated" tonnage requires testing by further drill holes before it can be quoted with confidence.

The tonnage quoted is only in the main body of wrigglite; it does not include (i) the complexly faulted folded and altered skarn east of Bismuth Creek beneath Hugo's Fault (ii) deep wrigglite and pyrrhotite skarn intersected in SMD 5 and SMD 9 west of line 500E (iii) the wrigglite bodies on sheet 2 intersected in SMD 17 and in SMD 23.

Amongst the assumptions in the calculations are:

(i) only open pittable wrigglite calculated. Where the overburden/wrigglite ratio exceeds about 2.5 : 1, the wrigglite is not included in the calculation.

(ii) density of wrigglite 3.3

(iii) density of overburden 2.5 (basalt, some Tertiary alluvium and sediment.)

(iv) open pit slope 45^{o}.

(v) in many places there is a grade boundary between wrigglite and fluorite bearing calc-silicate rock. Only mineralized rock with an approximate bulked average analysis of greater than 10% CaF_2 has been included in the calculation.

(c) Grade

The grade of wrigglite is approximate only, since only eight drill holes have penetrated "indicated" wrigglite. Table 1 summarizes weighted average grades. Average grade for the

052

whole wrigglite deposit is visually estimated from this table.

TABLE 1

WEIGHTED AVERAGE ANALYSES

DIAMOND DRILL HOLES, MOINA, WITHIN "INDICATED" WRIGGLITE

Hole No.	From metres	To metres	Interval metres	CaF_2 %	Sn ppm	W ppm	Remarks
ML 2	43.3	50.4	7.1	17.8	ca 800	ca 400	
	50.4	61.0	10.6	11.6	ca1400	ca 150	
	61.0	82.9	21.9	19.2	ca1500	ca 800	
	43.3	82.9	39.6		1350	540	bulked sample analysis
SMD 6	22.75	83.05	60.30	17.6	1400	910	
	22.75	67.70	44.95	19.5	1540	930	
SMD 7	1.00	55.00	54.00	20.9	1450	1030	
SMD 10	38.75	88.50	49.75	17.6	1320	535	0.35 interval of rich vein
	38.75	76.00	37.25	19.2	1300	500	excluded
SMD 11	31.00	74.00	43.00	16.9	1525	1020	1.35 interval of nil core recovery
	31.00	60.70	29.70	19.4	1540	1010	excluded.
SMD 15	33.00	105.00	72.0	18.0	1470	1250	
SMD 28	29.00	90.60	61.60	20.3	1740	940	
	90.60	101.00	10.40	10.1	1110	560	
	29.00	101.00	72.00	18.8	1650	890	
SMD 29	0.00	23.25	23.25	20.8	2180	2260	

Note: All intervals except for SMD 29 are approximate true thicknesses.

OS. 1144

DENSITY OF VARIOUS ROCK TYPES, MOINA. 922054

DEPARTMENT OF MINES—TASMANIA

TELEPHONES:
Metallurgical Research .. .. } 44 2431-2
Laboratory .. .. .. (2 lines)
Mines Inspection .. .. ..
Explosives & Inflammable Liquids .. ..

LAUNCESTON OFFICES
287 WELLINGTON STREET
SOUTH LAUNCESTON 7250

2nd February, 1978.

Comalco Exploration Office,
P.O. Box 691,
DEVONPORT 7310 Tas.

Attn. Mr. C. Weste.

Dear Sir,

Please find below results of samples submitted to us on the 27th January, 78. Would you advise if you want the pieces of drill core returned as they are intact.

	Reg. Nos.	Your Description			Density t/m³
	780146	ML 1A	868'	granite (altered)	2.57
	147	ML 2	1057.7	quartzite greisen	2.65
*	148	SMD 4	37.15	basalt	2.25
*	149	SMD 4	63.45	basalt	2.49
	150	SMD 7	27.00	wigglite	3.52
	151	SMD 7	49.70	calc silicate	3.49
	152	SMD 8	18.0	basalt	2.92
	153	SMD 9	15.50	limestone	2.67
	154	"	39.10	limestone	2.70
	155	"	70.00	limestone	2.72
	156	"	79.25	limestone	2.73
	157	"	94.60	pyrrhotite skarn	3.70
	158	"	109.00	pyrrhotite skarn	3.27
	159	SMD 10	90.80	sandstone	2.75
	160	Smd 11	47.30	wigglite	3.49
	161	SMD 12	118.70	metasiltstone	2.75

* These were determined when immersed weight became constant under normal atmospheric conditions. (i.e. bubbling had ceased) May still contain some trapped air.

Yours faithfully,

Senior Metallurgist.....

(H. K. Wellington)
Chief Chemist & Metallurgis

Fee: $80.00

APPENDIX 12

WRIGGLITE INDICATED TONNAGE CALCULATIONS

Sections used for the tonnage calculations are Fig's 6 to 10 attached. (These are merely part of the sections on plans TAS-79-). Each figure shows the area of wrigglite and the area of overburden used for each of the blocks on Fig. 5, attached.

The broad assumptions for the calculations are listed in the text. It must be emphasised that the figures cannot be quoted with confidence because of the relative lack of drill or surface information and the consequent interpretive nature of the sections in many places.

B BLOCK. 25m SE and 50m NW of Section B

Wrigglite 75m x area on section B = 75 x 11,000 = 825,000m^3

Overburden 75m x area on section B = 75 x 7075 = 530,625m^3

C BLOCK. 50m either side of Section C

Wrigglite 100m x area on section C = 100 x 22,300 = 2,230,000m^3

Overburden 100m x area on section C = 100 x 4375 = 437,500m^3

D BLOCK. 50m either side of Section D

Wrigglite 100m x area on section D = 100 x 23,300 = 2,330,000m^3

Overburden 100m x area on section D = 100 x 7025 = 702,500m^3

E BLOCK. 50m either side of Section E

Wrigglite 100m x area on section D = 100 x 18,200 = 1,820,000m^3

Overburden 100m x area on section D = 100 x 10,100 = 1,010,000m^3

F. BLOCK. 50m either side of Section F

Wrigglite 100m x area on section F = 100 x 9050 = 905,000m^3

Overburden 100m x area on section F = 100 x 7850 = 785,000m^3

TOTAL VOLUME WRIGGLITE 8,110,000m^3

Take density of wrigglite as 3.3

∴ TOTAL TONNES WRIGGLITE, indicated 26,763,000t

say 26,500,000t

TOTAL VOLUME OVERBURDEN 3,465,625m^3

Take density of overburden as 2.5

∴ TOTAL TONNES OVERBURDEN over indicated wrigglite 8,664,000t

say 8,500,000t

∴ Ratio indicated wrigglite to overburden 3.0 : 1

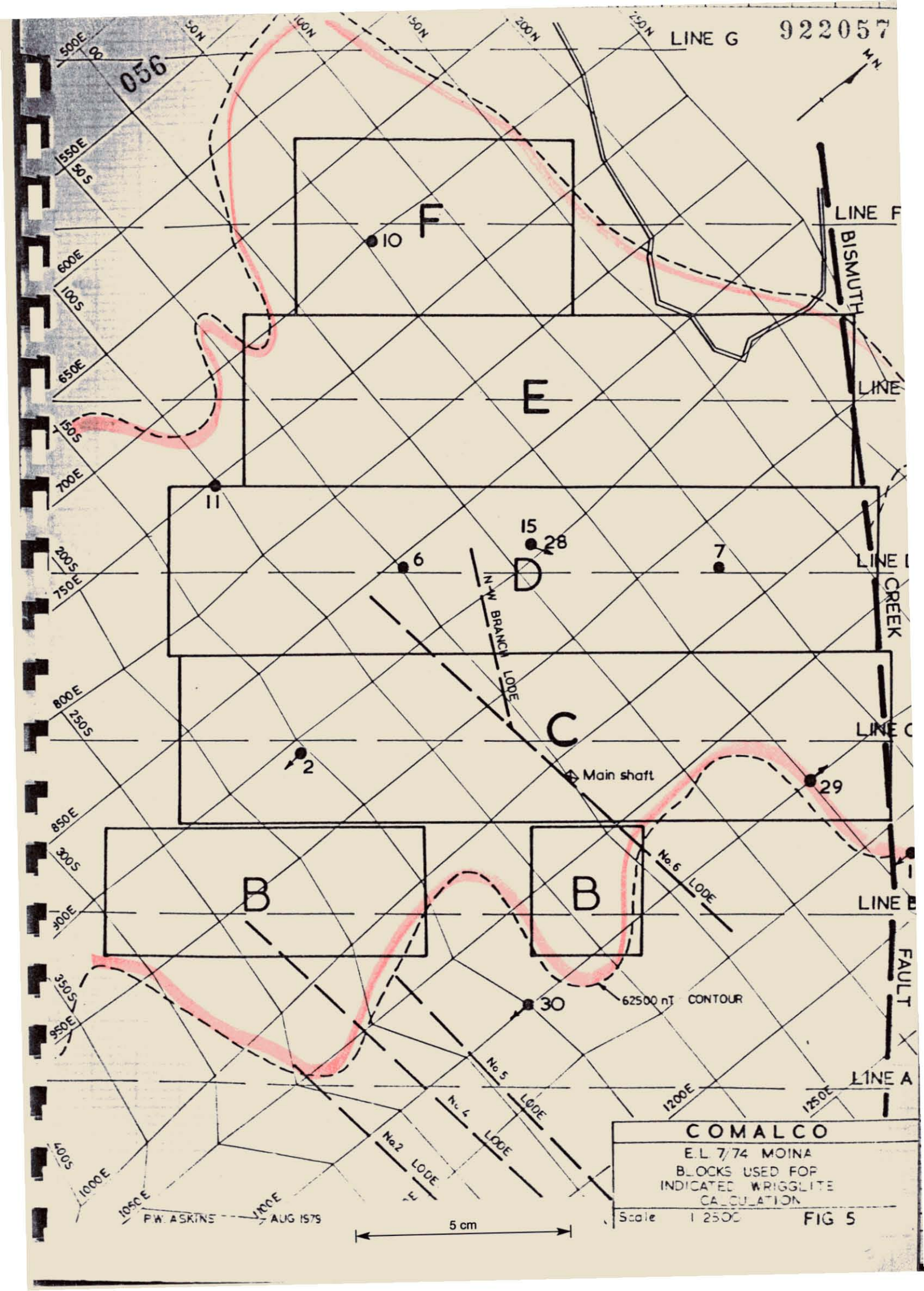
922057
LINE G
056
MN
LINE F
BISMUTH
LINE E
CREEK
LINE C
LINE B
FAULT
LINE A
F
E
D
C
B
B
10
11
15
28
6
7
2
29
30
Main shaft
NW BRANCH LODE
No.6 LODE
No.5 LODE
No.4 LODE
No.2 LODE
62500 nT CONTOUR
500E
550E
600E
650E
700E
750E
800E
850E
900E
950E
1000E
1050E
1100E
1150E
1200E
1250E
50N
100N
150N
200N
250N
50S
100S
150S
200S
250S
300S
350S
400S
P.W. ASKINS
AUG 1979
5 cm
COMALCO
E.L. 7/74 MOINA
BLOCKS USED FOR INDICATED WRIGGLITE CALCULATION
Scale 1:2500
FIG 5

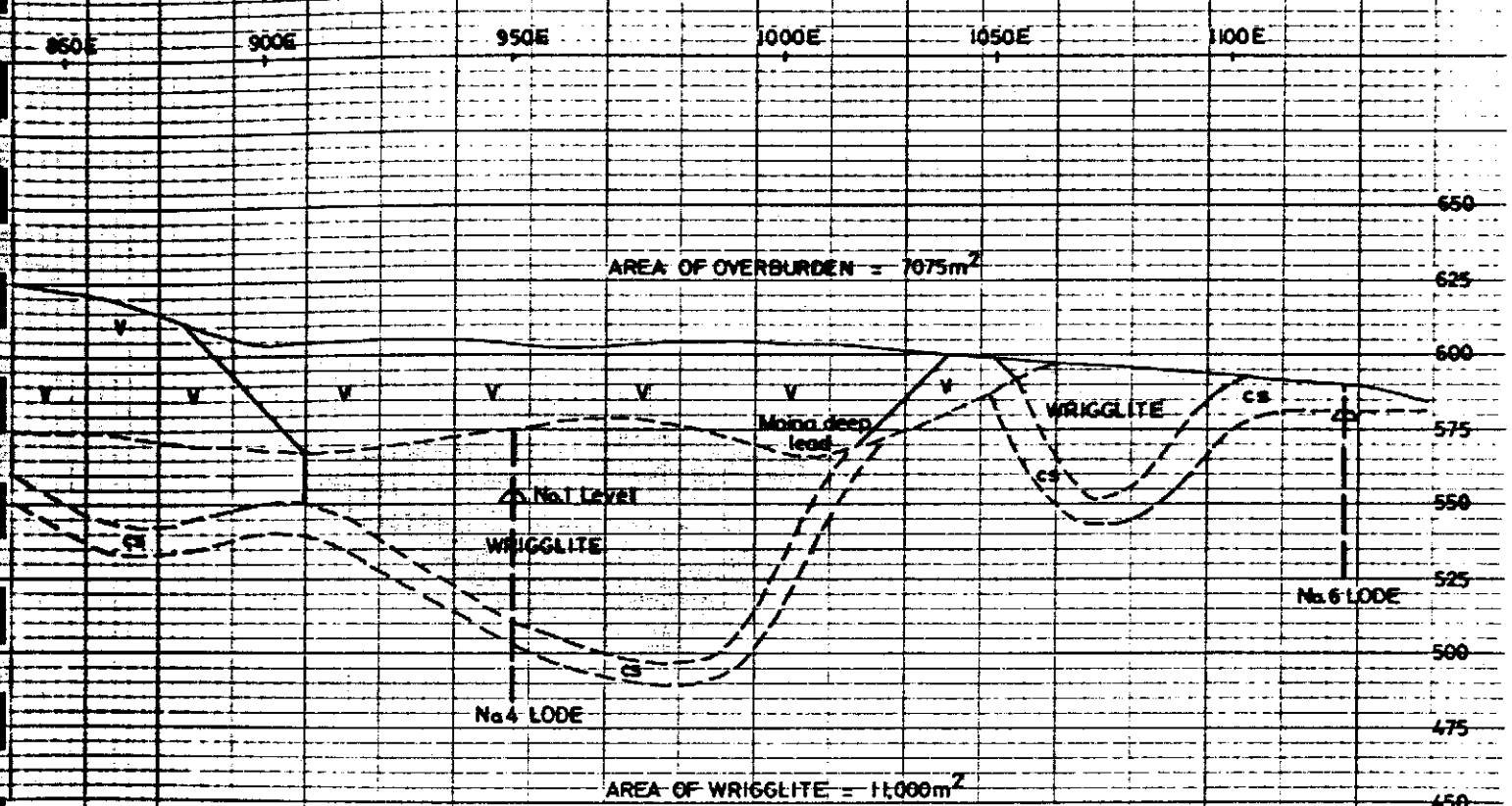

COMALCO

INDICATED WRIGGLITE

SECTION B

P.W.ASKINS
AUG. 1979

FIG. 6

922059

058

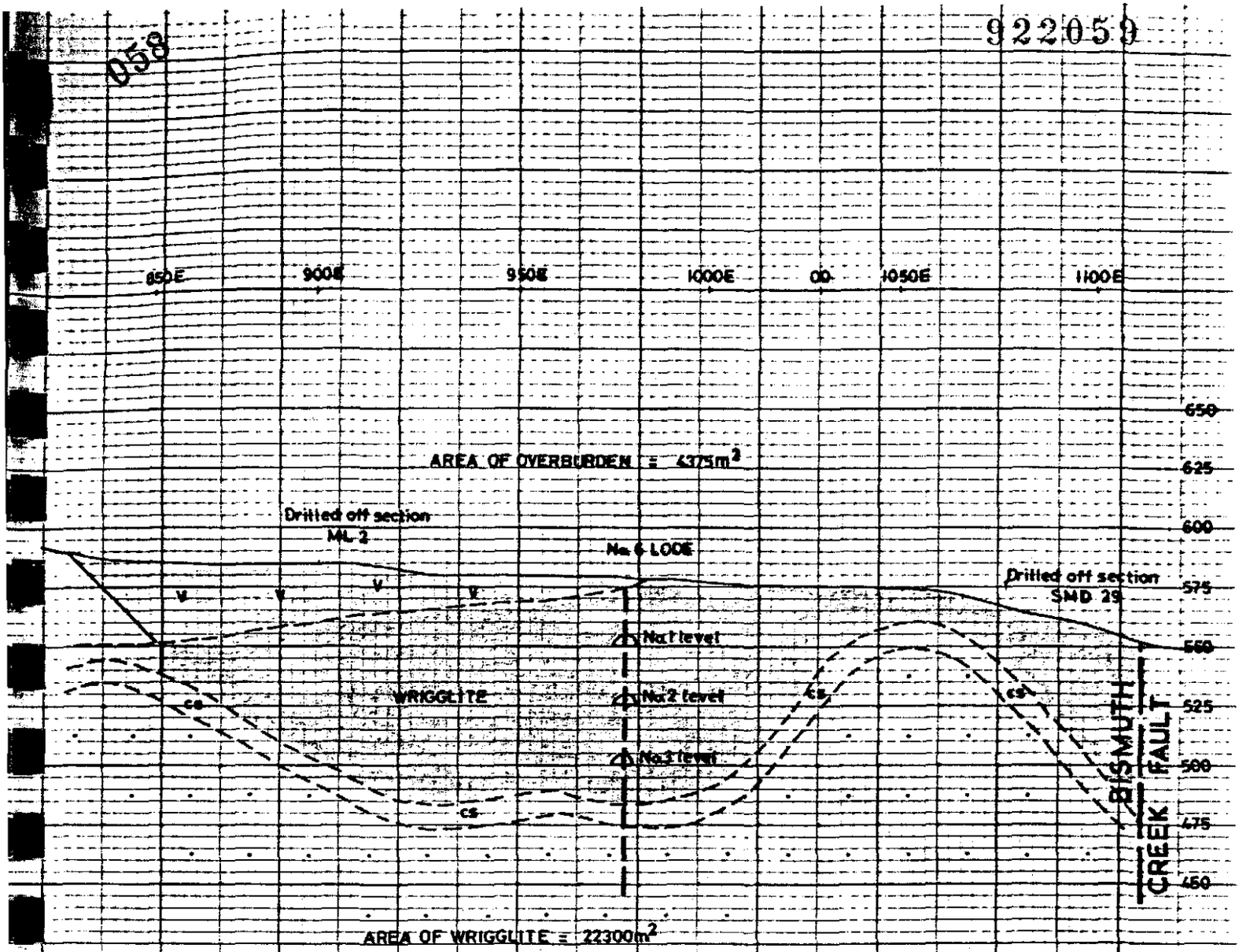

COMALCO

INDICATED WRIGGLITE

SECTION C

P.W.ASKINS

FIG. 7

922060

059

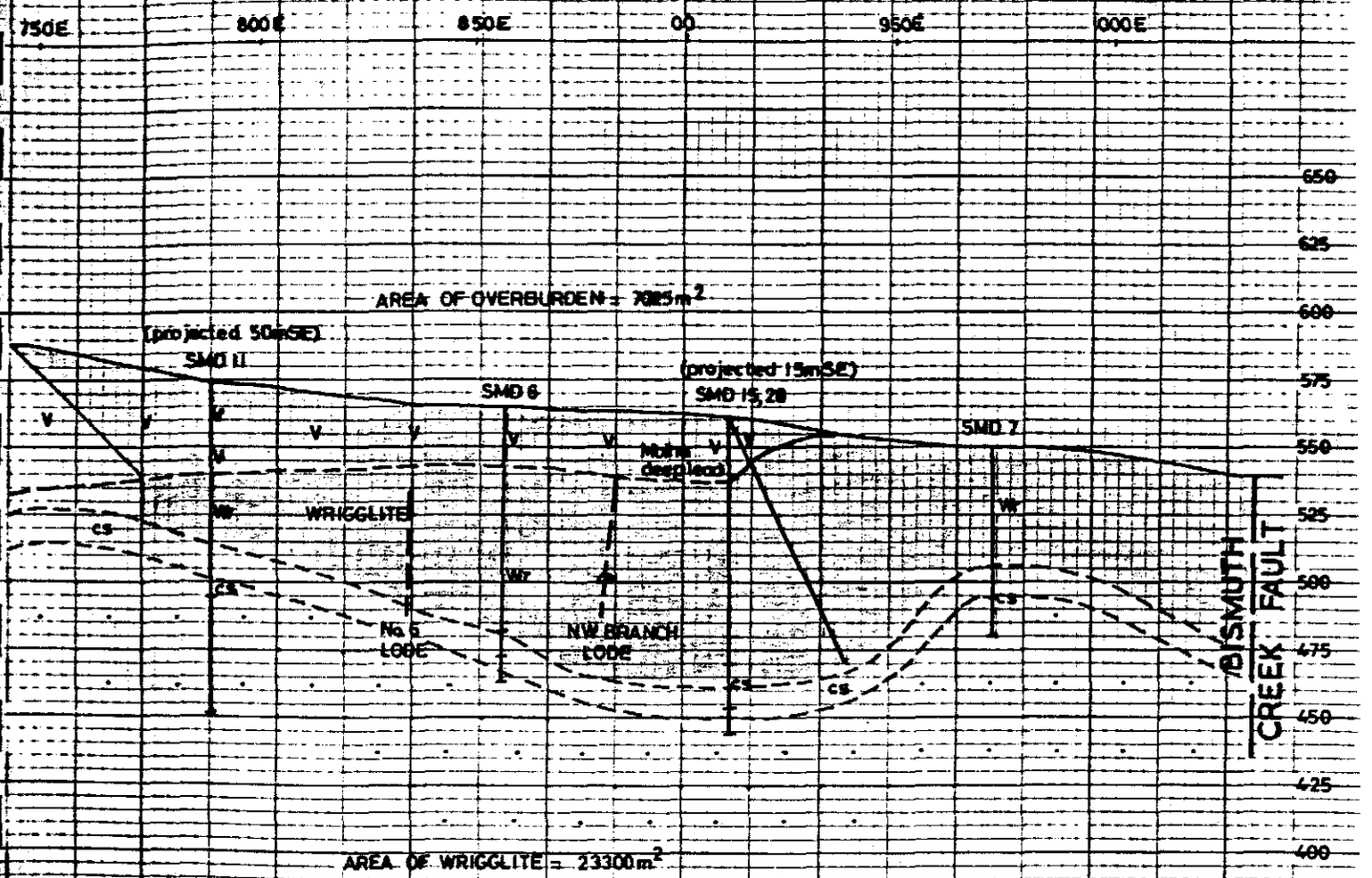

AREA OF WRIGGLITE = 23300m²

COMALCO

INDICATED WRIGGLITE

SECTION D

P.W. ASKINS
AUG. 1979

FIG. 8

922061

060

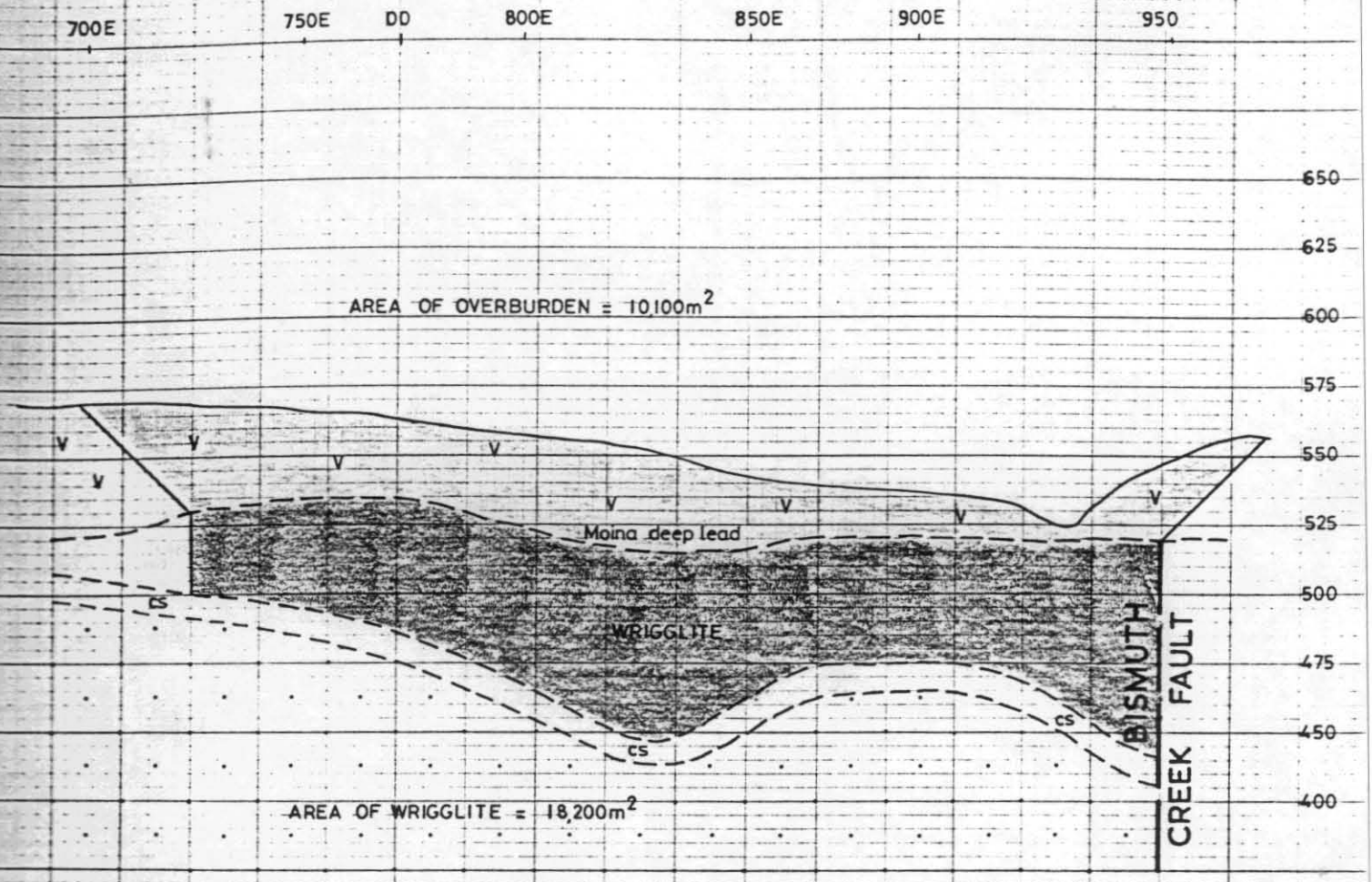

COMALCO

INDICATED WRIGGLITE SECTION E

P.W. ASKINS
AUG. 1979

FIG. 9

061

922062

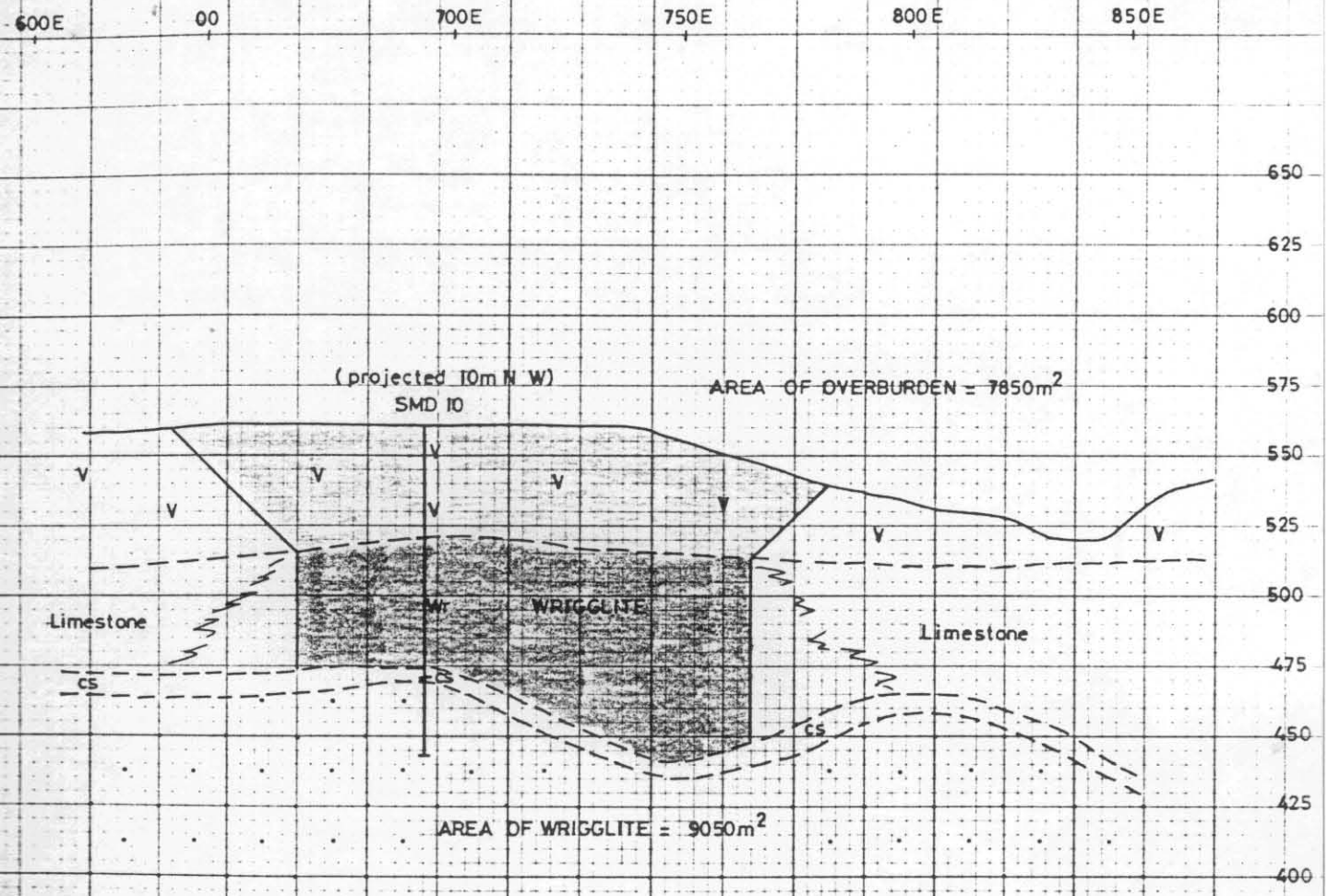

COMALCO

INDICATED WRIGGLITE SECTION F

P.W.ASKINS
AUG. 1979

FIG. 10

BENEFICIATION STUDIES

1. Askins, 1978

2. Askins, 1979

18. BENEFICIATION STUDIES.

A. GENERAL.

Beneficiation studies have been carried out on wrigglite by The Australian Mineral Development Laboratories (AMDEL) in Adelaide and by the Tasmanian Department of Mines in Launceston.

Amdel initially did work on chemical extraction of the fluorite from surface samples of wrigglite and subsequently carried out mainly flotation testing of a composite sample from drill core.

The Department of Mines has investigated,and is continuing to investigate, fluorite, tin and tungsten extraction on a bulk sample of wrigglite collected off dumps at the Shepherd and Murphy mine.

B. AMDEL INVESTIGATIONS.

(a) Chemical extraction of fluorite:

Aim and method

Amdel offered in late 1975 to try a roasting process to extract fluorite from Moina wrigglite. They had previously used their method in an ore that had not given acceptable flotation results.

The exact method remains confidential to Amdel, but is believed to be a roast at 400^{o}C with ammonium sulphate, and collection of gaseous fluorine compounds. Details of what is probably the method used are at the end of Appendix 28. (This method was published in Amdel report No.1178 in 1977).

Two samples, Moina 1 and Moina 2 were submitted to Amdel. Both are samples collected by A.H. Bartlett of wrigglite from outcrop adjacent to the old Shepherd and Murphy mill site.

Results

Only sample Moina 1 was tested. Full results are in Appendix 28.

Extraction of fluoride was 70%, but this initial work did not attempt to modify and optimize the method. The tin remained in the residue and so was not extracted.

The high iron content of the wrigglite caused a major wastage of the reagent, so no further work was carried out with this method; all further work was by more conventional

flotation means.

(b) Flotation extraction of fluorite:

Aim and methods

The aims were:

(i) to produce an acid grade fluorite concentrate at maximum recovery;

(ii) to study the feasibility of extraction of magnetite, cassiterite and scheelite.

A quotation was received from Amdel and the Colorado School of Mines for an initial beneficiation study of the Moina wrigglite. Amdel's quote was accepted because

(i) it was cheaper;

(ii) they had previously carried out beneficiation work on the Mt. Garnet wrigglite; and

(iii) liaison with Amdel as work proceeded would be easier.

A bulked sample of crushed split core from drill holes SMD 4, 5, 6, 7 was made up according to a recipe, as listed in Appendix 29. The sample contains both wrigglite and calc-silicate rock. The overall fluorite content was 16%, and Sn was 0.13%, WO_3 - 0.11%.

Full details of the mineralogical studies, magnetic separations and flotation testing are in Amdel's final report No.1147 (Feb 1977), in Appendix 29. (Data from Amdel's preliminary report and progress reports 1 and 2 are all covered in the final report and so only the final report is reproduced here).

Results

Full results of testing are in Amdel's final report in Appendix 29.

Amdel's final conclusions are:

(i) By fine grinding and flotation a concentrate assaying 92.5% CaF_2 with a recovery of 64.9% was produced from a feed assaying 16.5% CaF_2.

(ii) Removal of magnetite by magnetic separation applied to either the flotation feed or concentrate resulted in a high loss of fluorite due to the poor liberation characteristics of magnetite.

(iii) Grinding to 17 μm is necessary for good liberation of fluorite. Scheelite is well liberated at flotation sizes but little cassiterite is liberated above 9 μm. Much of the magnetite is liberated at 33 μm but finely disseminated magnetite is evident in grains finer than 15 μm.

(iv) The chief contaminants in the flotation concentrate are magnetite, calcite, scheelite and amphibole. Further flotation cleaning stages should reject calcite and amphibole, but the magnetite occurs as fine inclusions in the fluorite. Differential flotation of the scheelite from the fluorite has not been studied.

(v) It is unlikely that a high grade magnetite concentrate suitable for heavy medium use could be recovered from the ore because of the poor liberation characteristics of this mineral.

(vi) The composite ore sample contains 0.13% Sn, 45% of which is present in solid solution in garnet. The remaining tin is present as cassiterite which is too finely disseminated for physical beneficiation.

(vii) The composite ore sample contains 0.11% WO_3 as scheelite. This scheelite concentrated to 0.4% WO_3 with the fluorite during flotation but it is doubtful whether the scheelite could be recovered economically from this concentrate unless chemical treatment was carried out.

Discussion and recommendations

Amdel believe that it may be feasible to treat the Moina wrigglite by flotation to produce a low-grade concentrate at high recovery and then leach this concentrate to extract fluoride. They recommended that sufficient work be carried out to enable a preliminary assessment of the technical and economic feasibility of this process. This work has not been carried out.

My comments are:

(i) The bulk sample which Amdel investigated included some calc-silicate rocks from holes 4 and 5; these calc-silicate rocks are not within the "indicated" wrigglite of the resource tonnage calculations (Section 17). This can throw a bias on the bulk sample by changing grades, minerals present etc. The bulk sample when it includes calc-silicate rock is probably more representative of the deposit as a whole, but the initial investigation would have been simpler if only pure wrigglite had been studied.

(ii) Amdel have found that about half the tin is in solid-solution in garnet. I suspect that most of this garnet comes from the calc-silicate rocks and relatively little from the wrigglite (See table 3). Much of the calc-silicate rock occurs at the base of the wrigglite

so with selective mining calc-silicates can probably be largely eliminated, and a relatively pure wrigglite product mined. This relatively pure wrigglite possibly would have more tin in a recoverable form.

To resolve the tin problem work needs to be done on a purer bulk sample of wrigglite. Such a bulk sample was prepared for investigation by the Department of Mines.

(c) Pyrohydrolysis

Amdel have a method of extracting fluorite by pyrohydrolysi a process which yields HF using steam as the only reagent. When approached by us they suggested that trials be carried out. (Appendix 29A). No such work has yet commenced but it is recommended.

C. DEPARTMENT OF MINES INVESTIGATIONS.

(a) Exploratory project, investigation R 731:

Sample type and analyses

A sample of wrigglite uncomplicated by the presence of calc-silicate rocks was submitted to the Department of Mines for investigation. The sample was a 140 kg parcel of wrigglite made up of cobbles and boulders selected off the dump about 50 m NNE of the old main shaft of the Shepherd and Murphy Mine, and off a bulldozer costean spoil heap immediately adjacent to the old main shaft.

An analytical comparison of the bulk samples submitted to Amdel and the Department of Mines is:

	Amdel sample.	Mines, (R 731).
CaF_2	16.1%	20.0%
Sn	.13%	.22%
W	.08%	.14%

Full lists of available analyses of the Mines bulk sample are in Appendix 30. Analyses by Comalco laboratory, Amdel and the Mines Department are listed. The Mines Department analysis for fluorine (7.8%) is much lower than that of both Amdel and Comalco ($\sim$10%), however the Mines Department admit that their fluorine analyses are not consistent and "should be taken as indicative only".

Aim and methods

Comalco's aim when submitting the sample was the recovery of acid grade fluorite. The Department of Mines decided that an exploratory project was necessary, to fully determine the nature of the material submitted.

They carried out a series of scout tests applying normal concentration methods at three degrees of grinding. The concentration methods included heavy liquid separation, magnetic separation, gravity separation, and flotation of sulphides and fluorite. Full details are in Appendix 30.

Results

A full discussion of results is in a report entitled R 731, dated 21st December 1976, which is in Appendix 30. It was clear that very fine grinding of the wrigglite would be necessary to future work.

Conclusion

It was decided by H.K. Wellington (Mines Department) and A.H. Bartlett and P.W. Askins (Comalco) that the information emerging from the investigations would basically only mirror what Amdel had already determined. Therefore the future investigations were designed to accentuate problems which Amdel had not tackled, in particular scheelite recovery.

(b) Scheelite concentration project, investigation R 745.

Preliminary

As concluded above the exploratory project was requested to be continued with an emphasis on scheelite.

Thorough evaluation of scheelite recoveries had not been carried out by Amdel, partly because their bulk sample had a low tungsten content. Scheelite occurs in two main styles in the wrigglite: (i) as very fine grained scheelite disseminated within the fabric of the wrigglite. Under UV this fluoresces lime green and so is probably Mo rich; (ii) relatively coarse grained scheelite within the pink felspar veins which commonly penetrate the wrigglite. This generally fluoresces white and so is probably purer, with less Mo content.

It was thought that a thorough metallurgical evaluation of these styles of scheelite mineralization were warranted; scheelite could be more important economically than the tin. Assuming a mined recoverable grade of 0.1% WO_3 and prices of scheelite concentrate of $120/m.t.u. then this is worth $12 in-the-ground; - possibly sufficient to pay mining and milling costs.

Sample

The same sample as R 731 was used.

Methods

Successive grinding and concentration techniques were used to reduce a sample bulk of 95 Kg to a final particle size of - 53 μm. The ore was initially ball mill ground to -

-300 µm, producing the fractions + 170 µm, + 76 µm, + 53 µm and - 53 µm. The + 170 µm fraction was then subjected to magnetite separation on an Eriez drum type wet magnetite separator. The resulting non-magnetic fraction was then gravity concentrated on a laboratory Deister table and the concentrate produced was subjected to sulphide flotation. The flotation tailing was then dried and fed to a Rapid high intensity dry magnetic separator. This total process was repeated for each size fraction together with its appropriately sized and reground table tailing and Eriez magnetics. Thus by successive stages, the ore was concentrated at the following particle sizes.

Primary section	- 300 µm	+ 170 µm
Secondary section	- 170 µm	+ 75 µm
Tertiary section	- 75 µm	+ 53 µm
Quaternary section	- 53 µm	

Results

Full results in are Appendix 31 in the report entitled Comalco Limited - Moina wrigglite, R 745, dated 9th May 1978.

Both scheelite and cassiterite were difficult to recover. Scheelite overall recovery by tabling was only 33% producing a concentrate of only 22.7% WO_3. The problems are presence of scheelite-magnetite composites and that 39% of the overall WO_3 present was finer than 16 µm and unrecoverable by gravity concentration methods. (Furthermore 26% of the over-all WO_3 was finer than 9 µm!).

Recovery of tin in table concentrate was only 7%, producing a concentrate of only 7% Sn. This grade was raised to 21% Sn after dry magnetic separation, but recovery was then only 4% overall. 53% of the original tin was found to be in the sample in smaller than 16 µm particle size and 19% is locked in magnetite in a - 50 µm cleaner magnetics product.

A magnetite concentrate was produced which contained 82.5% magnetics (Davis Tube determination) and 63% HCl soluble iron. This could approach specifications suitable for coal washery purposes - (See Appendix 32 for such specifications)

Fluorite flotation was not attempted. 87% of the original fluorite was contained in the - 53 micron final gravity tailings.

Conclusion

These results are disappointing, but in view of the fine grain size of the wrigglite, not surprising. Considering

that the concentration methods were merely conventional gravity techniques, the results are somewhat encouraging.

Insufficient sample remained for future investigation.

(c) Scheelite concentration project, investigation R 758:

Because no further sample remained a one tonne parcel of wrigglite again from surface dumps was supplied.

This sample was collected by P. Askins and deliberately slightly biased by selection of pieces of wrigglite containing felspar veinlets. This was done in an effort to raise the head grade of scheelite and so make beneficiation tests a little easier.

A head assay by the Mines Department R 758 is:

Sn	0.3 %
WO_3	0.16%
S	0.8 %
Ca	12.7 %
Fe (total)	21.2 %
Fe (soluble)	20.4 %

No results of investigations have yet been received.

New techniques of flotation of scheelite in the presence of fluorite have been devised, see Appendix 33. Hopefully these methods can be attempted on the Moina wrigglite.

15. BENEFICIATION STUDIES

DEPARTMENT OF MINES INVESTIGATIONS

The Tasmania Department of Mines has continued beneficiation studies.

Scheelite and cassiterite concentration project, investigation R 758

Results have been received for initial work on this one tonne parcel of wrigglite from surface dumps. The entire one tonne has now been ground and processed.

This sample was collected by P. Askins and deliberately slightly biased by selection of pieces of wrigglite containing feldspar veinlets. This was done in an effort to raise the head grade of scheelite and so make beneficiation tests a little easier.

Head assays by the Mines Department R 758 are:

	19th May, 1978	1st February, 1979
Sn	0.3%	0.27%
WO_3	0.16%	0.19%
S	0.8%	0.8%
Ca	12.7%	12.8%
Fe (total)	21.2%	21.2%
Fe (soluble)	20.4%	20.4%

A complex grinding, tabling, magnetics and vanner circuit (plus some conventional flotation for sulphide recovery not cassiterite recovery) resulted in some significant conclusions, details of which are in Appendix 10.

(a) conventional gravity techniques are capable of producing a concentrate being 0.11% of the original mass containing 16.8% of the overall WO_3 at a grade of 24.8% WO_3 and 12.5% of the overall Sn at a grade of 31.2% Sn.

(b) 85% of the fluorine finishes in the vanner tailing product. The vanner tailing is 66.1% of the original mass and contains 59.1% of the original Sn and 51.9% of the original WO_3; That is about half of the Sn and WO_3 in the original sample reports with the fluorite and other calc-silicate minerals.

(c) the magnetic concentrate is 29.7% of the original mass and contains 20.2% of the original Sn and 14.4% of the original WO_3 and 11.7% of the original fluorine.

My comments are:

The Sn product from this study is as black cassiterite, and the WO_3 is as cream scheelite.

The Sn contained in the magnetite is about 20% of the overall Sn and is probably not recoverable. At least 12% of the Sn and17% of the WO_3 should be recoverable by conventional means as a by-product of fluorite flotation, but a critical question is how much of the Sn and WO_3 is irrecoverable (say finely dispersed in garnet or other calc-silicate minerals) in the vanner tailing where most of the fluorite is present.

The future direction of the investigations will be on the vanner tailings, as outlined in the letter 6th March 1979 in Appendix 10.

David Green has done some initial work on the vanner tailing to determine the tin distribution; his results are in Appendix 10. The work to date suggests that some cassiterite occurs as minute inclusions (not solid solution) in garnet and in fluorite. The results of the bulk of this study are awaited.

BILLITON INVESTIGATION

A 5kg sample was sent to Billiton Research Arnhem, via The Shell Company of Australia Ltd. Brief results of their investigation are in Appendix 11.

FINANCIAL FEASIBILITY

(Askins, 1978)

19. FINANCIAL FEASIBILITY STUDIES.

A. CAPTIVE SOURCE OF FLUORITE.

The beneficiation work done to date on the wrigglite has shown that it is feasible to remove fluorite, though with low recoveries. The wrigglite is therefore a satisfactory strategic captive source of fluorite for Comalco Limited's aluminium smelting operations at Bell Bay, Tasmania and Bluff, New Zealand.

The deposit is possibly the largest single fluorite resource in Australia.

B. COMMERCIAL RESOURCE.

(a) General:

The wrigglite is potentially a very large source of fluorite for the commercial market.

Based on purely commercial, largely overseas, sales of acid grade fluorite and by-product tin, a preliminary DCF study was carried out in July 1975, by G. Weste. (Appendix 34). This study was done before any drilling and showed that the wrigglite body was potentially economic. This was an encouragement for all the future investigations.

The beneficiation studies have since shown that the main problems affecting the wrigglite are the low attainable recoveries of CaF_2, Sn and W.

A recent brief financial analysis taking into consideration the available drilling and beneficiation information and revised metal prices is attached, Appendix 35.

(b) Conclusion:

The wrigglite body at Moina is a subeconomic source of CaF_2, Sn and W with presently known technology and commodity prices. It relies on all or some of the following factors to become economic.

(i) increased prices of CaF_2, Sn and W.

(ii) new beneficiation method to increase fluorite recoveries, and recoveries of by product cassiterite and scheelite.

(iii) higher Sn content in recoverable form in areas so far not drilled.

(iv) higher W content in recoverable form, say coarse scheelite in areas so far not drilled.

(v) sale of magnetite for say coal beneficiation.

(vi) sale of basalt overburden for say road-aggregate.

APPENDIX 35.

FINANCIAL ANALYSIS, MOINA WRIGGLITE:

SEPT. 1978 - (P. ASKINS)

ASSUMPTIONS:

1. 15 million tonnes 18% CaF_2, 0.1% WO_3, 0.1% Sn
2. Open pittable, ore : overburden 1 : 1
3. Thruput 1.5 million t/yr i.e. 10 yr mine life
4. Assume mill operates for 300 day/yr
5. Recoveries 60% CaF_2 as acid grade
   50% WO_3 as scheelite concentrate
   30% Sn as cassiterite concentrate
   (WO_3 and Sn recoveries are very optimistic).
6. Realized prices (using approximate current prices)

CaF_2	acid grade	\$ 80/t
WO_3	65% WO_3 as scheelite conc.	\$120/m.t.u.
Sn	clean cassiterite conc. say	\$ 90/m.t.u.

7. In-the-ground values, at quoted recoveries:

CaF_2	$\frac{18}{100} \times \frac{60}{100} \times 80$	=	\$ 8.60
WO_3	0.1 x 0.5 x 120	=	\$ 6.00
Sn	0.1 x 0.3 x 90	=	\$ 2.70
			\$17.30

8. Concentrate freight costs:

   for Sn, WO_3 negligible
   for CaF_2 assume concentrate sold F.O.B. Devonport. trucking 100 km to coast at say \$12/tonne.

9. No smelter costs since products sold as concentrates.
10. State Government royalties. Tasmania royalties, Sept. 78, are 2.5% of the gross value of production, or 5% of before tax profit, whichever is less. In this case 5% of before tax profit is less.
11. Ore mining cost \$1.20/tonne
12. Overburden removal cost \$1.20/tonne
13. Milling cost \$10.00/tonne (inflated from Erskine (1975), also approximate Renison cost).
14. Overhead, indirect costs \$1.50/tonne
15. Reclaimation costs negligible

16. Capital costs, No townsite necessary

Concentrator (concentrator is complex)	$30 million
Mine development and equipment	$ 4 million
Mine exploration and proving	$ 2 million
	$36 million

17. Capital expenditures each year of operation $ 2 million

18. Assume inflation and commodity prices rise sympathetically.

19. Depreciation of capital costs straight line method $3.6 million/year

OPERATING PROFITS CALCULATION

		Each year of Production.
Tonnes of ore milled		1,500,000
Grade of ore reaching mill		18% CaF_2 0.1% WO_3 0.1% Sn
Tonnes of products in mill feed	CaF_2	270,000
	WO_3	1,500
	Sn	1,500
Tonnes of products recovered	CaF_2	162,000
	WO_3	750
	Sn	450
Gross value of products recovered, $	CaF_2	12,960,000
	WO_3	9,000,000
	Sn	4,050,000
	TOTAL	26,010,000
Tonnes CaF_2 concentrate freighted 97% CaF_2 in concentrate, hence $\frac{162,000 \times 100}{97}$		167,000
Freight charges on CaF_2 concentrate, $ (Sn, WO_3 freight negligible)		2,004,000
No other significant charges, royalty to be figured on operating profit		-
Receipts after charges - equivalent to $16.00/tonne ore milled		say 24,000,000
Operating costs/tonne ore:		
mining ore + overburden	$ 2.40	
milling	$10.00	
overhead/indirect	$ 1.50	
say	$14.00	
Operating profit $16.00 - $14.00 = $2/tonne		$ 3,000,000

CASH FLOW CALCULATION

A detailed cash flow calculation is pointless because the $3 million annual operating profit would be insufficient over the life of the mine, 10 years, to repay the capital costs.

Each year

> Op.profit $3.0 million, less royalty of 5%, gives $2.85 million, minus depreciation $3.6 million means negative taxable income. Net profit after tax is therefore $2.85 million, less annual capital expenditures $2.million gives cash flow of only 0.85 million.

An operating profit exceeding 14 million per year would be necessary to generate a satisfactory cash flow exceeding $6 million per year and a DCF of near 15%.

CONCLUSION

The Moina wrigglite deposit is presently subeconomic.

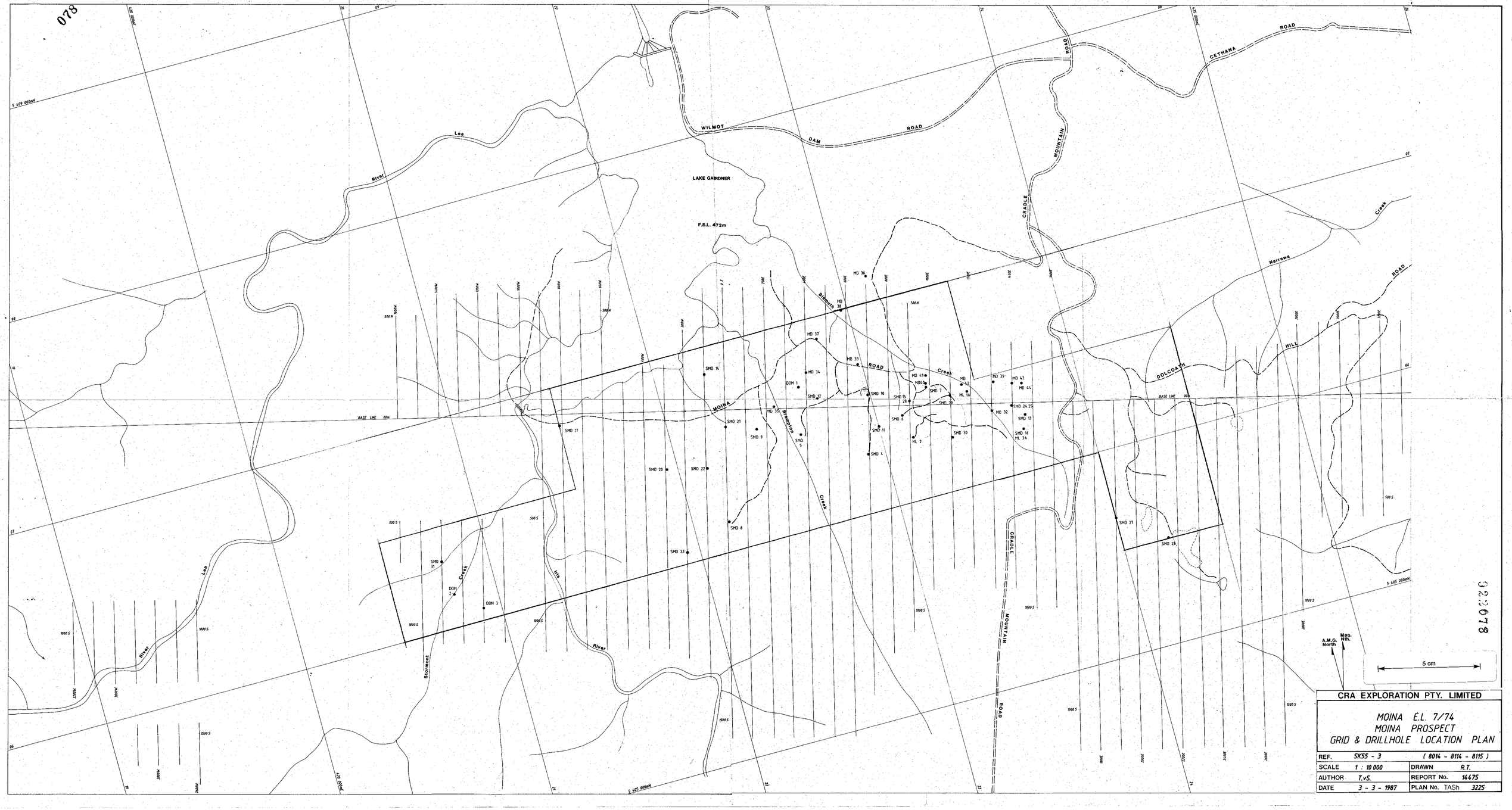

CRA EXPLORATION PTY. LIMITED

MOINA E.L. 7/74
MOINA PROSPECT
GRID & DRILLHOLE LOCATION PLAN

REF.	SK55 - 3	(8014 - 8114 - 8115)	
SCALE	1 : 10 000	DRAWN	R.T.
AUTHOR	T.v.S.	REPORT No.	14475
DATE	3 - 3 - 1987	PLAN No. TASh	3225

CRA EXPLORATION PTY. LIMITED

MOINA E.L. 7/74
MOINA PROSPECT
GEOLOGICAL PLAN

REF.	SK55 - 3	(8014 - 8114 - 8115)	
SCALE	1 : 10000	DRAWN	R.T.
AUTHOR	T.vS.	REPORT No.	14475
DATE	9 - 2 - 1987	PLAN No.	TASh 3290